



VCU

Virginia Commonwealth University
VCU Scholars Compass

Theses and Dissertations


Graduate School

2021

Intermittent Theta Burst Stimulation: Application to Spinal Cord Injury Rehabilitation and Computational Modeling

Neil Mittal
Virginia Commonwealth University

Follow this and additional works at: <https://scholarscompass.vcu.edu/etd>

 Part of the [Bioelectrical and Neuroengineering Commons](#), [Rehabilitation and Therapy Commons](#), and the [Translational Medical Research Commons](#)

© Neil Mittal, MD

Downloaded from

<https://scholarscompass.vcu.edu/etd/6829>

This Dissertation is brought to you for free and open access by the Graduate School at VCU Scholars Compass. It has been accepted for inclusion in Theses and Dissertations by an authorized administrator of VCU Scholars Compass. For more information, please contact libcompass@vcu.edu.

Intermittent Theta Burst Stimulation: Application to Spinal Cord Injury Rehabilitation and Computational Modeling

Partial fulfillment statement:

A thesis/dissertation submitted in partial fulfillment of the requirements for the degree of
Doctor of Philosophy at Virginia Commonwealth University.

Neil Mittal, MD, MS

© 2021 Neil Mittal, All Rights Reserved

College of Engineering, Biomedical Engineering
Rehabilitation Engineering to Advance Ability Lab (REALab)

December 8, 2021

Advisor

Carrie Peterson, PhD

Committee

Dean Krusienski, PhD, Christopher Lemmon, PhD, Ravi Hadimani, PhD, George Gitchel, PhD

Abstract

Loss of motor function from spinal cord injuries (SCI) results in loss of independence. Rehabilitation efforts are targeted to enhance the ability to perform activities of daily living (ADLs), but outcomes from physical therapy alone are often insufficient. Neuromodulation techniques that induce neuroplasticity may push the limits on recovery. Neuromodulation by intermittent theta burst transcranial magnetic stimulation (iTBS) induces neuroplasticity by increasing corticomotor excitability, though this has most frequently been studied with motor targets and on individuals not in need of rehabilitation. Increased corticomotor excitability is associated with motor learning. The response to iTBS, however, is highly variable and unpredictable, while the mechanisms are not well understood. Studies have proposed brain anatomy and individual subject differences as a source of variability but have not quantified the effects. Existing models have not incorporated known neurotransmitter changes at the synaptic level to pair mechanisms to cell output in a neural circuit. To use iTBS in practical rehabilitative efforts, the technique must either be consistent, have a predictable responsiveness, or present with enough mechanistic understanding to improve its efficacy.

To that effect, this study has two primary objectives for the improvement of rehabilitation techniques. The first is to establish how iTBS affects both a motor target and population that typically undergoes physical rehabilitation often with unsatisfactory outcomes, in this case the biceps brachii in individuals with SCI and relate the empirical effects of iTBS to individual anatomy. This will establish the consistency of the technique and predictability of its effects, relevant to rehabilitative efforts. The secondary objective is to create the foundation of a model that exhibits circuit organization, which would start the development of a motor neuroplasticity functional unit with simulation of the synaptic long-term potentiation (LTP) like effects of iTBS.

Summary of Methods: iTBS was performed targeting the biceps, on multiple cohorts, with changes in motor evoked potential amplitude (MEP) tracked after sham and active intervention. This was compared between nonimpaired individuals and those with SCI. Furthermore, iTBS of both biceps and first dorsal interosseus (FDI) was compared to simulation of TMS on MRI derived head models to establish the impact of individualized neuroanatomy. Finally, a motor canonical neural circuit was programmed to display fundamental physiological spiking behavior of membrane potentials.

Summary of Results: iTBS did facilitate corticomotor excitability in the biceps of nonimpaired individuals and in those with SCI. iTBS had no group-wide effect on the FDI, highlighting the variability in response to the protocol. TMS response (motor thresholds) and iTBS response (change in MEPs) both were related to parameters extracted from MRI-derived head models representing variations in individual neuroanatomy. The neural circuit model represents a canonical networked unit. In the future, this can be further tuned to exhibit biological variability and generate population-based values being run in parallel, while matching the understood mechanisms of neuroplasticity: disinhibition and LTP.

Conclusion: These studies provide missing information of iTBS responsivity by (1) determining group-wide responsiveness in a clinically relevant target; (2) establishing individual level influences that affect responsivity which can be measured prior to iTBS; and (3) beginning design of a tool to test a single neural circuit and its mechanistic responses.

Table of Contents

1	Introduction	1
1.1	Spinal Cord Injury and Motor Dysfunction	1
1.2	Neuromodulation.....	3
1.3	Representation of Neuron Function and Cortical Control	7
1.4	Limitations of Current Knowledge	11
1.5	Objective of Presented Research.....	13
1.6	Aims.....	14
2	The effect of intermittent theta burst stimulation on corticomotor excitability of the biceps brachii in nonimpaired individuals.....	15
2.1	Authors and Submission Details	15
2.2	Abstract.....	15
2.3	Introduction	16
2.4	Materials and methods.....	17
2.5	Results.....	22
2.6	Discussion.....	24
2.7	Conclusions	27
2.8	Supplemental	28
3	Intermittent theta burst stimulation modulates biceps brachii corticomotor excitability in individuals with tetraplegia	31
3.1	Authors and Submission Details	31
3.2	Abstract.....	31
3.3	Introduction	32
3.4	Methods.....	34
3.5	Results.....	38
3.6	Discussion.....	42
3.7	Limitations.....	43
3.8	Conclusions	44
3.9	Supplemental	45

4	Effect of Neuroanatomy on Corticomotor Excitability During and After Transcranial Magnetic Stimulation and Intermittent Theta Burst Stimulation.....	49
4.1	Authors and Submission Details	49
4.2	Abstract.....	49
4.3	Introduction	49
4.4	Methods.....	51
4.5	Results.....	62
4.6	Discussion.....	69
4.7	Limitations.....	71
4.8	Conclusion.....	71
5	Effect of Fiber Tracts and Depolarized Brain Volume on Resting Motor Thresholds during Transcranial Magnetic Stimulation	73
5.1	Authors and Submission Details	73
5.2	Abstract.....	73
5.3	Introduction	73
5.4	Methods.....	74
5.5	Results.....	78
5.6	Discussion.....	80
6	Motor Neural Circuit Simulated Response to iTBS	82
6.1	Script Repository.....	82
6.2	Context Overview: Existing Simulation in Neural Circuits and TMS	82
6.3	Specific Examples of Simulation Work and Theory: TMS, Neural Circuits, Hodgkin Huxley.....	82
6.4	Description of Completed Work	85
6.5	Future Work.....	91
7	Conclusion.....	93
8	Scientific Communications.....	95
8.1	Papers	95
8.2	Conference Posters and Presentations.....	95
9	Acknowledgements.....	97

10	Abbreviated <i>Curriculum Vitae</i>	98
11	References	99

Abbreviations and Acronyms

∞ : Equilibrium State	LTD: Long Term Depression
τ (tau): Time Constant	LTP: Long Term Potentiation
ADL: Activities of Daily Living	m: Activation Subunit (Sodium) Probability
AMPA: α -Amino-3-Hydroxy-5-Methyl-4-Isoxazolepropionic Acid	M1: Primary Motor Cortex
AMT _{target} : Active Motor Threshold of Target Motor Region	MEP: Motor Evoked Potential
B: Magnetic (e.g., B-field – Magnetic Field)	Mmax: Maximal Compound Action Potential
BSD: Brain-Scalp Distance	MRI: Magnetic Resonance Imaging
C: Capacitance	MSO: Maximum Stimulator Output
CCP: Corticomotor Conductance Potential	MT: Motor Threshold
cTBS: Continuous Theta Burst Stimulation	MVC: Maximum Voluntary Contraction
E: Electric (e.g., E-field – Electric Field)	n: Activation Subunit (Potassium) Probability
E _{channel} : Nernst Potential for Membrane Channel	Na ⁺ : Sodium
EEG: Electroencephalography	NMDA: N-Methyl-D-Aspartic Acid
EFS: Electric Field Strength	nMEP: Normalized Motor Evoked Potential
EMG: Electromyography	PEST: Parameter Estimation by Sequential Testing
EPOCS: Evoked Potential Operant Conditioning Software	RMT _{a-b} : RMT Difference Between Target Motor Region A and Target Motor Region B
ETL: Echo Train Length	RMT _{target} : Resting Motor Threshold of *Target Motor Region*
FCR: First Carpal Radialis Muscle	rTMS: Repetitive Transcranial Magnetic Stimulation
FDI: First Dorsal Interosseus Muscle	S: Neurotransmitter Channel Gating Fraction
FEA: Finite Element Analysis	SCI: Spinal Cord Injury
FPI: First Palmer Interosseus Muscle	SEM: Standard Error of the Mean
FTSA: Fiber Tract Surface Area	t: Time
G _{species} : Membrane Permeability to Species	TDCS: Transcranial Direct Current Stimulation
GABA: γ -Aminobutyric Acid	TE: Time Echo
h: Deactivation Subunit Probability	TFC: Tract Fiber Count
I: Current	TMS: Transcranial Magnetic Stimulation
IN: Interneuron	TR: Time Repetition
iTBS: Intermittent Theta Burst Stimulation	V: Volts
K ⁺ : Potassium	x: Ionic Channel Subunit Activation Probability
k_f & k_r : Rate Constants (Forward & Backward)	
LMEM: Linear Mixed Effects Model	

1 Introduction

1.1 Spinal Cord Injury and Motor Dysfunction

Spinal cord injuries (SCI) result in a loss of nervous transmission at the site of damage, disrupting the communication between the brain and the body. Among the various effects of SCI is the loss of transmission of motor control to the muscles from above the injury and a loss of sensory messaging from the below the injury. For individuals who have experienced SCI, improving motor function is a crucial part of rehabilitation efforts to enhance their quality of life. There are 288,000 individuals in the USA currently living with SCI, with 17,700 new cases annually; the most common form of SCI is incomplete tetraplegia, which can result from damage to the lower cervical spinal cord (C5-C8) and is characterized by deficits in upper limb function (Fig 1.1A) [1], [2]. With upper limb function being essential to perform activities of daily living (ADL), it is the most desired ability to be regained after injury at the cervical level [3]. One approach to improve the motor performance of upper limb muscles in individuals with incomplete SCI, is to strengthen the connection of spared corticospinal tracts through repetitive transcranial magnetic stimulation (rTMS). This has been demonstrated in studies such as those by Belci et al and Benito et al, which targeted rTMS to the thenar and leg representations of the primary motor cortex (M1), respectively, and showed significant improvements in motor function as assessed by the American Spinal Injury Association Impairment Scale [4], [5].

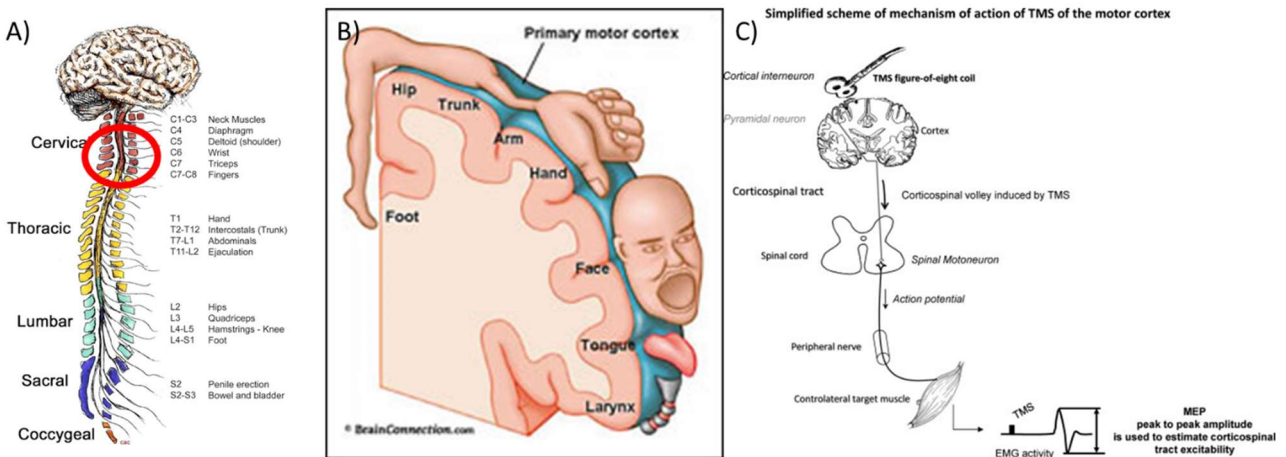


Fig 1.1: Relevant Physiology. (A) C5-C8 spine anatomy is displayed (Image Source: Reeves Fondation). (B) A motor homunculus shows the representations of motor control regions of the primary motor cortex (Image Source: NPR). (C) The corticomotor pathway between the primary motor cortex and upper limb is part of the corticospinal pathway from the brain [6].

Motor function of specific body regions is associated with organized cortical regions as well, with greater neuron density and cortical surface area dedicated to body targets that require greater control, such as the hands and fingers (Fig 1.1B, 1.1C) [7]–[9]. The motor map, or motor homunculus, is a dynamic map that evolves and changes with learning and physical activity [10]. After SCI, the map changes, with regions dedicated to parts of the body with severely reduced function overwritten by

those that remain, a natural process of innate neuroplasticity that is essential for rehabilitative efforts [6], [11]–[17].

The impact of motor loss particularly, is an immediate and profound reduction in independence. ADLs such as locomotion, tooth-brushing, self-feeding, and other forms of routine selfcare, depend heavily on coordinated control of the upper limbs with strength [3], [18], [19]. Individuals with incomplete tetraplegia may retain some upper limb function, but frequently not enough to maintain a level of independence with which they are satisfied [3], [20], [21]. Higher function can relate to greater satisfaction in the longer term for recovery, but the perceived function and self-efficacy or independence are as or more critical than objective functional metrics [22]–[24]. While there is some room for recovery with time in some cases, often limited by the amount of function at the start of rehabilitation, the nerves themselves do not regenerate and reform coordinated connections to fully restore the level of strength or control from before injury [25], [26]. Upper limb function has been shown to be the most desired ability to regain for individuals with SCI [3].

1.1.1 Rehabilitative Efforts

Current rehabilitative efforts are focused on preserving and restoring motor control over regions of the body that are not fully impaired, with a focus on maximizing ability to perform ADLs [27]–[29]. Restoration of function can be achieved through interventional techniques and device-mediated support to replace or compensate for lost functionality [30]. To that effect, if the goal of physical therapy is to improve quality of life and independence, skill acquisition is centered on retraining to replace lost function with new and compensatory movement techniques, with efforts made to minimize further loss of function over time in a combination of physical training, ergonomics, and functional electrical stimulation [27]–[29], [31], [32]. This often results in learning new ways to grip and manipulate objects without the use of distinct fingers or a strong hand grasp. Current physical rehabilitative therapy methods include strength and resistance training to build motor strength, aerobic conditioning to maintain endurance, and skills training for dexterity [27]. Skills training has a focus on movements that can restore any degree of independence by promoting self-completion of ADL's [27]. Elbow extension, for weight transfer and chair control, for example, is an important component of physical therapy, and even surgical interventions in the form of upper limb reconstructions where healthy biceps brachii (biceps) or brachioradialis muscle, tendon, or nerve tissue is repurposed for elbow extension [33]–[35]. Surgical intervention necessitates its own rehabilitation process, with similar focus but a greater weight on motor re-education to repurpose elbow flexors as extensors [35], [36]. Other movements that are of high rehabilitative value are elbow flexion and grip strength, as these movements allow for gripping and manipulation of the world around the patient [37].

Using metrics of restoration of ADL's and satisfaction of quality of life, rehabilitative efforts as they stand are inconsistent in their outcomes and largely not optimally successful [3], [21]. Because lost neurons do not get replaced, and axonal regrowth has only limited organization, damage to the

corticospinal tract continues to limit functional recovery. The initial degree of injury and disability often limits the degree of recovery [3], [20], [21]. Patients are often dissatisfied by their degree of independence and levels of function, as well as with the length and difficulty of their rehabilitative plan [3], [20], [21].

1.2 Neuromodulation

Neuromodulation techniques can affect the communication of the neuromuscular system. For example, electromagnetic stimulation at the level of the cortex has been used to trigger peripheral responses and may assess the communicability of the corticomotor tract [6], [11], [38]–[43]. Some neuromodulation methods are advantageous for being noninvasive, such as transcranial direct current stimulation (tDCS) and transcranial magnetic stimulation (TMS). In certain paradigms such as repetitive and patterned stimulation, these techniques have also manipulated the excitability of the cortical (cortical excitability) and downstream pathways (cortico-* excitability), changing their level of excitability rather than simply eliciting response, which has resulted in investigations of their potential as therapeutic techniques [44].

Neuromodulation techniques are currently in use both clinically and in research. TMS has been used for cortical mapping studies and motor dysfunction assessment or treatment in research [6]. Clinically, TMS is used to treat refractory depression, as a more focal alternative to electroconvulsive therapy [45], [46]. Physical therapy and motor skills practice both are forms of neuromodulation, inducing activity dependent or practice based plasticity [47], [48]. These are indirect effects, as the intervention does not directly target neuron function. Physical therapy and motor skills practice are examples of physical rehabilitation techniques and skill acquisition used by healthy individuals [12]. Certain pharmacologic drugs and stimulation based techniques that affect mood and attention are also neuromodulating; these direct techniques target synaptic function and shift the balance of neurotransmitters [49], [50]. Psychiatric medicine makes extensive use of neuromodulation pharmacology to regulate and treat mood and attention disorders. Anti-spasticity medications such as baclofen work at the level of interneuron and inhibitory signaling modulation in the central nervous system to affect the neuromuscular system below.

Cortical motor map changes after an injury, cortical map changes after rehabilitation, and effects of neuromodulation are all examples of neuroplasticity [11], [16], [17], [51]. The central nervous system is not a static system and undergoes dynamic change as it functions and processes stimuli [11], [16], [17]. These changes are driven at the level of the synapses between neurons, as the balance of neurotransmitters, receptors, and currents, shift and modify the connectivity between neurons. Corticomotor excitability is the degree to which signals will propagate and transmit down the motor pathway, which is enhanced by facilitatory plasticity, or diminished by inhibitory plasticity. Previous research has highlighted the role of changes in corticomotor excitability individuals with tetraplegia and biceps brachii tendon transfer to extend the elbow, which was positively correlated to elbow extension

strength [52]. Even small improvements in force can reflect more substantial effects in rehabilitation [53].

There is promise in pairing direct neuromodulation that increases corticomotor excitability with physical therapy to improve skill acquisition and thus rehabilitation outcomes [11], [40]–[43]. Research has shown that elbow extension strength is related to corticomotor excitability, and facilitatory neuromodulation techniques can increase corticomotor excitability [11], [40]–[43], [52]. Furthermore, improved motor function and skill acquisition are associated with increased corticomotor excitability, which can be measured via electromyography (EMG) by an increase in the amplitude of motor-evoked potentials (MEPs) induced by external stimuli [6], [54], [55]. These effects have been demonstrated primarily in human iTBS studies, which targeted distal muscles of the upper limb in non-impaired (with respect to spinal cord injury and tetraplegia) populations (i.e. first dorsal interosseous (FDI) & flexor carpi radialis (FCR)) [38], [56]. Therefore, using these methods could improve rehabilitation outcomes. For example, after biceps-to-triceps tendon transfer to restore elbow extension in individuals with tetraplegia, the biceps must undergo motor re-learning to extend the elbow. Previous work suggests that these individuals may benefit from increased biceps corticomotor excitability [52].

1.2.1 *Transcranial Magnetic Stimulation*

TMS is noninvasive, low risk, focal, and versatile. As a result, this technology has been used to aid in mapping of the cortex quickly, accurately, and inexpensively [6], [57], and it's currently used to treat refractory depression and other neuropsychiatric conditions with FDA approval [45], [46]. Current work in our lab also is applying single pulse TMS as a diagnostic tool, for assessing the strength of corticomotor connectivity after SCI by comparing the forces generated by voluntary contraction to the extra force generated above by an exogenous cortical stimulation at the same time. Furthermore, TMS, in both single pulse TMS and rTMS protocols, as previously mentioned, has been applied in number of clinical and research settings for sensory, mood, and motor function, and TMS has been shown to be able to alter the cortical motor network [6], [39], [51], [54], [57].

TMS works by inducing a current on the cortical surface, from an induction coil placed above the head (Fig 1.2A) [6], [39], [57]. This current depolarizes superficial and deep layer excitatory neurons and generates an action potential. Direct stimulation of the cortical output at the deeper layers causes direct stimulation down the corticospinal tract, referred to as a D-wave (Fig 1.2B) [6], [39]. Indirect stimulation of this tract due to the signal volleys sent from the depolarized superficial layer neurons that follow presents in a series of I-waves [6], [39]. These waves together trigger a muscular response, the MEP, that can be measured by EMG (Fig 1.2B). MEPs are used as a measurement of corticomotor excitability [6], [39]. The likelihood of a signal to induce a MEP is related to its strength, and the stimulation intensity needed to do so at least half of the time, at sufficient magnitude, is referred to as a motor threshold (MT), which can be evaluated at rest, the resting motor threshold (RMT), or during voluntary activation of the motor target, the active motor threshold (AMT) [6], [39]. AMT is usually

found at lower intensity than RMT as the tract is primed by the voluntary activation [6], [39], [49], [50], [58], [59].

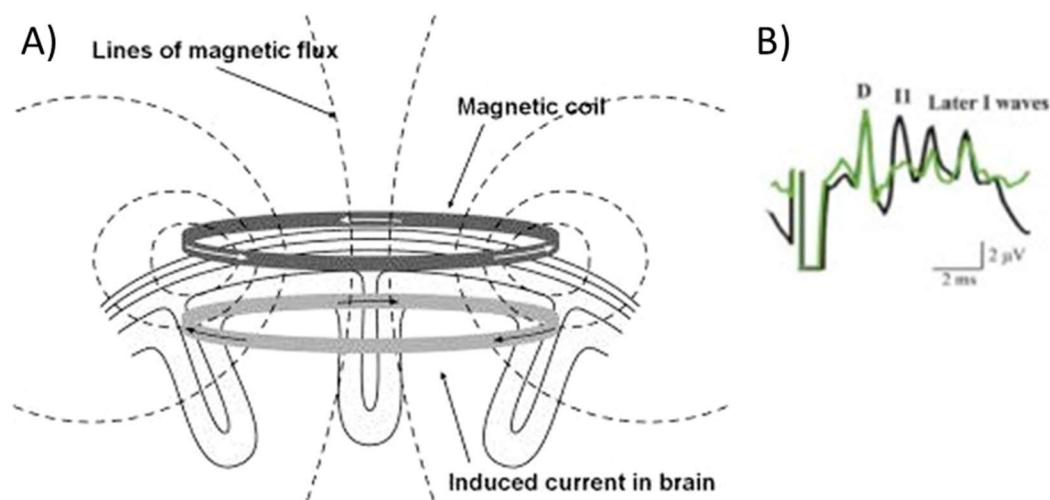


Fig 1.2: TMS Physical Mechanism. (A) The magnetic coil discharges, single coil shown [60]. The rapid generation and cessation of the magnetic field induces a current which can be applied to the cortical surface. (B) The descending volley comprises a D wave (green line) and a series of I waves (black line) are shown, which summate in the muscle as the motor evoked potential [39].

Neuromodulatory effects of TMS are largely mediated by rTMS protocols, as opposed to single pulse TMS [6]. Uniform frequency protocols can take upwards of 15 minutes, with variable outcomes and effects, often which are transient [6], [57]. Therefore, uniform rTMS, while useful, is inherently a limited approach.

1.2.2 Intermittent Theta Burst Stimulation

Theta burst stimulation is a unique and flexible form of rTMS that allows for shorter protocols [54], [61]. These are pattern-based bursts of stimulation based on the theta brain wave found in electroencephalogram (EEG) readings, representative of electrical activity at the frequency of 4-10 Hz depending on the source or species [6]. These waves are found in rodents during exploration, short term memory storage, and REM sleep, from 6-10 Hz in the hippocampus [39]. When delivered continuously (cTBS), the effect has been shown to be inhibitory, lowering corticomotor excitability in studies focused largely in the first dorsal interosseus muscle (FDI) of healthy, adult, human hands [39], [54]. When delivered intermittently (iTBS), in similar study cohorts the effect has been excitatory [6], [38], [39]. TBS is thought to trigger an influx of calcium ions, the rate and magnitude of which then effect excitation or inhibition [6], [39], [62]. This is referred to as long term potentiation (LTP) or depression (LTD) like effects, as they excite or inhibit respectively similarly to the mechanisms of LTP and LTD, mediated by calcium currents and NMDA receptors [6], [39], [54], [63]. iTBS is associated with increasing late I-waves, while cTBS depresses early I-waves [39].

iTBS is a short protocol, under 3 minutes, of low intensity bursts of high frequency stimulation [54]. It is associated with excitatory effects that last upwards of 30 minutes after stimulation and has been most studied in distal muscles of the upper limb in humans (i.e. first dorsal interosseous (FDI) & flexor carpi radialis (FCR)) [6], [38], [39], [54]–[56], [64]. These studies have shown that the effect of iTBS is in fact variable, between studies and even within individuals on repeated sessions.

The key limitation to iTBS and TMS based neuromodulatory techniques at this time is variability of the effect on corticomotor excitability. While there are conventionally held views on the effects, numerous studies have shown that high variability and at times no effect or even opposite effects on corticomotor excitability are obtained by common protocols [38], [39], [65]–[72]. Across paradigms, motor targets, and cohorts, high variability is inherent in TMS data. MEPs in particular are also prone to high variability as a measurement, further compounding the potential unreliability of TMS protocols [73], [74].

1.2.3 Neuroanatomy and TMS Simulation

Anatomy has been studied as a modifier of TMS outcomes but is poorly understood and largely not controlled in most studies. The conduction of the induced current from TMS is dependent on the morphology and material properties of what is stimulated [54], [75]. Communication of the stimulation is carried through the relevant fiber tract, such as the corticospinal tract for corticomotor control [54], [75]. Depolarization of motor cortex neurons elicits responses to TMS, so individual differences in neuroanatomy should impact the response to TMS between individuals and motor targets [8], [76]–[80]. Brain scalp distance has been associated with TMS response variability [79], [81] but is limited as a one-dimensional parameter that ignores composition of tissue between scalp and cortex, so better metrics that can account for multiple dimensions and complex tissue properties are needed [80].

Neuroanatomical modeling has been paired with neuromodulation simulation, including finite element TMS simulation of MRI-derived head models [79], [80]. Such models have allowed for individually accurate *in silico* representations of both brain morphology and coil shape [82]. From such studies, the simulated induced cortical electric field strength has been used as a more nuanced metric of neuroanatomy [81].

Fiber tractography has also provided another route to individualized and accurate modeling of the relevant anatomy of neuromodulation [83]. These MRI-derived models can provide parameterization of the connective tracts from the cortex to spine. Both of these neuroanatomical simulation techniques, however, have been used predominantly isolated from empirical data and have not been used for a rehabilitation relevant target of iTBS.

1.3 Representation of Neuron Function and Cortical Control

1.3.1 Neural Circuits

Unlike neuroanatomical models, which provide insights at the organism level, cellular level models can be used for more mechanistic studies [63]. However, such studies can be opaque to the internal machinery of neuroplasticity, proposing numerical representations that do not have direct physiological analogues; or pair schematic structure with validated mechanisms but not test the constructed representation [84]. Organizing neural function into a circuit enables the development of models based on them in a number of contexts, from network oscillation baseline activity, to subthreshold communication, from mouse models of neurotransmitter focused ganglion models to primate and human sensory function [85]–[88]. TMS mechanisms and learning have been discussed with neural circuit paradigms used for context, though in some cases without actual definition of the circuitry [89]–[91]. A neural circuit is a population of neurons that are synaptically linked and perform a distinct task [92]. They are generally considered the smallest functional subunit of discrete neural activities and can be linked to scale up and form large brain networks [92]. A “canonical circuit” can be used as a representative of a symbolic neural circuit for most simple stimulation response functions [93]–[95]. Circuit paradigms are implicated in neuroplasticity, as evidence suggests that plastic reorganization is a result of change at the level of synapses, affecting the circuits in which they are found [6].

A canonical circuit has been used in the development or conceptualization of circuit pathways. This canonical circuit is a starting point for neural circuit modeling or the understanding of circuit-organized processes [93]–[95]. Connections can incorporate time and spatial organization and be visualized abstractly or algorithmically. One presentation of a neural circuit is as an electrophysiological model, presenting each element in the circuit by its electrophysiological contribution [96]–[100]. Cellular function for neuronal signal transmission can be conceptualized as the development, propagation, and effects of action potentials between cells based on their internal compartmental electrochemical physiology. Doing so enables a neural circuit to be presented as an electrical circuit diagram, linking circuits together to represent cellular compartments.

A neural circuit structure is the basis for the current understanding of a variety of physiological and pathological functions. Oscillatory activity in the basal ganglia has been modeled, using neural circuits as the basis [85]. Associative learning is dependent on thalamic based circuits, such as the fear circuit that pairs pain and flinching to non-noxious stimuli [101], [102]. Neurodegenerative cognitive disease such as Alzheimer’s dementia or Parkinson’s disease are understood to have links to dysfunction in a basal ganglia circuit, the Papez circuit [103]–[105]. In both examples, studies have used circuit paradigms to improve understanding and propose treatment, such as the use of deep brain stimulation of the Papez circuit.

1.3.2 Hodgkin and Huxley Membrane Potential Modeling of Electrophysiology

Hodgkin and Huxley developed a conductance-based model of action potential generation in neurons [106]. This work converted the electrophysiology of nervous conduction to a series of equations that allowed for voltage dependent ion currents and the reactive synaptic currents that we see empirically. Their model used ionic mechanisms to generate membrane potential change, as a function of probabilities that determine the permeability of the membrane to unique ionic species (Fig 1.3) [106]. Ionic gradients were represented as voltage sources, and membrane permeability to said ionic species were analogous to resistors. The instantaneous permeability to any ionic species was determined as a voltage dependent probability [106]. The applications of such presentation have been expanded to include full networks of other neuronal compartments and full neurons, such as dopamine bursting neurons, especially for *in silico* experimentation [88], [107]. For example, individual cell compartments can be presented as a collection of unique channels, and linked together, and full cells represented this way can be strung compartment to compartment (Fig 1.4). This paradigm has been applied in larger neural circuits, albeit randomly connected, to show that cellular ion concentrations and cellular network behavior are closely linked [108].

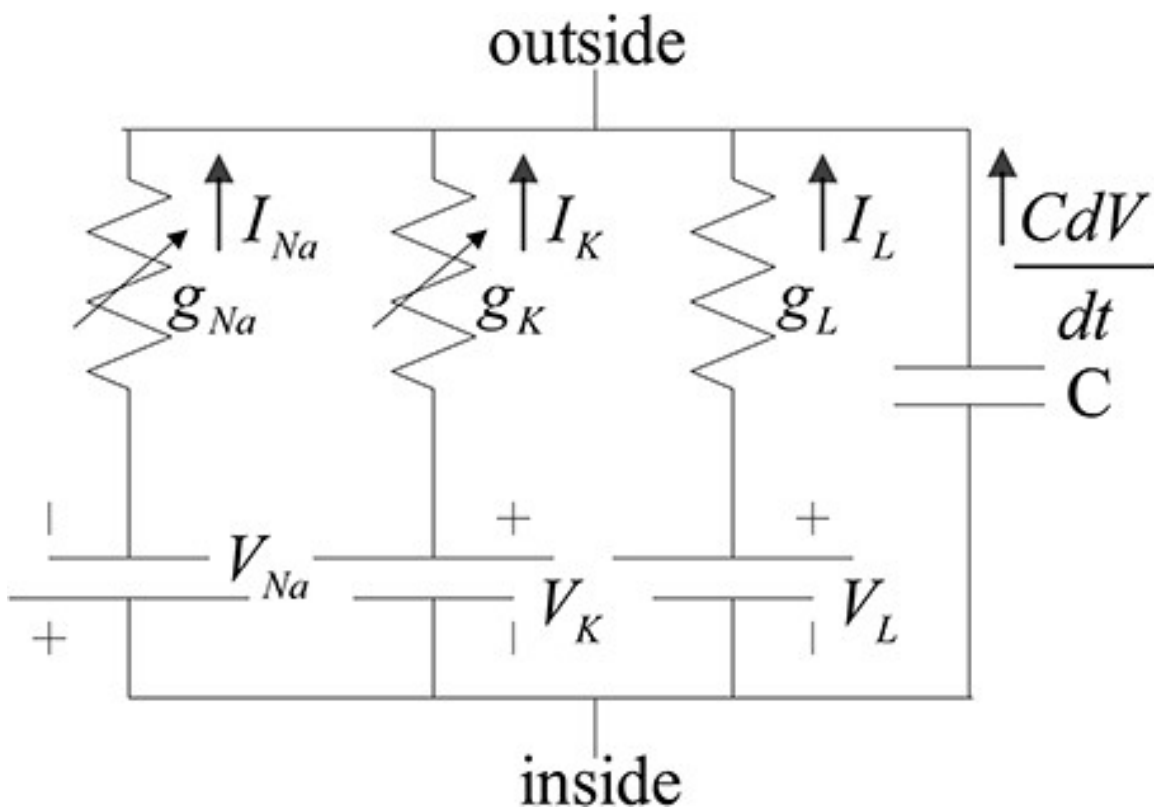


Fig 1.3: Circuit diagram of a neuronal axonal membrane patch [106]. Ionic gradients and permeability can be represented as voltage sources and resistors, across the insulating capacitance of a phospholipid bilayer cell membrane.

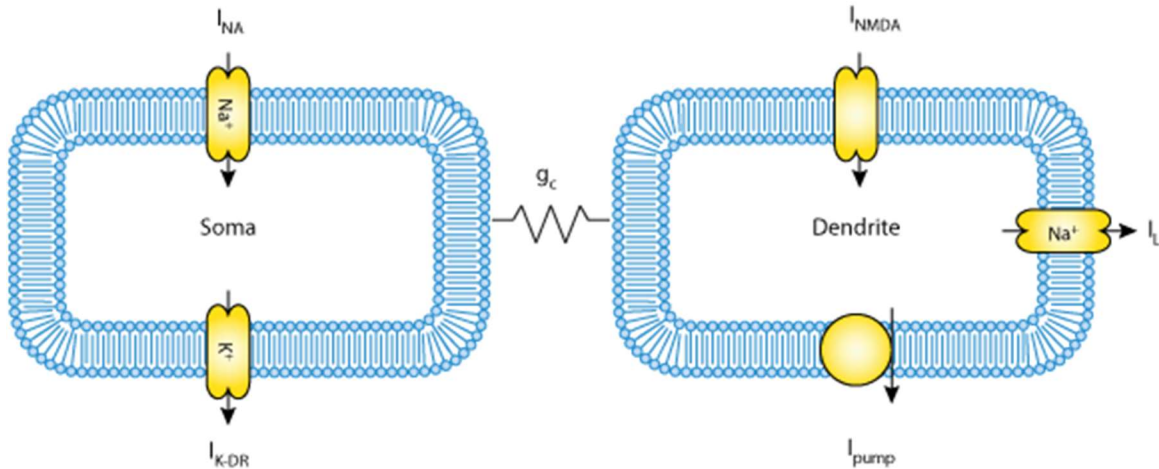


Fig 1.4: Compartmental representation of a dopamine bursting neuron [108]. Schematic shows unique parameters that define the soma, in this model represented by transmitting channels for sodium and potassium associated with action potentials; and the dendrite, in this model represented by neurotransmission reception and homeostatic pumps.

Empirically, patch clamp experiments have validated this circuit conception, and this technique remains involved with mathematical modeling of membrane function [109], [110]. It is through rudimentary voltage clamp experimentation mediated intracellular recording that Hodgkin and Huxley determined that the membrane permeability was dynamic and responsive to voltage, with respect to specific ions, in the generation of an action potential [110]. Patch clamp techniques involve using a glass pipette filled with an ionic solution to lock membrane potentials or currents locally, and a probe can measure cellular behavior as a function of the clamp parameters, allowing for the observation of transient currents as small as 0.5 pA and brief as 0.5 mS, consistent with individual channel protein opening and closing [111]. It is the “gold standard” for ion channel screening, with high signal to noise ratio and time scale resolution [112], though due to high labor requirements it is a poor choice for large throughput experimentation. Patch clamp experiments have been used extensively in ion channel monitoring experiments, such as tracking calcium flow for neurons and muscular cells [113]. It has also been involved in drug delivery studies and cellular communication studies of synaptic interactions [112], [114]. More recently, adaptations to the technique have been used to characterize membrane behavior of intracellular organelles, such as endolysosomes, in the follow-up to proteomic studies of lysosomal storage disorders [115]. In another application, patch clamp techniques and circuitry models of cellular components were used in studies of membrane capacitance regarding polarization behavior of dorsal root ganglion neurons and correlated to empirical work [96]. As such, patch clamp techniques have served as validation of electric circuit modeling approaches.

Synaptic communication follows similar circuit behavior, with postsynaptic function presented as dependent on presynaptic voltage [116], [117]. In this way, neurotransmitter transmission is converted to current, and can be wired into a circuit diagram. Probabilities are controlled less by receptor subunit behavior as in ionic channels, and more by gating subunits in the receptors [116], [117]. In the case of

LTP, for example, rapid or large depolarizations result in activation of N-methyl-D-aspartate (NMDA) receptors, resulting in upregulation of α -amino-3-hydroxy-5-methyl-4-isoxazolepropionic acid (AMPA) receptors and therefore glutamate or excitation sensitivity (Fig 1.5) [118].

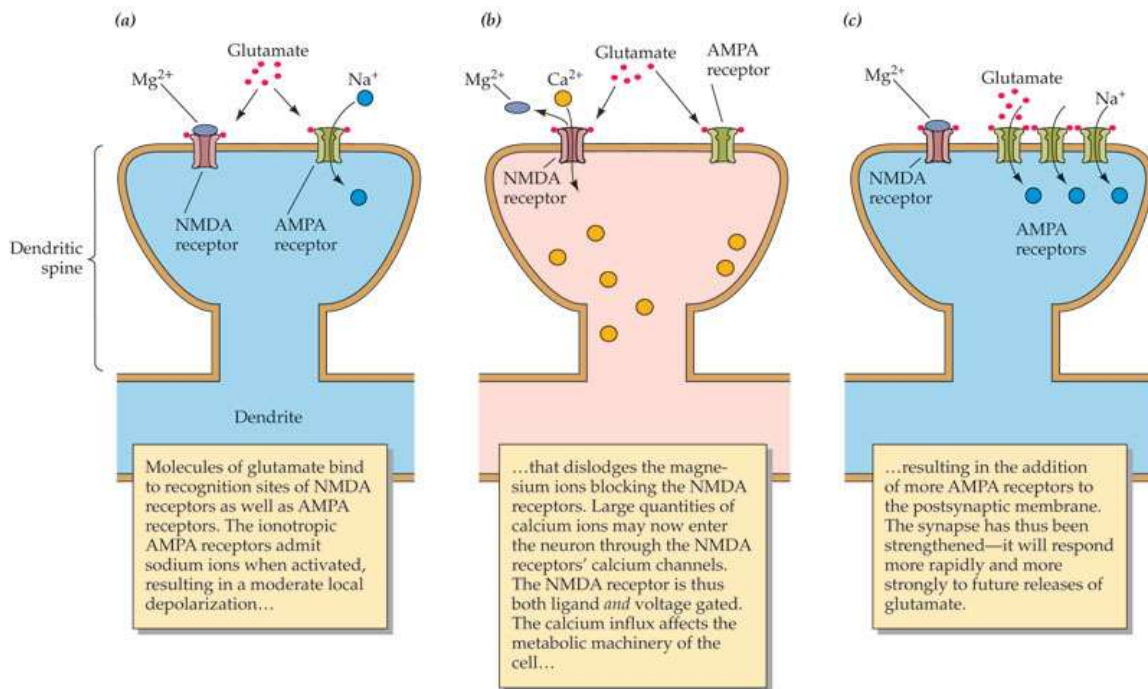


Fig 1.5: Schematic for LTP. Activation of NMDA receptors results in upregulation of AMPA receptors and an increase in glutamate sensitivity in excitatory cells. (Image Source: <https://2e.mindsmachine.com/asf04.02.html>, now https://learninglink.oup.com/access/watson3e-instructor-resources#tag_all-chapters)

The Hodgkin Huxley concept has been incorporated into neural circuit modeling to characterize the behavior of spiking neurons [119], [120]. Further specifics of a methodology used to represent cellular function as a circuit diagram is discussed in Approach, Aim 3 (1.6). Further discussion regarding the conceptualization of a neural circuit is also discussed in Approach, Aim 3 (1.6).

1.3.3 Applications of Combining Electrophysiology Circuit Representation with Neural Circuit Paradigms

This electrophysiological approach allows for the transformation of a cellular membrane into circuit elements, which further enables the diagramming of a neural circuit [120]. This style of cellular modeling has been used to represent a variety of neural functions, from crustacean pacemaker neuron networks, to specific communication mechanisms such as feed forward inhibition, to large-scale human neuron networks of tunable randomized connections that could be stimulated *in silico* [97]–[100]. Electrophysiological modeling has been used for example to explain sensory function and to drive pharmaceutical development [121], [122].

Currently, the description of function within a neural circuit paradigm is in high demand. In the conceptualization of neural control and function, communication that can be presented in discrete elements of input-output relationships is desirable for linking structure, function, genetics, behavior, and technological implications [123]. Development can be discussed in terms of the appearance of behavioral and functional circuits in the brain, and the paradigm serves to provide a basis for discussion of behavior, genetics, environmental influence, and pathology [124]. Modifications of circuits have been examined for how they might alter or improve learning [90]. In other cases, neural circuits as the representation of a functional unit serve as a focus or target point to provide a context for the phenomena being observed (e.g., gene expression in the development of behavioral function units) [125]. Recent trends in habit-formation research have focused on the proposal of neural circuits or orienting the patterns of behavior around them [126].

1.4 Limitations of Current Knowledge

A broader understanding of the efficacy of iTBS is needed to inform the design of combinatorial therapies to improve motor function. Prior studies examining the effects of iTBS on corticomotor excitability have targeted the distal muscles of the upper limb, particularly the FDI [6], [38], [39], [54], [55], [64]. The FDI is easier to target with stimulation relative to more proximal muscles, such as the biceps brachii, as distal muscles have a higher density of corticospinal neurons projecting to the muscle and larger motor map areas that are more accessible to TMS [7], [8]. However, proximal muscles may be in need of rehabilitation and serve as suitable targets for iTBS [6], [38], [39], [52], [71]. For example, after biceps-to-triceps tendon transfer to restore elbow extension in individuals with tetraplegia, the biceps must undergo motor re-learning to extend the elbow. Previous work suggests that these individuals may benefit from increased biceps corticomotor excitability [52]. However, the effects of iTBS targeted to distal muscles (e.g., the FDI) may not translate to the biceps due to differences in corticospinal control [9].

While the effects of iTBS have been demonstrated in non-impaired populations, there have been limited studies which have investigated its effects in individuals with SCI. Most of these studies have targeted iTBS to the M1 region of upper and lower limb muscles to evaluate its ability to modulate spasticity [127], [128]. However, evidence from an SCI study in rodents has shown that iTBS is able to facilitate MEPs and improve motor function after injury [129]. Subsequently, Fassett et al. investigated the effects of iTBS on corticomotor excitability (measured by MEPs) of the FCR in humans with cervical SCI and found MEPs to be reduced in the majority of instances post stimulation [69]. While these findings contradict what has been found in non-impaired populations and SCI animal studies, the results indicate that iTBS is able to modify corticomotor excitability in humans with SCI, which warrants further investigation.

Further research is needed to investigate the potential for iTBS to increase corticomotor excitability in individuals with SCI and how it differs from the observed effects in the non-impaired

population. While the distal upper limb has been the focus of previous iTBS research, the biceps may be a more functionally relevant target for rehabilitation in individuals with low cervical (C5-C8) SCI. Additionally, the biceps can be transferred to restore elbow extension function for some individuals with tetraplegia, supporting the need for motor re-education [33], [37]. As mentioned, previous work shows a positive relationship between the corticomotor excitability of the transferred biceps and elbow extension strength [52]. This further suggests that the biceps may be a functionally relevant target for iTBS in individuals with tetraplegia.

Variability is observed in iTBS studies across populations, both within and between subjects [38], [39], [65]–[72]. Parameters affecting this variability include genetic factors, age, neurotransmitter and receptor variation, transient alertness, and engagement [39], [71], [130]. While recent meta-analysis has suggested that response to theta burst stimulation can be somewhat predicted based on a battery of demographical and procedural details such as age, time of day, and baseline response to TMS, the variability inherent in TMS studies continues to make difficult the drawing of broad conclusions in its efficacy and has even been linked to methodology [39], [71], [130]. Different motor regions have unique parameters, such as surface area or neuron density, that make them easier or harder to target and thus dissimilarly responsive to TMS techniques [7], [8]. Furthermore, most studies have focused on non-impaired individuals, rather than those who have the corticospinal changes present in individuals with motor impairments and dysfunctions, such as those with SCI. However, regardless of the population or motor target, the neuromodulatory impact of iTBS is not predictable. Despite the importance of understanding intrasubject response variability for both investigating mechanisms of neuroplasticity induction and the therapeutic application of iTBS there are very few studies investigating the causes and responses both in healthy participants and clinical populations. Furthermore, individual anatomy has been implicated as a factor but is not generally included in most iTBS protocols [39].

The mechanisms of iTBS have been studied but understanding is limited [63], [84]. While LTP-like plasticity and disinhibition both have been implicated, neither has been shown mechanistically how their contributions result in corticomotor excitability changes or how they interact [63], [84], [98], [99], [131]–[134]. Individual mechanisms have been simulated, but not combined, or not with an organized network structure that a neural circuit would provide [63], [84], [98], [99]. In some cases, complexity has been prioritized, but without physiologically relevant organization, resulting in modeled neuronal network responses to TMS, but no organized network that represents a physiologically relevant system [99], [100]. Similar work has been completed using animal data, with more organization, but without any correlation to human studies [135]. Other than LTP-like plasticity and disinhibition being contributory, not much is explicitly defined in how iTBS effects excitation. These properties themselves have not been tested in an organized system or paired with a scalable subunit, a neural circuit, that would allow for the representation of complex cortical networks [98], [99], [135]. Cited examples have either failed to represent synaptic behavior, ignored canonical circuit structure, or have lacked organization in favor of large network cell populations with random connectivity between cells.

Furthermore, most have focused on stimulus-response behavior, rather than effects of neuromodulatory interventions such as iTBS.

Because the response to iTBS is variable and unpredictable and unknown in a target relevant to rehabilitative efforts, iTBS is limited in its potential application as an adjunct to therapy. Existing simulation work has not yet paired the known mechanistic effects to an organized network of cellular function, and therefore improvements to the technique cannot be proposed to increase its viability by increasing its consistency, predictability, or individually tailoring the technique.

1.5 Objective of Presented Research

To contribute to future improvements in the application of iTBS, these projects had two primary objectives (Figure 1.4 **Error! Reference source not found.**). First, a foundation for the effects of iTBS on a rehabilitation relevant target was needed. Characterization of the response to iTBS targeting the biceps brachii of individuals with SCI used a non-impaired cohort as comparison. Further investigation related the individual anatomy and response to iTBS using MRI. Second, the development of a motor neural circuit was started, to in the future simulate LTP-like effects of iTBS and disinhibition. This circuit will establish the dependence of response to iTBS on known mechanistic effects of iTBS, in a scalable unit that could be later used as a building block for wider cortical networks. These objectives comprise three aims.

1.6 Aims

1.6.1 *Aim 1: Quantify the effect of iTBS on biceps corticomotor excitability in individuals with SCI.*

We applied both active and sham iTBS to the motor cortical region associated with biceps activity in both non-impaired (with respect to SCI and tetraplegia) and those with SCI, then compared the change in amplitude of motor evoked potentials (MEP) of the biceps as a measurement of corticomotor excitability. It was expected that MEPs would be greater after active iTBS, representing increased neuroplasticity, regardless of participant group. See Sections 2 and 3.

1.6.2 *Aim 2: Correlate individual level brain anatomy and functional activity to response to iTBS.*

We simulated electric fields over participant specific brain MRIs and identified the induced electric field strength at M1. We characterized the geometry of corticomotor fiber tracts. We collected the MEP response to an iTBS protocol performed on the same participants targeting both the biceps and FDI. We correlated simulation parameters of current strength and fiber tract geometry with empirical measures of TMS (RMT) and iTBS (MEPs) response, to determine the effect of anatomy. It was expected that individual level anatomy, motor regional anatomy, and functional brain activity would affect iTBS response. See Sections 4 and 5.

1.6.3 *Aim 3: Develop a model of neuromodulatory effect on synaptic communication.*

I designed a neural circuit that models the functional behavior of a canonical neural circuit using a simplified MATLAB function library, based on physiologically relevant cellular parameters. This serves as a basis for future work involving outfitting the synapses with neuroplastic mechanisms to simulate facilitated cellular priming and communication. It was expected that this circuit would present physiologically realistic spiking patterns from an outputting neuron, with a firing rate that could be modulated by its inputter and inhibitor circuit co-members. See Section 6.

2 The effect of intermittent theta burst stimulation on corticomotor excitability of the biceps brachii in nonimpaired individuals

2.1 Authors and Submission Details

N. Mittal, B. Majdic, A. Sima and C. Peterson, "The effect of intermittent theta burst stimulation on corticomotor excitability of the biceps brachii in nonimpaired individuals", *Neuroscience Letters*, vol. 764, p. 136220, 2021. Available: 10.1016/j.neulet.2021.136220.

IRB Approval: VCU IRB HM20010643

Clinical Trials Registration: clinicaltrials.gov NCT03277521

Data Repository: Open Science Framework –

https://osf.io/f6ur7/?view_only=6db94d7460674a928166b53df54b0149

2.2 Abstract

Intermittent theta burst stimulation (iTBS) is a form of repetitive transcranial magnetic stimulation (TMS) that can increase corticomotor excitability in distal upper limb muscles, but the effect on the more proximal biceps is unknown. The study objective was to determine the effect of iTBS on corticomotor excitability of the biceps brachii in non-impaired individuals. Ten individuals completed three sessions, and an additional ten individuals completed one session in a secondary study; each session included sham and active iTBS. Resting and active motor thresholds (RMT, AMT) were determined prior to sham and active iTBS. Motor evoked potentials (MEPs) in response to single pulse TMS served as our measure of corticomotor excitability. In our primary cohort, MEPs were recorded with biphasic stimulation to accurately capture the same neurons affected by biphasic iTBS. MEPs were recorded at an intensity of 120% of RMT, or for instances of high RMTs, 100% of the maximum stimulator output (MSO), at baseline, and 10, 20, and 30 minutes after iTBS. MEPs were normalized by the maximum voluntary isometric muscle activity. In the secondary, MEPs were recorded with monophasic stimulation, which increased our ability to record MEPs at 120% of RMT. Linear mixed effects models were used to determine the effect of iTBS on normalized MEPs (nMEPs), with analyses to evaluate the interaction of the biceps AMT:RMT ratio as a measure of corticomotor conductance. Change in nMEPs from baseline did not differ for the active and sham conditions ($p = 0.915$) when MEPs were assessed with biphasic stimulation. With MEPs assessed by monophasic stimulation, there was an increase in biceps nMEPs after active iTBS, and no change in nMEPs after sham. Our results suggest that when RMTs are expected to be high when measured with biphasic stimulation, monophasic stimulation can better capture changes in MEPs induced by iTBS, and biphasic stimulation appears limited in its ability to capture changes in biceps MEPs in nonimpaired individuals. In both cohorts, increased corticomotor excitability after iTBS occurred when the biceps AMT:RMT ratio was high. Thus, the

AMT:RMT ratio may be a predictive measure to evaluate the potential for iTBS to increase biceps corticomotor excitability.

2.3 Introduction

Priming the corticospinal system with non-invasive brain stimulation prior to motor training can further enhance training induced motor re-learning [40]–[42]. Increased corticomotor excitability of upper limb muscles is also associated with motor recovery, motor learning and skill acquisition [11], [43]. Intermittent theta burst stimulation (iTBS) is a form of repetitive transcranial magnetic stimulation (TMS) that can increase corticomotor excitability as measured by motor evoked potentials (MEPs) in response to single pulse TMS [136]. iTBS protocols deliver repetitive, high frequency TMS pulses at subthreshold intensities with increased corticomotor excitability aftereffects lasting up to 30 minutes [6], [38], [39], [54]. The mechanistic understanding to date is that iTBS can induce long-term potentiation of cortical neurons [6], [63], [137]. As a result, iTBS has been evaluated as a priming technique for improving individuals' motor functional outcomes after neurologic injury, with previous success in those recovering from stroke [40], [138]–[140].

A broader understanding of the efficacy of iTBS to modulate corticomotor excitability is needed to inform the design of combinatorial therapies to improve motor function. Prior studies examining iTBS effects on corticomotor excitability have targeted the distal muscles of the upper limb, particularly the first dorsal interosseous (FDI) [6], [38], [39], [54], [64]. The FDI is easier to target with stimulation relative to more proximal muscles, such as the biceps brachii, as distal muscles have a higher density of corticospinal neurons projecting to the muscle and larger motor map areas that are more accessible to TMS [141]–[144]. However, proximal muscles may be in need of rehabilitation and serve as suitable targets for iTBS [28], [29]. For example, after biceps-to-triceps tendon transfer to restore elbow extension in individuals with tetraplegia, the biceps must undergo motor re-learning to extend the elbow. Previous work suggests that these individuals may benefit from increased biceps corticomotor excitability [52]. However, the effects of iTBS targeted to distal muscles (e.g., the FDI) may not translate to the biceps due to differences in corticospinal control.

The purpose of this study was to determine the effect of iTBS on corticomotor excitability of the biceps in non-impaired individuals. Since the effects of iTBS have shown to be variable across sessions [68], [72], we tested participants across three sessions to evaluate the reproducibility of iTBS aftereffects [38], [56], [68]. Based on the expectation that iTBS promotes long-term potentiation of cortical neurons [39], [54], we hypothesized that relative to baseline, biceps corticomotor excitability would be increased following active iTBS, and unchanged following sham iTBS. This assessment was performed using biphasic stimulation, to ensure the response was elicited using similar stimulation as iTBS on the same neuron pools [145], [146], and to better model the clinical setting with a single stimulator. However, as monophasic stimulation is associated with greater response at lower stimulation intensities [58], this

study was also repeated in a new group of participants with monophasic stimulation-elicited responses, to account for potential under-stimulation induced variability using the biphasic stimulator [6].

2.4 Materials and methods

2.4.1 Participants

This study comprised 40 independent sessions completed by a total of 20 nonimpaired participants. 10 nonimpaired individuals were recruited, equally divided by gender (5 men, 5 women) and aged between 18 and 38 years (mean = 25.3 years, standard deviation = 5.6 years); each individual in the initial cohort completed three independent sessions of the iTBS protocol. A second cohort of 10 nonimpaired individuals, 7 females, 3 males, aged 19 to 32 years (mean 23.5 ± 5 years), each completed one session of the iTBS protocol (see Monophasic Stimulation Assessment). Individuals with active motor thresholds (AMT) greater than 72% of maximum stimulator output (MSO) on their first RMT measurement were excluded. This criterion ensured iTBS could be delivered at 80% of AMT by the stimulator, as the iTBS intensity was limited to a maximum of 57% MSO as a manufacturer safety feature. All participants were screened to ensure safety of the TMS protocols [147] and provided informed consent. The protocol was approved by the Institutional Review Board of Virginia Commonwealth University.

Repeated sessions were conducted to investigate independence of sessions and intrasubject variability [38], [56]. Each session was separated by a minimum of three days to prevent the potential for carry over effects from one session to another [57] and held in early afternoons to control for variability from diurnal effects. Participants were seated in a chair with their dominant arm at rest, the elbow in 90° flexion, and the forearm supinated, wearing a neck brace to minimize head movements and improve coil positioning (Fig 2.1).

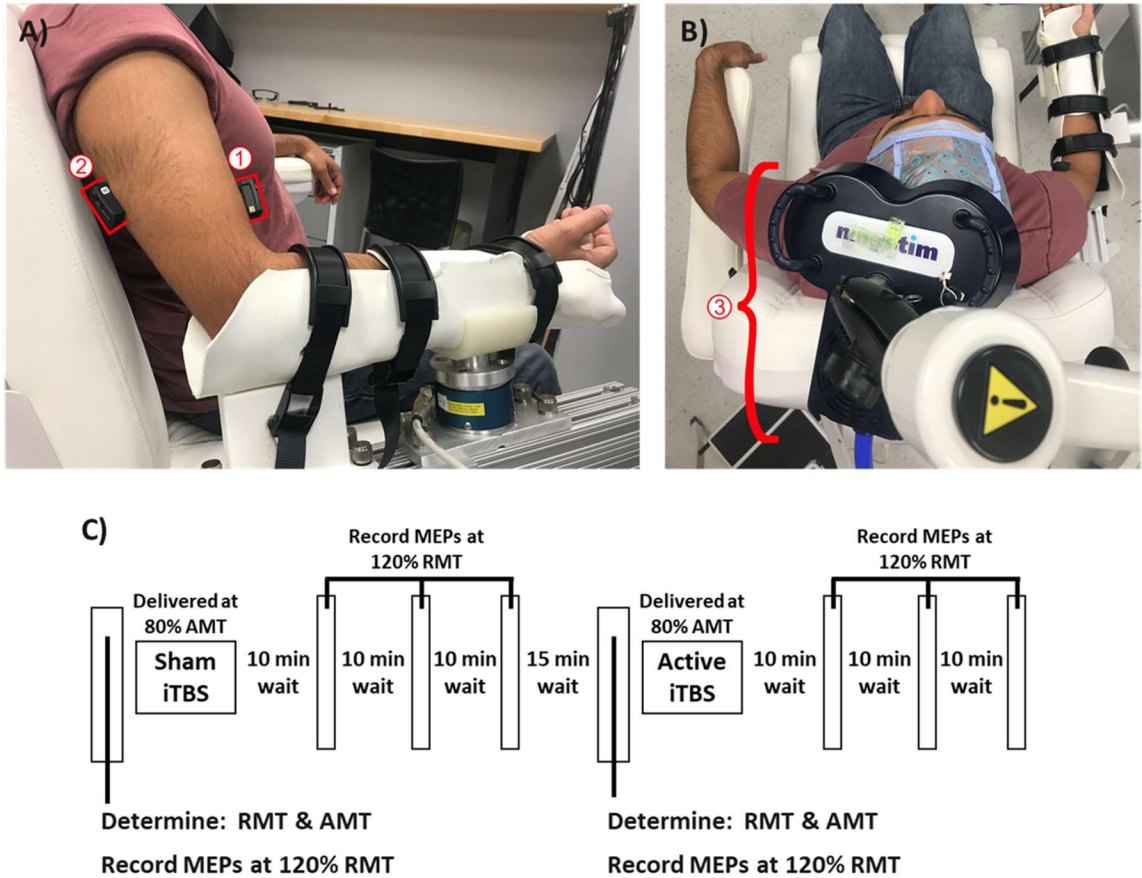


Fig 2.1: Experimental setup and structure of iTBS sessions. (A) Participants were seated with their forearm supported against gravity with EMG sensors placed on their biceps (1) and triceps (2). (B) The TMS coil (3) was held tangentially to the scalp and was placed over the biceps brachii representation of the motor cortex. The coil handle was pointed posteriorly and laterally at a 45 degree angle from the midline to induce a biphasic posterior-anterior then anterior-posterior current within the motor cortex. (C) Before each application of iTBS, biceps brachii RMTs, AMT, and baseline MEPs were recorded. The intensity of all iTBS pulses was 80% of AMT, though the sham coil did not pass this intensity through for sham iTBS. MEPs were recorded at 10-minute intervals following iTBS at an intensity of 120% of RMT.

2.4.2 Overview of Experimental Protocol

Resting and active motor threshold (RMT, AMT), and baseline corticomotor excitability were determined for the biceps brachii. Baseline corticomotor excitability was determined as the average of MEP amplitudes collected in response to single pulse TMS at an intensity of 120% of RMT. iTBS was delivered, after which MEPs were again recorded at intervals 10, 20, and 30 minutes post-iTBS (Fig 1). This was performed for both sham and active iTBS with participants receiving a 15-minute break in between. Sham iTBS was always performed prior to active iTBS.

2.4.3 Electromyography

Electromyography (EMG) data were recorded from the dominant arm of each participant using a Trigno™ Wireless System (Delsys, Natick, MA). Surface EMG electrodes were placed on the long head of the biceps and the lateral head of the triceps (for monitoring purposes). Electrode placement was verified by functional muscle testing. EMG signals were amplified (x1000), bandpass-filtered (20-450 Hz) prior to A/D conversion (Micro 1401 MkII, Cambridge Electron Design, Cambridge, UK), and sampled at 2000 Hz with Spike 2 software (Cambridge Electron Design, Cambridge, UK).

2.4.4 Locating the Cortical Hotspot

Single pulse TMS was delivered to the motor cortex contralateral to the resting arm using a Super Rapid² Plus¹ stimulator (Magstim, Whitland, UK) via a Magstim 70 mm figure-of-eight double air film coil (3910-00). This stimulator was used to deliver both single pulse TMS and iTBS to better simulate a clinical environment in which more than stimulator/coil may be infeasible, and to target and test similar neural networks responsive to biphasic stimuli. The vertex at the intersection of theinion-nasion and inter-aural lines were marked on a cap fitted on the participant's head. The coil was held tangentially on the scalp via a support stand. The coil center was located at a distance about 5 cm from the vertex and the coil was rotated 45 degrees from the midline to induce a biphasic posterior-to-anterior (PA), then anterior-posterior (AP) cortical current across the central sulcus (*FigB*). From that initial coil location, the exact hotspot for the biceps was identified through a cortical mapping procedure to determine the coil location and orientation evoking the largest peak-to-peak amplitude MEP using the lowest stimulation intensity [58], [148]. The hotspot location and coil orientation were marked on the participant's cap.

2.4.5 Motor Thresholds & Corticomotor Excitability

RMT was defined as the lowest stimulus intensity that induced MEPs of $\geq 50 \mu\text{V}$ in at least 5 of 10 consecutive stimuli with the target muscle fully relaxed [149]. AMT was defined as the stimulus intensity that elicited a MEP of $\geq 200 \mu\text{V}$ in at least 5 of 10 consecutive stimuli recorded during sustained isometric contraction of $10 \pm 5\%$ of the participant's maximum effort [149]. Maximum effort was measured by the average EMG in the highest 0.5 s period of a 5 s isometric maximum voluntary contraction (MVC), averaged across 3 trials. Stimulus intensity was determined using an adaptive parameter estimation by sequential testing (PEST) software developed by Borckardt et al., in order to limit stimuli before iTBS [150]. PEST is a triangulating software that has been validated for the purpose of capturing motor thresholds with fewer stimulations than manually counting at set stimulation intensities and making minor adjustments to determine the threshold [150]. Evoked Potential Operant Conditioning Software developed and shared by the National Center of Neuromodulation for Rehabilitation was used to record motor thresholds and display effort levels for feedback to participants.

2.4.6 Intermittent Theta Burst Stimulation Protocol

iTBS was applied using a Magstim Super Rapid² Plus¹ stimulator and a Magstim 70 mm double air film coil (3910-00) following the seminal [54] and now common protocol applied to motor areas [6], [38], [54], [56], [68]. iTBS applied to the biceps cortical hotspot consisted of three pulses presented at 50 Hz, repeated every 200 ms for 2 s at an intensity of 80% of the participant's AMT, repeated every 8 s for 600 pulses [39], [54]. During sham iTBS, a Magstim 70 mm double air film sham coil (3950-00) was used, which looks identical to the active coil and made similar noises without delivering any stimulation. Participants were kept unaware of the type of stimulation they were receiving.

2.4.7 Monophasic Stimulation Assessment

A Magstim BiStim² stimulator and a Magstim D70 Alpha figure-of-eight coil (4150-00) was used to determine RMT and deliver single pulse TMS, therefore better ensuring biceps RMT would remain low enough to record suprathreshold MEPs. The protocol was otherwise unchanged, and a LMEM was used to assess the effect of iTBS on this post hoc cohort (Fig 2.2).

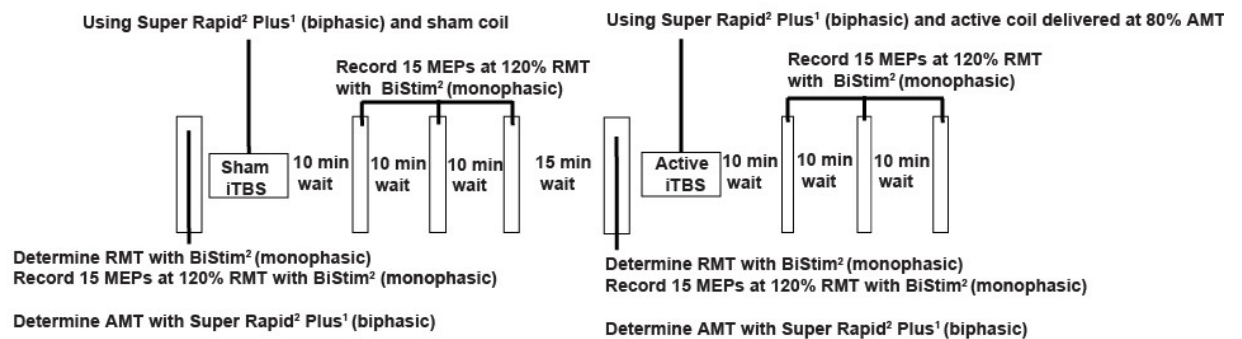


Fig 2.2: iTBS session structure: post hoc study. The iTBS protocol was repeated for one session each in a new cohort of ten nonimpaired individuals, using monophasic PA stimulation for RMT and MEP recordings. All other procedures were kept identical to the primary study.

2.4.8 Data Processing

Peak-to-peak MEP amplitudes in response to single pulse TMS were calculated from the biceps EMG data using purpose-written code in MATLAB (MATLAB v 9.7.0.1190202, MathWorks Inc., USA). The root mean square (RMS) amplitude was calculated over a 50 ms window for the evoked response (starting 12-62 ms after the TMS pulse), and a 50 ms window prior to the TMS pulse (pre-stimulus). Instances where the pre-stimulus RMS amplitude was greater than the evoked response RMS amplitude, or where voluntary activation was detected, were discarded [73]. Raw MEPs from a single iTBS session of a representative participant are shown in Fig 2.3. During the time points in which MEPs were recorded (i.e., 10, 20, 30 min post-iTBS), we delivered no more than 25 stimulations per time point. Across the 30 sessions, an average of 12.3 ± 5 MEPs per time point remained after discarding as described. MEP amplitudes were normalized by, and are presented as a percentage of, the participants'

MVC EMG from the corresponding session. Normalized MEPs (nMEPs) served as our measure of corticomotor excitability, with the average of nMEPs collected prior to iTBS serving as the baseline.

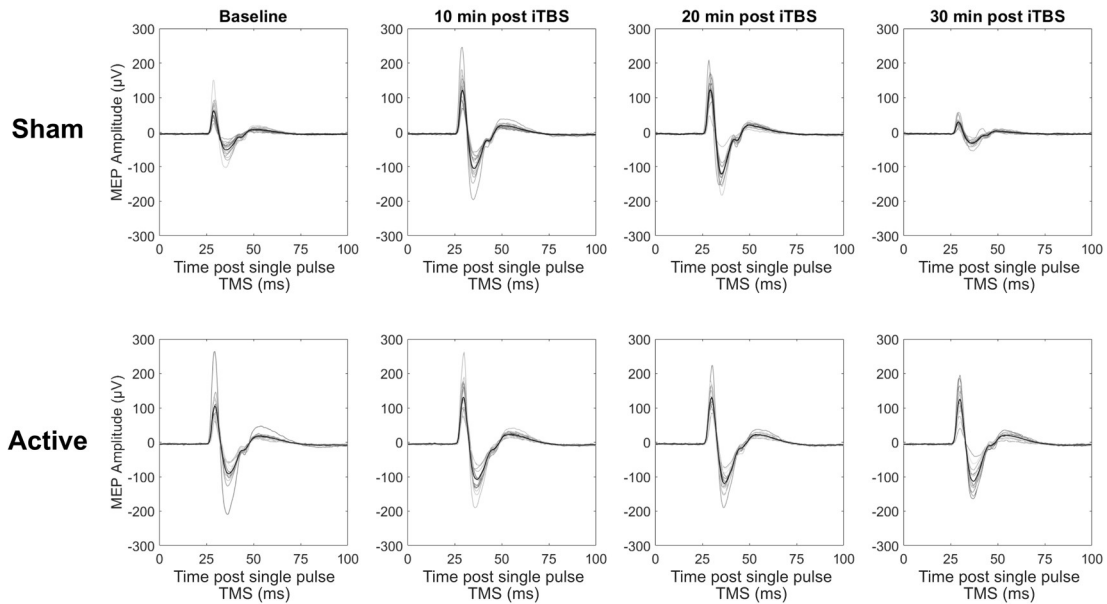


Fig 2.3: Raw Motor Evoked Potentials (MEPs) from a Representative Subject. Biceps MEPs were collected pre-iTBS (baseline), and at 10, 20, and 30 min post-iTBS. The horizontal axis depicts time post single pulse TMS (ms). Grey lines depict individual MEPs (overlaid trials for demonstration) and the black line represents the average MEP.

2.4.9 *A priori Sample size justification*

The standard deviation of the average active-sham differences in nMEPs was empirically solved for, accounting for a within-subject correlation of 0.5 and three observations per person using a marginal standard deviation of 0.09. The true difference between active and sham protocols was assumed to be 5% of the nMEP, with a standard deviation of 9%. Power was then computed based on the sample size ($n = 10$ participants; 30 independent sessions) and standard deviation (0.073). Ten participants would achieve at least 80% power using a two-sided test of the overall mean using a repeated measures model [152].

2.4.10 *Statistical Analyses*

The effects of active and sham iTBS on nMEPs were analyzed with a linear mixed effects model (LMEM) to assess the difference between baseline and post-iTBS nMEPs with purpose-written R code based on the LME4 package [153], [154]. The model had a nested random effect of session within participant to account for potential relationships between nMEPs of the same session or participant, and within each time period post-iTBS. Stimulation type (i.e., active or sham), time (i.e., 10, 20 or 30 minutes post-iTBS), and their interaction were included as fixed effects. A Kenward-Rogers adjustment

was used to adjust for estimated random effect parameters [155]. Friedman’s test was used to evaluate the reproducibility of the baseline nMEP, RMT, and AMT values [156]–[158]. A LMEM evaluating for the effects of session and its interaction with stimulation type on nMEPs was also performed to confirm independence of sessions.

2.4.11 Corticomotor Conductance Potential

The biceps AMT:RMT ratio (i.e., AMT of the biceps divided by RMT of the biceps) was evaluated within a linear mixed effects model to assess a main effect and interactions with time and stimulation type to account for the effects of corticomotor conductance potential on nMEPs. Corticomotor conductance refers to the synaptic conductance along the corticospinal pathway being stimulated during a given session [49], [50]. Motor thresholds reflect this conductance as they are determined by the synaptic permeability between neurons along the corticomotor tract at rest (RMT) and during activation (AMT). Therefore, the biceps AMT:RMT ratio served as a representation of the corticomotor conductance potential across states of activation [58], [59]. We evaluated the effect of corticomotor conductance on nMEPs because nMEPs represent instantaneous corticomotor excitability driven by shifts in sodium channel currents and are affected by gamma aminobutyric acid receptor modulation [49], [50].

2.5 Results

2.5.1 Reproducibility of Baseline Measures and Independence of Sessions

Biceps AMT was reproducible across sessions ($p_{\text{AMT}} = 0.0546$), while biceps RMT and baseline nMEPs were not reproducible across sessions ($p_{\text{RMT}} = 0.006$, $p_{\text{nMEPs}} < 0.001$) (*Table 2.1*). Individual motor thresholds for each session can be found in the supplementary material (*Table S2.1, S2.2*). Session and stimulation type had no interaction that affected nMEP amplitude ($\chi^2 = 0.07$, $p = 0.794$).

Table 2.1: Baseline metrics prior to iTBS presented as mean \pm one standard deviation.

	Session 1	Session 2	Session 3	All Sessions
<i>MVC EMG (mV)</i>	250.56 \pm 112.6	284.69 \pm 123.2	283.48 \pm 130.6	272.91 \pm 119.1
<i>Prior to Sham iTBS</i>				
<i>Biceps RMT^a</i>	89.5 \pm 9	87.6 \pm 13	88.4 \pm 14	88.5 \pm 12
<i>Biceps AMT^b</i>	60.3 \pm 8	58.5 \pm 9	55.1 \pm 9	57.9 \pm 9
<i>Baseline nMEP^c</i>	0.0489 \pm 0.049	0.0447 \pm 0.045	0.0347 \pm 0.037	0.0429 \pm 0.044
<i>Prior to Active iTBS</i>				
<i>Biceps RMT</i>	89.0 \pm 10	90.6 \pm 12	86.1 \pm 14	88.6 \pm 12
<i>Biceps AMT</i>	59.8 \pm 6	60.0 \pm 6	50.0 \pm 9	56.6 \pm 8
<i>Baseline nMEP</i>	0.0594 \pm 0.057	0.0452 \pm 0.049	0.0445 \pm 0.042	0.0499 \pm 0.051

a) RMT: resting motor threshold as percent of maximum stimulator output (% MSO); b) AMT: active motor threshold as % MSO; c) nMEP: normalized MEPs, as percent of maximum voluntary contraction EMG (% MVC)

2.5.2 Change in normalized MEPs post-iTBS

Change in nMEPs from baseline did not differ for the active and sham conditions as indicated by no interaction between the type of stimulation and time post-iTBS ($\chi^2 = 0.32$, $p = 0.570$) in the analysis of the linear mixed effects model (Fig 2.4), as measured by biphasic stimulation.

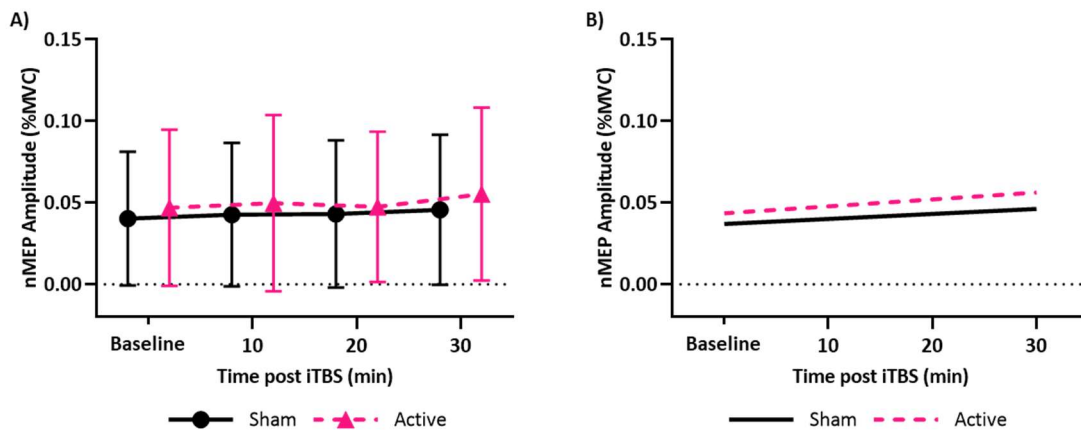


Fig 2.4: No change in corticomotor excitability over time for active and sham iTBS. Average biceps nMEP amplitudes across all sessions are shown for the pre-iTBS and each post-iTBS time point. (A) Empirically collected: mean biceps nMEP amplitudes (group average N = 30 sessions); error bars represent \pm one standard deviation from the mean. (B) Modeled nMEPs from the linear mixed effects model based on these data. The effect of active and sham stimulation was not different as measured with biphasic stimulation induced nMEPs.

In the monophasic stimulation group, however, there was an excitatory effect of iTBS ($\chi^2 = 6.0$, $p = 0.014$) (Fig 2.5). The effect of active iTBS was to increase nMEPs post-iTBS and the increase in nMEPs exceeded the effect of sham iTBS.

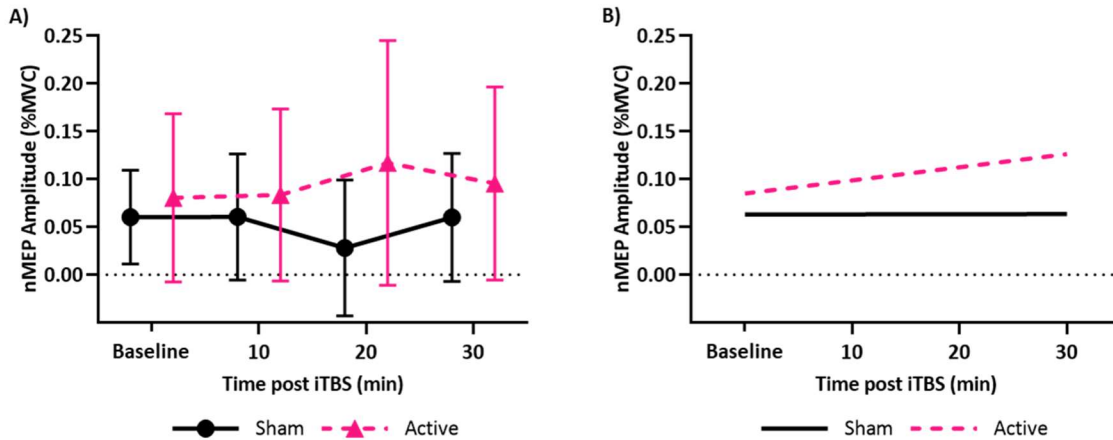


Fig 2.5: Change in corticomotor excitability when MEPs are assessed with monophasic stimulation.

Average biceps nMEP amplitudes across all control study sessions are shown for the pre-iTBS and each post-iTBS time point. (A) Empirically collected: mean biceps nMEP amplitudes (group average $N = 30$); error bars represent \pm one standard deviation from the mean. (B) Modeled nMEPs from the linear mixed effects model based on these data.

2.5.3 Corticomotor Conductance Potential

The biceps AMT:RMT ratio (measure of corticomotor conductance potential) and nMEPs were negatively correlated, and the negative correlation depended on stimulation type. As the AMT:RMT ratio decreased, nMEPs increased, and at a greater rate after sham relative to active iTBS ($\chi^2 = 13.1$, $p < 0.001$). This suggests that a negative relationship between AMT:RMT ratio and nMEP amplitude was depressed by active iTBS stimulation (Fig S2.1).

2.6 Discussion

The primary objective of this study was to determine the effect of iTBS on the corticomotor excitability of the biceps in nonimpaired individuals. A secondary objective was to assess the reproducibility of iTBS effects across three sessions. We hypothesized that biceps corticomotor excitability would be increased following active iTBS. This hypothesis was supported only when MEPs were assessed using monophasic stimulation. Also, iTBS effects assessed across multiple sessions were found to be unrelated for the same participant. Our results suggest that when RMTs are expected to be high when measured with biphasic stimulation ($\geq 84\%$ MSO), monophasic stimulation can capture changes in MEPs induced by iTBS. Further, our results suggest that in nonimpaired individuals, biceps RMTs assessed with biphasic PA-AP stimulation typically exceed 84% MSO, such that suprathreshold

(120%) biphasic stimulation is not possible. Overall, biphasic stimulation appears limited in its ability to capture changes in biceps MEPs in nonimpaired individuals.

Our results support that the stimulus waveform and the resulting induced current in the brain is important in the assessment of iTBS induced changes in MEPs. Although the effect of stimulus waveform has been studied extensively for single pulse TMS targeting motor cortical areas projecting to hand muscles [145], [159]–[161], induced current effects on more proximal muscles of the upper limb, such as the biceps brachii, remains to be fully elucidated. Direct monosynaptic corticospinal projections are more prominent for hand muscles relative to the biceps [68], [162]–[166]. Thus, differences in corticospinal control between proximal and distal muscles may affect the efficacy of TMS waveforms and should be investigated in future studies. TMS studies targeting hand muscles report greater efficacy of single pulse monophasic stimulation that induces a PA current in the brain relative to biphasic stimulation that induces a PA then AP current in the brain by reduced RMT with monophasic PA stimulation [145], [167]. In the nonimpaired biceps, we also found reduced RMT with monophasic PA stimulation relative to RMT with biphasic PA/AP stimulation.

Our findings contribute to the accumulating evidence that factors influencing iTBS induced changes in MEPs include (at least) the motor cortical target (i.e., muscle or muscle group of interest), the current waveform and direction used to deliver iTBS and assess MEPs, and whether iTBS is delivered in a single or repeated format. The lack of an effect of iTBS on corticomotor excitability when MEPs are assessed with biphasic stimulation is not limited to the current study. Tse et al. assessed MEPs with biphasic stimulation after iTBS targeting the FDI in fifteen participants; after a single session of iTBS there was no change in MEPs as assessed by biphasic stimulation at an intensity needed to induce MEPs of about 1 mV amplitude [168]. However, Tse et al. found increased FDI MEPs with biphasic stimulation when iTBS was repeated with a 15 minute interval. Their findings suggest there are conditions in which biphasic stimulation can detect iTBS induced changes in MEPs. Notably, the direction of the biphasic stimulation induced in the brain and the stimulator models differed between the Tse et al. and our current study. In contrast to our results and the findings of Tse et al, a study by Zafar et al. found iTBS targeting a hand muscle (abductor digiti minimi) cortical hotspot increased MEPs relative to baseline regardless of the waveform in which iTBS was delivered and assessed [169]. Zafar et al. tested both waveforms and directions in our study (biphasic PA/AP and monophasic PA), although with a different stimulator and coil model, and their RMT values allowed for suprathreshold stimulation (at 120% RMT) in all study participants. In our study, biceps RMTs were high with biphasic stimulation such that it was not always possible to assess MEPs at 120% RMT.

Continuous theta burst stimulation (cTBS) is another form of theta burst stimulation which can reduce corticomotor excitability possibly through long-term depression of synaptic plasticity [54], [67], [170]. Martin et al. found that cTBS had no effect on biceps corticomotor excitability, despite observing large and long-lasting inhibition in most participants when the FDI was targeted [68]. Our results were similar to the findings of Martin et al., with high variability in the biceps MEPs both before and after

theta burst stimulation. While the mechanisms of iTBS and cTBS differ, the high variability in MEPs could be a reason for the lack of group findings after TBS as assessed with biphasic stimulation [68], [71], [73], [171]. Variability may be due to the preferential activation of different intracortical networks, history of physical activity, timing, age, and genetic differences potentially including brain-derived neurotrophic factor genotype [65], [71], [158], [171]–[173]. While accounting for all of these factors was beyond the scope of this study, within-participant variability was assessed using a session response analysis in our primary cohort via session effects on the linear mixed effects model.

The AMT:RMT ratio, representative of the conductive potential of the corticomotor pathway, may be a predictive measure to evaluate the potential for iTBS to increase biceps corticomotor excitability. We found that biceps corticomotor excitability was negatively correlated with an individual's corticomotor conductance (i.e., biceps AMT:RMT ratio), and this negative correlation was reduced by active iTBS. Active iTBS increased nMEPs at higher corticomotor conductance (i.e., higher AMT:RMT ratios), indicating that there was a nonuniform response to active iTBS. As previously stated, motor thresholds reflect corticomotor conductance as they are determined by the synaptic permeability between neurons along the corticomotor tract at rest (RMT) and during activation (AMT) [6], [49]. In our study, low AMT:RMT ratios represent a corticomotor pathway with less potential for change, while high ratios represent a conductive pathway which would be more likely to benefit from iTBS. Thus, future work should investigate the AMT:RMT ratio as a predictive measure of individuals who may be most responsive to iTBS.

In this study, only the biceps AMT was found to be reproducible across sessions with biphasic stimulation (reproducibility was not assessed with monophasic stimulation due to single sessions), suggesting activation provides a more robust baseline measure relative to measures at rest. This agrees with the interpretation that muscle contraction provides the corticospinal tract with a greater degree of organization; contraction increases the membrane conductance of the neurons, placing neuron membrane potentials in a more primed state to depolarize [58], [174]. When at rest, the corticomotor tract of a muscle is relatively disorganized; the membrane potential of each neuron along the pathway is less uniform and less primed to depolarize relative to an active muscle state. Thus, AMT thresholds are typically lower than RMT for a given stimulus waveform [50], [58], [59], [175]. Our finding of reproducible biceps AMT with biphasic stimulation across sessions is important for the design of studies and rehabilitation where iTBS is to be delivered and assessed (in terms of MEPs) with one biphasic stimulator. Future studies targeting muscles with high motor thresholds in which only biphasic stimulation is feasible or desired should consider assessing MEPs pre and post iTBS as a percentage of AMT, rather than RMT, or other biomarkers of cortical excitability.

This study was designed to use a single stimulator to induce plasticity and assess MEPs in similar populations of neurons and to represent the clinical application of iTBS where only one stimulator may be available. However, a low peak intensity of our biphasic stimulator and coil, imposed by the manufacturer as a safety feature, resulted in many of our participants having RMT values \geq 84% MSO.

Thus, in 42 out of 60 instances we could not assess biceps corticomotor excitability by recording MEPs at 120% RMT. This issue was addressed by using a separate monophasic stimulator to evaluate RMT and MEPs in an additional subject cohort as RMT of the biceps when determined by a monophasic stimulator are typically 50-60 %MSO [58]. Indeed, in our additional cohort, the average biceps RMTs prior to sham and active iTBS were lower with monophasic relative to biphasic stimulation and there was an effect of active iTBS on MEPs when MEPs were assessed with monophasic stimulation. A potential limitation is the use of MEPs to capture changes due to iTBS. The multiple neural circuits contributing to MEPs make interpretation of changes in normalized MEP amplitude difficult [176]. We analyzed MEPs because MEPs remain a conventional approach to measuring corticomotor excitability at the time of stimulation. Another potential limitation is that sham stimulation was always delivered prior to active stimulation. While this was done to prevent any response to active stimulation biasing the response to sham, we cannot exclude the possibility of an order effect. Our sample size may be considered small, however, it was established through statistical consultation. Lastly, with the effects of iTBS being first evaluated 10 minutes after stimulation, it is possible that more immediate effects were not captured. However, the post-iTBS time points replicated previous work in other muscles [38], [56], [177] and were focused on the time frame most relevant and realistic to pairing with motor therapy, which would likely begin a few minutes after iTBS priming.

2.7 Conclusions

There was an increase in biceps corticomotor excitability when MEPs were assessed with monophasic stimulation. When RMTs are expected to be high when measured with biphasic stimulation ($\geq 84\%$ MSO) for the muscle of interest, monophasic stimulation may capture changes in MEPs induced by iTBS. In our cohort, biceps RMTs assessed with biphasic PA-AP stimulation typically exceeded 84% MSO, such that suprathreshold biphasic stimulation was not possible. Future studies targeting muscles with high motor thresholds in which only biphasic stimulation is feasible or desired should consider assessing MEPs pre and post iTBS as a percentage of AMT, rather than RMT, or other biomarkers of cortical excitability. Our results also supported the independence of iTBS response between sessions for the same participant and proposed a potential predictive parameter in the corticomotor conductance potential.

2.8 Supplemental

Table S2.1: Motor thresholds by session in primary cohort prior to iTBS presented as percent maximum stimulator output (%MSO).

<i>Participant</i>	Session 1				Session 2				Session 3			
	Biceps RMT ^a Prior to Sham iTBS	Biceps AMT ^b Prior to Sham iTBS	Biceps RMT Prior to Active iTBS	Biceps AMT Prior to Active iTBS	Biceps RMT ^a Prior to Sham iTBS	Biceps AMT ^b Prior to Sham iTBS	Biceps RMT Prior to Active iTBS	Biceps AMT Prior to Active iTBS	Biceps RMT ^a Prior to Sham iTBS	Biceps AMT ^b Prior to Sham iTBS	Biceps RMT Prior to Active iTBS	Biceps AMT Prior to Active iTBS
01	90	52	100	61	100	48	100	56	100	60	100	51
02	77	56	83	56	85	50	88	60	95	65	88	54
03	100	68	87	60	61	53	67	56	61	58	59	60
04	100	71	100	69	90	67	100	74	96	68	98	59
05	84	56	85	64	86	63	95	54	85	56	74	44
06	85	53	83	49	97	60	95	67	77	42	88	42
07	95	68	100	59	100	46	100	55	100	45	100	34
08	88	62	74	52	83	66	85	61	100	54	83	58
09	100	67	100	68	100	72	100	57	100	60	100	53
10	76	50	78	60	74	60	76	60	70	43	71	45
<i>Mean ± SD</i>	89.5 ± 9	60.3 ± 8	89.0 ± 10	59.8 ± 6	87.6 ± 13	58.5 ± 9	90.6 ± 12	60.0 ± 6	88.4 ± 14	55.1 ± 9	86.1 ± 14	50.0 ± 9

a) RMT: resting motor threshold as percent of maximum stimulator output (%MSO) measured with biphasic PA/AP stimulation; b) AMT: active motor threshold as %MSO measured with biphasic PA/AP stimulation.

Table S2.2: Motor thresholds and maximum voluntary contraction (MVC) in post hoc cohort prior to iTBS presented as mean \pm one standard deviation.

<i>Participant</i>	Age	MVC EMG RMS (mV)	Prior to Sham iTBS			Prior to Active iTBS		
			Biceps RMT ^a	Biceps AMT ^b	Average Baseline nMEPs ^c	Biceps RMT	Biceps AMT	Average Baseline nMEPs
01	21	411.0	57	68	0.066	61	68	0.059
02	24	118.0	62	60	0.067	67	58	0.112
03	19	183.2	100	70	0.011	100	74	0.011
04	20	144.6	49	67	0.024	65	74	0.032
05	23	185.2	86	72	0.041	87	73	0.025
06	19	453.2	61	70	0.136	85	48	0.102
07	32	184.1	100	72	0.023	100	73	0.012
08	26	128.9	69	57	0.078	78	52	0.12
09	29	256.0	44	44	0.093	47	46	0.292
10	27	112.2	100	62	0.065	100	65	0.055
<i>Mean \pm SD</i>	23.5 \pm 5	217.63 \pm 121.1	72.8 \pm 22	64.2 \pm 9	0.0602 \pm 0.049	79.0 \pm 19	63.1 \pm 11	0.0820 \pm 0.084

a) RMT: resting motor threshold as percent of maximum stimulator output (% MSO) measured with monophasic stimulation inducing an AP current in the brain; b) AMT: active motor threshold as % MSO measured with biphasic PA/AP stimulation; c) nMEP: normalized motor evoked potential (%MVC) measured with monophasic AP stimulation, presented as mean \pm standard deviation

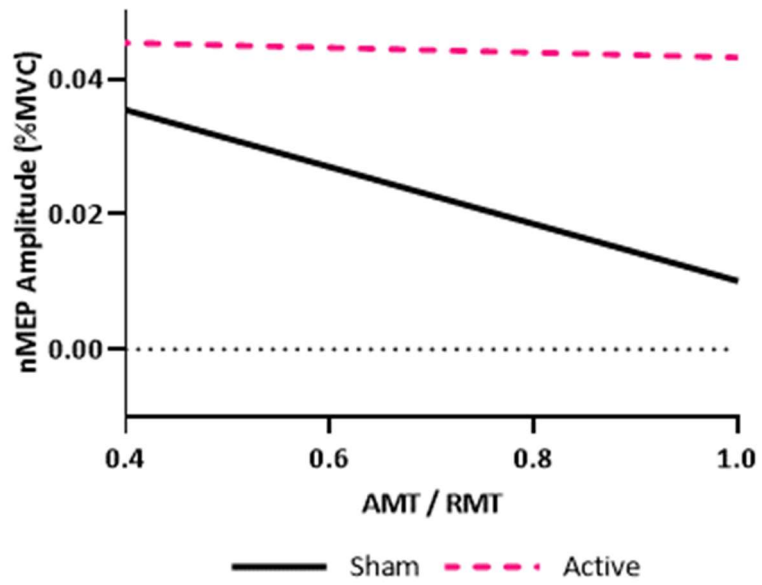


Fig. S2.1: Relationship between AMT:RMT ratio and nMEP amplitude

nMEP amplitude and the AMT:RMT ratio were negatively correlated; the magnitude of this correlation was reduced by active iTBS. The nMEPs were modeled across AMT:RMT ratios ranging from 0 to 1 based on recorded threshold values.

3 Intermittent theta burst stimulation modulates biceps brachii corticomotor excitability in individuals with tetraplegia

3.1 Authors and Submission Details

N. Mittal, B. Majdic and C. Peterson, "Intermittent Theta Burst Stimulation Modulates Biceps Brachii Corticomotor Excitability in Individuals with Tetraplegia", Submitted to *The Journal of NeuroEngineering and Rehabilitation*, 9-20-2021. Available (Preliminary Preprint): 10.21203/rs.3.rs-907901/v1, Submission ID: JNER-D-21-00301.

IRB Approval: VCU IRB HM20010643

Clinical Trials Registration: clinicaltrials.gov NCT03277521

Data Repository: Open Science Framework –

https://osf.io/za78p/?view_only=1f23b70066d64faba087b2b4c0784baa

3.2 Abstract

Objectives: Intermittent theta burst stimulation (iTBS) is a form of repetitive transcranial magnetic stimulation (TMS) that can increase corticomotor excitability of hand muscles in individuals with spinal cord injury (SCI). The objective of this study was to determine the effect of iTBS on the corticomotor excitability of the biceps brachii in individuals with tetraplegia.

Methods: Ten individuals with low cervical SCI (C5-C8) and ten nonimpaired individuals completed three independent sessions. Motor evoked potentials (MEPs) served as our measure of corticomotor excitability and were collected before and after iTBS. MEPs were normalized by the electromyography corresponding to maximum voluntary contraction and analyzed using linear mixed effects models to determine the effect of iTBS (active or sham) on normalized MEPs (nMEPs). iTBS effects were compared to a ratio of active and resting motor thresholds as a measurement of corticomotor conductance potential.

Results: Relative to sham, active iTBS increased nMEPs over time ($p < 0.001$) in individuals with SCI, but not nonimpaired individuals ($p = 0.915$). The amplitude of nMEPs were correlated with the biceps corticomotor conductance potential ($p < 0.001$), with nMEPs decreasing as the ratio increased at different rates after sham or active iTBS.

Conclusions: Preliminary results suggest that iTBS increases biceps corticomotor excitability in individuals with tetraplegia with effects that may be predicted by corticomotor conductance potential.

3.3 Introduction

Spinal cord injury (SCI) often results in deficits in voluntary control of muscles due to injury induced necrosis and partial or complete loss of conduction in neural pathways. The most common neurological classification of SCI is tetraplegia, which results from injury to the cervical spinal cord and is characterized by deficits in upper and lower limb function [2], [178]. Upper limb function is the most important resource for individuals with tetraplegia and is rated to be the most desired ability to regain after cervical SCI before bowel, bladder, sexual function, or walking ability [3]. Thus, improving upper limb function is a crucial part of rehabilitation to enhance an individual's independence and quality of life. One approach to improve voluntary control of upper limb muscles is to strengthen the connection of spared corticospinal tracts through repetitive transcranial magnetic stimulation (rTMS) [179]–[181]. High frequency (i.e., > 5 Hz) rTMS can increase corticospinal and primary motor cortex (M1) excitability [173]. Several studies have applied rTMS over the arm and leg motor representations in the M1 in nonimpaired individuals and in patients with motor impairments to increase corticospinal and M1 excitability, voluntary motor control, and motor learning processes [38], [69], [182], [183]. Although the effectiveness using different forms of rTMS in nonimpaired individuals and patients with motor impairments are variable [38], [56], [57], [180], rTMS may represent a useful technique to improve upper limb function after SCI, particularly when paired with other therapies.

A greater understanding of the utility of rTMS to improve upper limb function after SCI is needed. High-frequency rTMS protocols have been tested in individuals with tetraplegia to improve upper limb motor and sensory function in five studies to date, all of which targeted stimulation to hand representations in the M1 [5], [69], [128], [179], [184]. Five sessions of rTMS alone (i.e., without adjunct therapy) improved hand motor and sensory function in one study [5]. However, in a larger study involving five sessions of rTMS, results showed only modest improvement in hand motor and sensory function, which was not statistically different from sham effects, and there was no change in clinical neurological assessment [179]. In another study, addition of rTMS to repetitive task practice training over three sessions demonstrated a greater effect size for improvement in grasp strength and hand function relative to repetitive task practice alone [184]. Only two studies have evaluated a more specific pattern of rTMS known as intermittent theta-burst stimulation (iTBS) targeting the upper limb in individuals with tetraplegia [69]; these studies demonstrated safety and feasibility [128], and modifiability of corticomotor excitability [69]. Commonly, iTBS involves 2 seconds of TBS trains repeated every 10 seconds for a total of 20 cycles (600 pulses) delivered over a 190 second period [39], [54], [185]. iTBS has gained much interest, arguably due to its efficacy, short stimulation period, and effects lasting up to 60 minutes post-stimulation [186], making iTBS well suited as a neural priming adjunct to motor training exercises.

Further research is needed to investigate the potential for iTBS to increase the excitability of the corticospinal motor system (hereafter referred to as corticomotor excitability) in individuals with tetraplegia. Effects of iTBS have been demonstrated primarily in nonimpaired humans with stimulation

applied to hand representations in the M1 and motor-evoked potentials (MEPs) recorded from the first dorsal interosseous (FDI) [39], [185], [186]. A meta-analysis of studies in nonimpaired participants found that iTBS applied for 190 s significantly increases corticomotor excitability, as measured by MEPs, lasting up to 60 min with a mean maximum potentiation of $35.54 \pm 3.32\%$ [186]. The mechanisms of these effects are believed to be due to changes in neural circuits in the cortex, perhaps involving long-term potentiation of cortical synapses [187], [188]. Evidence from SCI studies in rats suggests that iTBS is able to facilitate MEPs and improve forelimb motor function after injury [129], [189], consistent with the mechanistic understanding of iTBS [187], [188]. However, Fassett et al. [190] investigated the effects of iTBS on corticomotor excitability of the flexor carpi radialis in humans with cervical SCI and found corticomotor excitability (i.e., MEPs) to be reduced in the majority of instances after a single session of active M1 stimulation. While the results of Fassett et al. contradict previous findings in nonimpaired subjects and animal models of SCI, the results indicate that iTBS is able to modify corticomotor excitability in humans with tetraplegia, which warrants further investigation.

Depending on the specific injury and needs of an individual with tetraplegia, the biceps brachii may be responsive to iTBS and a functionally relevant target for rehabilitation. The biceps may be particularly responsive to iTBS in individuals with tetraplegia because: the biceps typically remains with some spared motor pathways and function after injury at or below C6 as the biceps is primarily innervated at the C5 and C6 levels [191], and biceps motoneurons receive more corticospinal monosynaptic facilitation relative to its antagonist [192], [193]. Additionally, the biceps is relevant for upper limb rehabilitation in tetraplegia as the biceps can be transferred to restore elbow extension for some individuals with tetraplegia [64], [194]. After tendon transfer surgery, an individual with tetraplegia undergoes rehabilitation to promote motor re-education of the transferred biceps to extend the elbow. In our previous work, we found a positive relationship between the corticomotor excitability of the transferred biceps and elbow extension strength, suggesting that increased biceps corticomotor excitability may improve the outcomes of tendon transfer surgery [52].

We present a sham-controlled pilot study to provide the first characterization of iTBS-induced effects targeting the biceps brachii in individuals with tetraplegia. The purpose of this study was to determine the effect of iTBS on corticomotor excitability of the biceps in individuals with tetraplegia and nonimpaired subjects. The nonimpaired control group is included to provide a context for the potential effects of iTBS in individuals with SCI. We hypothesized that biceps corticomotor excitability, as measured by MEPs, would be increased relative to baseline following active iTBS relative to sham iTBS in both subject groups. This hypothesis was based on the expectation that iTBS promotes long-term potentiation within cortical neurons. Since the effects of iTBS can be variable across sessions [38], [56], [68], we tested participants across three sessions to evaluate the reproducibility of iTBS aftereffects.

3.4 Methods

3.4.1 Participants

Ten individuals (8 men, 2 women) with cervical SCI aged between 23 and 53 years (mean age = 35.7 years, standard deviation = 13 years) completed this pilot study. SCI participant characteristics are provided in Table 3.1. Inclusion criteria required SCI participants to be between the ages of 18 and 65 years old and have an injury to the lower cervical spinal cord (C5-C8) at least one year prior to the date of participation. Exclusion criteria included presence of concurrent severe medical illness, including unhealed decubiti, use of baclofen pumps, existing infection, cardiovascular disease, significant osteoporosis, history of pulmonary complications, or any contraindication to TMS. Ten nonimpaired individuals (5 men, 5 women), aged between 18 and 38 years (mean age = 25.3 years, standard deviation = 5.6 years) also participated. Nonimpaired individuals with active motor thresholds (AMT) greater than 71% of maximum stimulator output (MSO) during the first assessment were excluded. This criterion was needed to ensure iTBS could be delivered at 80% of AMT by the stimulator, as the iTBS stimulation intensity was limited to a maximum of 57% MSO as a manufacturer safety feature. All participants were screened to ensure safety of the TMS protocols and provided informed consent. The protocol was approved by the Institutional Review Board of Virginia Commonwealth University.

Table 3.1: Demographic and injury information from all participants with spinal cord injury are shown. M, male; F, female; C, cervical level injury (i.e. C5); ISNCSCI, International Standards for Neurological Classification of Spinal Cord Injury (A = no motor or sensory function is preserved in the sacral segments; B = sensory function is preserved below the level of injury, but no motor function; C = motor function is preserved below the level of injury, more than half the muscles have a grade < 3; D = motor function is preserved below the level of injury, at least half the muscles have a grade \geq 3; E = motor and sensory function are normal).

ID	Age	Gender	Injury level	Years post-injury	ISNCSCI score
1	23	M	C5-C6	7	C
2	26	M	C7	2	B
3	25	M	C5	2	A
4	42	M	C6	5	D
5	29	M	C5	4	A
6	52	F	C6	15	A
7	53	M	C6	17	A
8	32	M	C5-C6	9	B
9	30	M	C5-C6	4	A
10	52	F	C5-C8	10	D

Each participant completed three independent sessions of the iTBS protocol, yielding 30 independent sessions in the nonimpaired group, and 30 independent sessions in the SCI group. This number of sessions was established through statistical consultation and was similar to a previous study that investigated continuous TBS [68]. Repeated sessions were conducted to investigate independence of sessions and intrasubject variability, similar to previous work [38], [56]. Each session was separated by a minimum of three days to prevent the potential for carry over effects from one session to another [57]. To control for variability that may result from diurnal effects, sessions were scheduled for early afternoons. In each session, participants were seated in a chair with their dominant arm at rest, the elbow in 90° flexion, and the forearm supinated (Fig 3.1). During portions of the protocol involving TMS, participants wore a neck brace to minimize head movements.

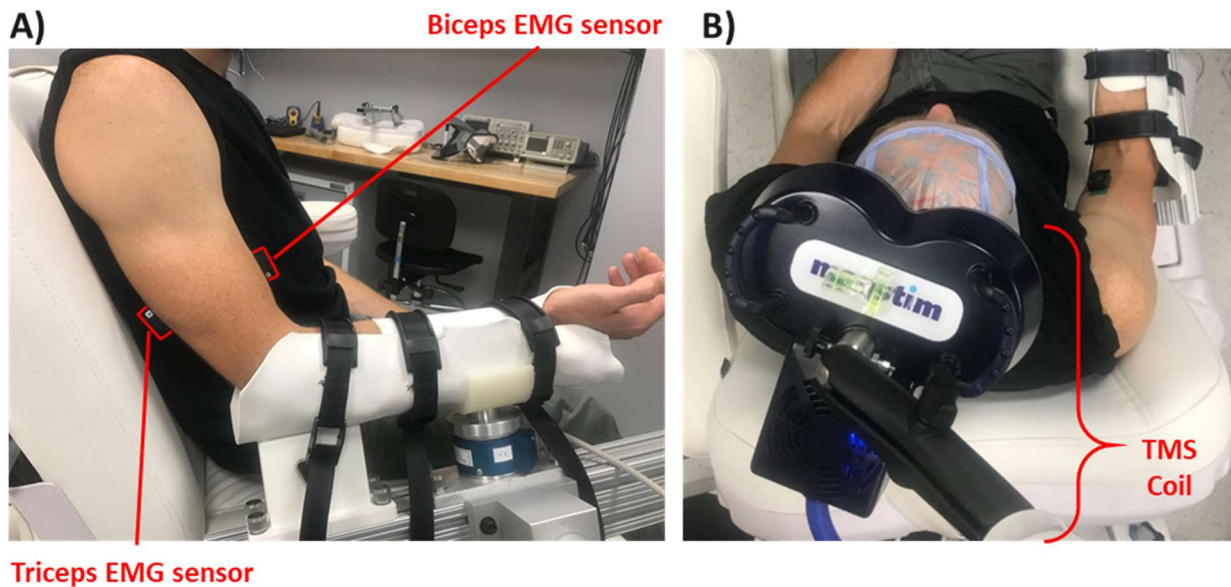


Fig 3.1: Setup for iTBS sessions. (A) Participants' forearms were supported in the horizontal plane with EMG sensors on the biceps and triceps; (B) The TMS coil was placed tangentially over the scalp above the biceps representation of the motor cortex, oriented to induce a biphasic posterior-anterior then anterior-posterior current within in the motor cortex.

3.4.2 Experimental Protocol

At the beginning of each session, the biceps resting motor threshold (RMT), active motor threshold (AMT), and baseline corticomotor excitability (MEPs prior to iTBS) were recorded (Fig. 2). iTBS was then delivered, after which MEPs were recorded at intervals 10, 20, and 30 minutes post-iTBS (Fig 3.2). This process was performed for both sham and active iTBS with participants receiving a 15-minute break in between. Sham iTBS was always performed prior to active iTBS to prevent the possibility of effects from active iTBS lingering throughout the sham portion of the study. Participants were blinded to the stimulation type.

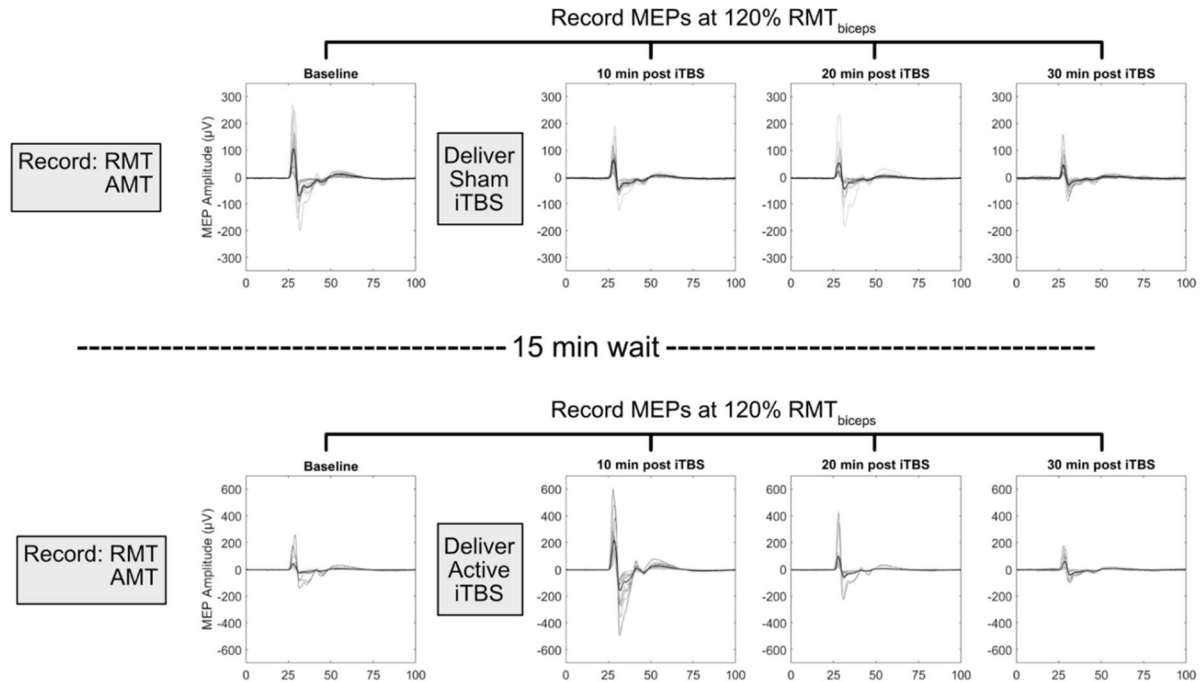


Fig 3.2: Experimental design of each session. Before each application of iTBS, single pulse TMS was used to determine RMT, AMT, and collect baseline MEPs for the biceps. The intensity of iTBS was set to 80% of AMT. Single pulse TMS was used to record MEPs at 10-minute intervals following iTBS, at an intensity of 120% RMT. Data shown represent the processed and collected raw MEPs of a single session from a representative participant. Grey lines represent individual MEPs and the black line represents the average MEP. Horizontal axis depicts time post single pulse TMS (ms).

3.4.3 Electromyography

Electromyography (EMG) data were recorded from the long head of the biceps and lateral head of the triceps (for monitoring) of the dominant arm of each participant using a Trigno™ Wireless System (Delsys, Natick, MA). Surface EMG electrode placement was verified by functional muscle testing. EMG signals were amplified ($\times 1000$), bandpass-filtered (20-450 Hz) prior to A/D conversion (Micro 1401 MkII, Cambridge Electron Design, Cambridge, UK), and sampled at 2000 Hz with Spike 2 software (Cambridge Electron Design, Cambridge, UK).

3.4.4 Single Pulse Transcranial Magnetic Stimulation

Single pulse TMS of the motor cortex was applied opposite to the resting arm using a Super Rapid² Plus¹ stimulator (Magstim, Whitland, UK) via a 70 mm figure-of-eight coil (P/N 3910-00). To better simulate a clinical environment where likely only one stimulation device would be available, this stimulator was used to deliver single pulse TMS and repetitive iTBS. The vertex at the intersection of the inion-nasion and inter-aural lines were marked on a fitted cap and used to identify the starting point for the coil center, 5 cm from the vertex and rotated 45 degrees from the midline. The coil was held

tangentially on the scalp via a support stand. The exact hotspot for the biceps was identified (and marked on the participants cap) as the coil location and orientation evoking the largest peak-to-peak amplitude MEP using the lowest stimulation intensity from a biphasic current oriented posterior to anterior then anterior to posterior across the central sulcus.

3.4.5 Motor Thresholds & Corticomotor Excitability

Resting and active motor thresholds were determined as the lowest stimulus intensity that induced MEPs in at least 5 of 10 consecutive stimuli, either at rest (RMT) and of $\geq 50 \mu\text{V}$ with the biceps fully relaxed, or with muscle activity (AMT) and of $\geq 200 \mu\text{V}$ [149]. Muscle activity was generated by sustained isometric contraction of $10 \pm 5\%$ of the participant's maximum effort [58]. Maximum effort was measured by the average EMG in the highest 0.5 s period of a 5 s isometric maximum voluntary contraction (MVC), averaged across 3 trials. Thresholds were found via validated adaptive parameter estimation by sequential testing (PEST) software [150]. Evoked Potential Operant Conditioning Software developed and shared by the National Center of Neuromodulation for Rehabilitation was used to record motor thresholds and display effort levels for participants.

3.4.6 Intermittent Theta Burst Stimulation Protocol

iTBS was applied using a Magstim Super Rapid² Plus¹ stimulator and Magstim 70 mm figure-of-eight double air film coil (3910-00) following a protocol [54] commonly applied to motor areas [6], [38], [56], [68]. iTBS comprised three pulses at 50 Hz, repeated every 200 ms for 2 s at an intensity of 80% of the participant's AMT [39], [54]. Two second bursts were repeated every 8 s for a total of 600 pulses [54]. During sham iTBS, a Magstim 70 mm figure-of-eight double air film sham coil (3950-00) was used which looked and sounded identical to the active coil without delivering stimulation. Participants were blinded to the type of stimulation they were receiving.

3.4.7 Data Processing

For each session, peak-to-peak MEP amplitudes in response to single pulse TMS were extracted from the biceps EMG data using purpose-written code (MATLAB v 9.7.0.1190202). The root mean square (RMS) amplitude was calculated over a 50 ms window for the evoked response (starting 12-62 ms after the TMS pulse), and a 50 ms window prior to the TMS pulse (pre-stimulus). Instances where the pre-stimulus RMS amplitude was greater than the evoked response RMS amplitude, or where voluntary activation was detected, were discarded [73]. MEP amplitudes were then normalized by, and are presented as a percentage of, the recorded EMG MVC. Normalized MEPs (nMEPs) served as our measure of corticomotor excitability, with the average of nMEPs collected prior to iTBS serving as the baseline.

3.4.8 *Statistical Analyses*

The effects of iTBS on nMEPs were analyzed with linear mixed effects models (LMEM) using purpose-written R code based on the LME4 package [153], [154]. The model had a nested random effect of session within participant to account for potential relationships between nMEPs of the same session or participant, and within each time period post-iTBS. Coil (i.e., active or sham), time (i.e., 10, 20 or 30 minutes post-iTBS), and their interaction were included as fixed effects to investigate the difference in nMEPs between baseline and post-iTBS, and the differences in post-iTBS nMEPs after active or sham stimulation. A Kenward-Rogers adjustment was used to adjust for estimated random effect parameters [155]. To investigate the effect of repeated sessions and confirm the independence of sessions of the same participant, we repeated our LMEM with sessions as a fixed effect. To establish any differences between the populations' baseline excitability, baseline metrics (RMT, AMT, and baseline nMEPs) were also compared between the nonimpaired and SCI groups using a two-tailed Mann-Whitney test.

3.4.9 *Corticomotor Conductance Potential*

The biceps AMT/RMT ratio (i.e., AMT of the biceps divided by RMT of the biceps) was evaluated within a linear mixed effects model to assess a main effect, and interactions with time and type of stimulation, to account for the effects of corticomotor conductance potential on nMEPs. By corticomotor conductance potential, we refer to the synaptic conductance gradient between different states of activation along the corticospinal pathway being stimulated during a given session [49], [50]. Motor thresholds reflect this conductance as they are determined by the synaptic permeability between neurons along the corticomotor tract at rest (RMT) and during activation (AMT) [58], [59]. Therefore, we defined the biceps AMT/RMT ratio as a representation of the corticomotor conductance potential across states of activation. We evaluated the effect of corticomotor conductance on nMEPs because nMEPs represent instantaneous corticomotor excitability driven by shifts in sodium channel currents and are affected by gamma aminobutyric acid receptor modulation [49], [50].

3.4.10 *Post hoc Analysis*

In most sessions (25 out of 30), due to RMT values being greater than 84% MSO in at least one RMT measurement, we were unable to record MEPs at stimulus intensities of 120% of RMT, introducing possible under-stimulation increased MEP variability [6]. Thus, we evaluated if the nMEP amplitudes were dependent on RMT using the aforementioned LMEM with RMT as a fixed effect.

3.5 **Results**

3.5.1 *Availability of Data and Materials*

The dataset supporting the conclusions of this article is available in the Open Science Framework [https://osf.io/za78p/?view_only=1f23b70066d64faba087b2b4c0784baa].

3.5.2 *Change in Normalized MEPs post-iTBS*

In individuals with SCI, there was an effect of active iTBS relative to sham stimulation over time ($p < 0.001$, $\chi^2 = 18.6$) with active iTBS causing an increase in nMEPs from baseline. For each time point, the average nMEP amplitude is presented in Fig 3.3A. Modeled nMEPs resulting from the LMEM are presented in Fig 3.3B for both the active and sham conditions. In nonimpaired individuals, change in nMEPs from baseline did not differ for the active and sham conditions as indicated by no interaction between the type of stimulation and time post-iTBS ($p = 0.915$) in the analysis of the LMEM (Fig 3.3C). When comparing the SCI group to the nonimpaired group, there was an interaction between group and stimulation type within the LMEM ($p = 0.012$, $\chi^2 = 6.4$) (Fig 3.3D).

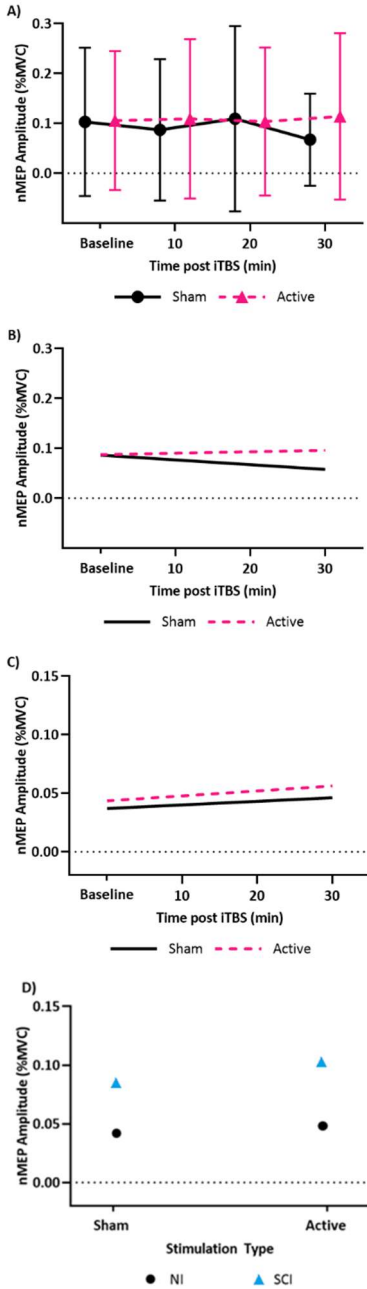


Fig 3.3: Time differentiated normalized motor evoked potential amplitudes (nMEP) from (A) recorded data and (B, C, D) linear mixed effects model (LMEM). (A) Mean nMEP amplitudes for each time point across all 30 sessions for active and sham iTBS are presented for participants with SCI. Error bars represent one standard deviation from the mean. (B) In the SCI group, the LMEM shows a significant difference over time in nMEP amplitudes depending on the type of iTBS, active or sham. (C) In the nonimpaired group, the LMEM does not show an effect of stimulation type on nMEP amplitude. (D) There was a difference in the effect of iTBS between groups, based on the LMEM, consistent with the excitation seen in the SCI group and not seen in the nonimpaired group. Each point represents all nMEPs across all sessions, for the given group and stimulation type.

nMEPs were independent of session, suggesting no carryover effects and no relationship between sessions within a participant ($p = 0.074$, $\chi^2 = 3.2$).

With regards to group baseline metrics, there was a difference in baseline nMEPs ($p < 0.001$) between the nonimpaired and SCI groups. There was no difference between the two groups with respect to MVC EMG ($p = 0.90$), RMT ($p = 0.081$), AMT ($p = 0.50$), or motor threshold ratio ($p = 0.89$). Group average baseline metrics are provided in Table 3.2. Individual participant motor thresholds and MVC values can be found in the Supplementary Material (Tables S3.1, S3.2, and S3.3).

Table 3.2: Baseline biceps metrics for the nonimpaired and SCI groups. Data presented by means within the group across all sessions and the standard deviation (mean \pm std). (*) Represents significant difference ($p < 0.05$) between groups. The AMT/RMT ratio represents the corticomotor conductance potential.

	Nonimpaired	Spinal Cord Injury
MVC EMG (mV)	274 \pm 12	250 \pm 18
RMT (%MSO)	88.5 \pm 11	92.1 \pm 11
AMT (%MSO)	57.3 \pm 8	66.4 \pm 21
AMT/RMT Ratio	0.67 \pm 0.1	0.69 \pm 0.2
Baseline nMEP *	0.0403 \pm 0.041	0.1031 \pm 0.148

3.5.3 Corticomotor Conductance Potential

In the SCI group, there was a significant interaction between the biceps AMT/RMT ratio (i.e., corticomotor conductance potential) and stimulation type. While both sham and active iTBS showed a negative relationship with corticomotor conductance potential, nMEPs associated with sham stimulation had lower nMEP amplitudes. Sham associated nMEPs also changed at a lower rate as the corticomotor conductance potential increased ($p < 0.001$, $\chi^2 = 15.2$). Consequently, as the corticomotor conductance potential approached zero, nMEP amplitudes were greater indicating a higher degree of excitation relative to sham (Fig. S3.1A). There was an interaction between the corticomotor conductance potential and group ($p < 0.001$, $\chi^2 = 13.3$) suggesting that while this parameter has predictive potential across both groups, the exact correlation is group specific (Fig. S3.1B). There was no difference in corticomotor conductance potential between groups ($p = 0.89$) (Table 3.2).

3.5.4 Post hoc Results

There was a relationship in the SCI group between RMT and nMEP ($p < 0.001$, $\chi^2 = 7.7$). There was no relationship between nMEPs and RMT in the nonimpaired group ($p = 0.47$, $\chi^2 = 0.5$).

3.6 Discussion

The primary objective of this study was to determine the effect of iTBS on the corticomotor excitability of the biceps as measured by MEPs in response to TMS in individuals with tetraplegia and nonimpaired individuals. A secondary objective was to assess the reproducibility of iTBS effects across three sessions. We hypothesized that in both subject groups, biceps corticomotor excitability (i.e., normalized MEPs) would be increased following active iTBS relative to baseline, and biceps corticomotor excitability would be unchanged following sham iTBS relative to baseline. This hypothesis was supported in the SCI group; there was an increase in nMEP amplitude after active iTBS relative to sham. This hypothesis was not supported in the nonimpaired group; there was no change in biceps nMEPs after either active or sham iTBS. These findings suggest that iTBS has more homogeneous facilitatory effects in the biceps in individuals with incomplete tetraplegia than nonimpaired individuals, likely due to changes in corticomotor control after motor function loss.

The results from this study reinforce that corticomotor excitability is modifiable with iTBS in individuals with tetraplegia. This supports the modifiability findings from Fassett et al. in which iTBS was targeted to the flexor carpi radialis in individuals with tetraplegia [69]. While their results showed MEP reduction following iTBS, this could be due to differences in the targeted cortical motor region, or other factors influencing responses to iTBS. Previous studies have indicated that changes induced by iTBS in nonimpaired individuals depend on the cortical region targeted due to inherent differences in corticospinal control among muscles [68]. The findings from this study suggest that this may also be true for individuals with SCI, which could be further affected by the degree of damage to a muscle's corticospinal tracts after injury, which is non-uniform after SCI [195].

Our results suggest that individuals with SCI exhibit a more homogeneous facilitatory response to iTBS targeting the biceps than nonimpaired individuals. In contrast to the nonimpaired group, the more uniform response of the SCI group may be the result of neuroplastic changes that occur post injury. For instance, the post-SCI system exhibits reduced intracortical inhibition and therefore greater neuroplastic response from disinhibition of gamma-Aminobutyric acid (GABA) transmitting interneurons to compensate for the loss of corticospinal axons [196]. Additionally, corticomotor plasticity can make alternate use of neural circuits that no longer have a functional muscular target available, as cortical map representation of nonparalyzed or less paralyzed muscle increases at the expense of paralyzed muscle [166]. This process can be facilitated by electrical stimulation along the corticomotor pathway; reactivation of neural circuits has been demonstrated after noninvasive electrical spinal neuromodulation in individuals with SCI, making them more responsive to facilitatory techniques, such as those for bladder control [197]. These results in spinal stimulation are relevant to our results in cortical stimulation because below-injury reorganization enhances excitability of motor pathways, reflective of cortical motor representation changes [15], and reorganization occurs above injury in the cortical projection system [14]. Corticospinal neurons projecting to the hand can branch to the arm which can improve voluntary upper limb movement of retained functional regions after reorganization

[166]. Finally, while the lack of an effect of iTBS in the nonimpaired group was unexpected because meta-analysis suggests that iTBS is regarded as excitatory when targeting distal hand muscles, responsiveness has been seen to vary across individuals and within repeated sessions of the same individual [38], [39], [56], [72].

Within both the SCI and nonimpaired groups, there was a significant interaction between the corticomotor conductance potential and stimulation type (active or sham), which demonstrated that individuals presenting with lower ratios were more responsive to active iTBS than those with higher ratios. While there was a groupwide response to iTBS in our SCI group, the interaction of group with corticomotor conductance potential suggests that the magnitude of the response may be predictable. For individuals with tetraplegia, low ratios may indicate that the corticospinal tract of the muscle has potential to increase its conductance from iTBS, while high ratios could indicate that the corticospinal tract of the muscle is less likely to respond to iTBS. This interaction between the corticomotor conductance potential and type of stimulation was similarly found in the nonimpaired group. Thus, the corticomotor conductance potential could be used as a predictive measure of an individual's responsiveness to iTBS. Future studies should investigate motor threshold changes as a potential effect of iTBS.

Our results further highlight the differences in corticomotor excitability between the nonimpaired and SCI populations, the effect of the corticomotor conductance potential, and how these population differences can affect the response to iTBS. While proximal muscles of the upper limb are likely to be less impaired relative to distal muscles after SCI, these muscles cannot necessarily be considered analogous to nonimpaired muscles [195]. This is demonstrated by our findings that the baseline nMEPs are higher in the SCI group relative to the nonimpaired group, which is consistent with other studies [15], [198]. Furthermore, while the groups respond within different regions of the corticomotor conductance potential profile, this work indicates that the corticomotor conductance potential has viability for predicting the effect of iTBS in both groups, despite the various neuroplastic changes that occur after SCI.

We assessed how corticomotor conductance potential affected nMEPs and the efficacy of iTBS in either nonimpaired individuals and those with SCI. We hypothesized that corticomotor excitability, as measured by nMEPs, would relate to the interaction between corticomotor conductance potential and stimulation type (i.e. active or sham iTBS). This hypothesis was supported; the motor threshold ratio was found to be negatively correlated with nMEPs and had a significant interaction between coil type.

3.7 Limitations

This study used a single stimulator to represent the clinical environment in which iTBS may be delivered and MEPs assessed with the same device. However, most of our participants had RMT values \geq 84% MSO. Thus, we could not assess biceps corticomotor excitability (i.e., MEPs) at stimulus intensities

of 120% RMT resulting in potential under-stimulation and greater MEP variability [6]. This potential limitation could be addressed by using a monophasic stimulator to evaluate RMTs and collect MEPs. RMT of the biceps when determined by a monophasic stimulator are typically 50-60 %MSO [58]. We evaluated the relationship between nMEPs and RMT to determine if under-stimulation influenced our results and found no correlation in the nonimpaired group, but there was a correlation in the SCI group. However, despite recording MEPs at less than 120% of RMT in many of the SCI subjects, the effect of iTBS was still significantly facilitatory in the SCI group as a whole (i.e., MEPs increased after iTBS relative to baseline). Another potential limitation is that sham stimulation was always delivered prior to active stimulation. While this was done to prevent any response to active stimulation biasing the response to sham within the same session, we cannot exclude the possibility of an order effect. It is also possible that effects of iTBS within the first 10 minutes were not captured due to the 10 minute interval schedule of MEP elicitation that was chosen based on previous work targeting other muscles [38], [56], [177]. The time frame was chosen for relevance as an adjunct to rehabilitation protocols which would begin a few minutes after iTBS priming. Also, in some iTBS sessions of our SCI group, AMT was greater than 72% MSO, although this was an exclusion criterion of the first session. AMT greater than 72% MSO would dictate an iTBS intensity of greater than 57% MSO, whereas safety limitations in our stimulator imposed by the manufacturer held maximum iTBS intensity to 57% MSO. In these individuals, 57% MSO was used for their iTBS, and potential under-stimulation during iTBS delivery was still insufficient to obscure the effect of iTBS in this SCI group. Finally, as the sample size is limited, our results should be confirmed in a larger clinical trial.

3.8 Conclusions

Our results indicate that the biceps brachii is a responsive target for iTBS to increase corticomotor excitability in individuals with tetraplegia, emphasizing the potential of iTBS as an adjunct to physical therapy for motor rehabilitation. Furthermore, our comparison with the nonimpaired group provides evidence for differences in effects of iTBS between nonimpaired and SCI groups suggesting that neuroplastic changes after SCI play a role in the neuromodulation susceptibility of a motor cortical target. Therefore, further research is needed to confirm our preliminary findings in a larger clinical trial, investigate how muscle target and injury level influence effects of iTBS, and establish the amount of corticomotor excitability change that is needed to affect rehabilitation outcomes and functional ability.

3.9 Supplemental

Table S3.1: Motor thresholds by session in SCI participants prior to iTBS presented as percent maximum stimulator output (%MSO).

<i>Participant</i>	Session 1				Session 2				Session 3			
	Biceps RMT ^a Prior to Sham iTBS	Biceps AMT ^b Prior to Sham iTBS	Biceps RMT Prior to Active iTBS	Biceps AMT Prior to Active iTBS	Biceps RMT ^a Prior to Sham iTBS	Biceps AMT ^b Prior to Sham iTBS	Biceps RMT Prior to Active iTBS	Biceps AMT Prior to Active iTBS	Biceps RMT ^a Prior to Sham iTBS	Biceps AMT ^b Prior to Sham iTBS	Biceps RMT Prior to Active iTBS	Biceps AMT Prior to Active iTBS
01	95	57	95	51	84	47	92	34	98	47	97	47
02	80	34	82	53	100	20	80	41	88	45	88	59
03	81	53	77	58	85	55	80	54	98	53	91	42
04	93	74	95	74	100	100	94	79	90	75	97	79
05	100	68	100	69	100	70	100	80	100	56	100	66
06	100	100	100	100	100	100	100	100	100	100	100	94
07	100	67	100	70	100	57	100	66	100	51	100	48
08	67	43	71	45	57	53	66	56	65	50	81	53
09	100	70	87	59	87	61	91	63	91	66	100	79
10	100	100	100	100	100	93	100	88	100	100	100	100

a) RMT: resting motor threshold as percent of maximum stimulator output (% MSO) measured with biphasic PA/AP stimulation; b) AMT: active motor threshold as % MSO measured with biphasic PA/AP stimulation.

Table S3.2: Motor thresholds by session in the nonimpaired participants prior to iTBS presented as percent maximum stimulator output (%MSO).

<i>Participant</i>	Session 1				Session 2				Session 3			
	Biceps RMT ^a Prior to Sham iTBS	Biceps AMT ^b Prior to Sham iTBS	Biceps RMT Prior to Active iTBS	Biceps AMT Prior to Active iTBS	Biceps RMT ^a Prior to Sham iTBS	Biceps AMT ^b Prior to Sham iTBS	Biceps RMT Prior to Active iTBS	Biceps AMT Prior to Active iTBS	Biceps RMT ^a Prior to Sham iTBS	Biceps AMT ^b Prior to Sham iTBS	Biceps RMT Prior to Active iTBS	Biceps AMT Prior to Active iTBS
01	90	52	100	61	100	48	100	56	100	60	100	51
02	77	56	83	56	85	50	88	60	95	65	88	54
03	100	68	87	60	61	53	67	56	61	58	59	60
04	100	71	100	69	90	67	100	74	96	68	98	59
05	84	56	85	64	86	63	95	54	85	56	74	44
06	85	53	83	49	97	60	95	67	77	42	88	42
07	95	68	100	59	100	46	100	55	100	45	100	34
08	88	62	74	52	83	66	85	61	100	54	83	58
09	100	67	100	68	100	72	100	57	100	60	100	53
10	76	50	78	60	74	60	76	60	70	43	71	45

a) RMT: resting motor threshold as percent of maximum stimulator output (%MSO) measured with biphasic PA/AP stimulation; b) AMT: active motor threshold as %MSO measured with biphasic PA/AP stimulation.

Table S3.3: Maximum Voluntary Contraction (MVC) EMG value by session in both groups prior to iTBS.

<i>Participant</i>	<i>Group</i>	<i>Session 1 MVC^a</i>	<i>Session 2 MVC</i>	<i>Session 3 MVC</i>
01	NI ^b	228.3	100.0	239.5
02	NI	204.8	85.0	240.3
03	NI	96.4	61.0	96.0
04	NI	162.0	90.0	210.6
05	NI	442.6	86.0	354.9
06	NI	392.5	97.0	527.7
07	NI	281.8	100.0	446.2
08	NI	233.7	83.0	183.3
09	NI	339.6	100.0	329.5
10	NI	143.7	74.0	206.9
01	SCI ^c	418.3	607.7	638.2
02	SCI	454.0	495.4	431.6
03	SCI	123.9	235.2	385.3
04	SCI	99.1	80.1	96.8
05	SCI	368.4	276.1	270.6
06	SCI	55.1	42.5	61.1
07	SCI	275.0	285.1	282.2
08	SCI	277.2	129.8	322.3
09	SCI	70.7	73.5	108.8
10	SCI	45.2	57.1	55.3

a) MVC: maximum voluntary contraction (mV); b) NI: nonimpaired group; c) SCI: spinal cord injury group.

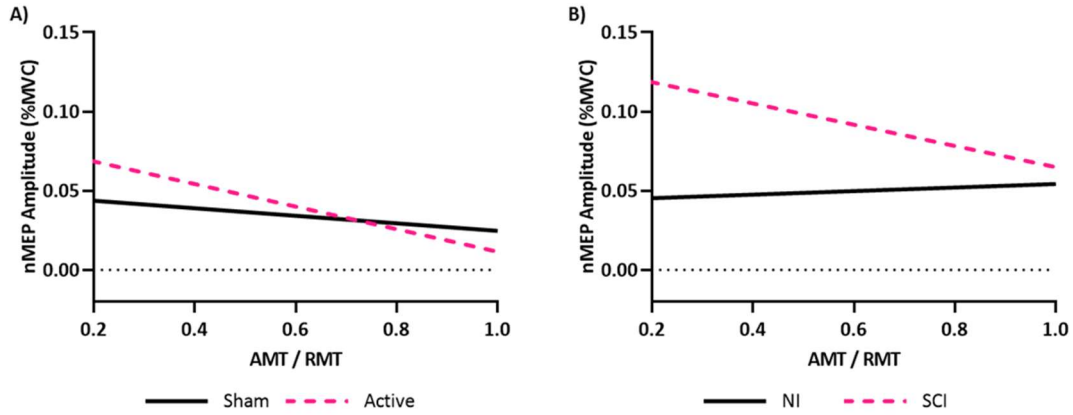


Fig S3.1: Interaction Between Corticomotor Conductance Potential (AMT/RMT) and Group, and their Effect on Modeled nMEPs.

A) There was a negative correlation between corticomotor conductance potential and nMEP amplitude that differed by stimulation type suggesting that at lower corticomotor conductance potentials, individuals in either group are more responsive to iTBS. (B) The effect of corticomotor conductance potential on nMEP amplitude was unique by group across both stimulation types suggesting that low corticomotor conductance potentials were associated with greater disparity in stimulation efficacy between the groups.

4 Effect of Neuroanatomy on Corticomotor Excitability During and After Transcranial Magnetic Stimulation and Intermittent Theta Burst Stimulation

4.1 Authors and Submission Details

N. Mittal, B Thakkar, C Hodges, C Lewis, Y Cho, RL Hadimani, CL Peterson, “Effect of Neuroanatomy on Corticomotor Excitability During and After Transcranial Magnetic Stimulation and Intermittent Theta Burst Stimulation”, Submitted to *Human Brain Mapping*, 10-25-2021. Submission ID: HBM-21-1017.

IRB Approval: VCU IRB HM20018505

Clinical Trials Registration: clinicaltrials.gov NCT04586387

Data Repository: Open Science Framework –

https://osf.io/qtxn4/?view_only=54a0e81eeb3e44f8a90971cbbd07c433

4.2 Abstract

Individual neuroanatomy can influence motor responses to transcranial magnetic stimulation (TMS) and corticomotor excitability after intermittent theta burst stimulation (iTBS). The purpose of this study was to examine the relationship between individual neuroanatomy and both TMS response measured using resting motor threshold (RMT) and iTBS measured using motor evoked potentials (MEPs) targeting the biceps brachii and first dorsal interosseus (FDI). Ten nonimpaired individuals completed sham-controlled iTBS sessions and underwent MRI, from which anatomically accurate head models were generated. Neuroanatomical parameters established through fiber tractography were fiber tract surface area (FTSA), tract fiber count (TFC), and brain scalp distance (BSD) at the point of stimulation. Cortical magnetic field induced electric field strength (EFS) was obtained using finite element simulations. A linear mixed effects model was used to assess effects of these parameters on RMT and iTBS (post-iTBS MEPs). FDI RMT was dependent on interactions between EFS and both FTSA and TFC. Biceps RMT was dependent on interactions between EFS and both FTSA and BSD. There was no groupwise effect of iTBS on the FDI but individual changes in corticomotor excitability scaled with RMT, EFS, BSD, and FTSA. iTBS targeting the biceps was facilitatory, and dependent on FTSA and TFC. MRI-based measures of neuroanatomy highlight how individual anatomy affects motor system responses to different TMS paradigms and may be useful for selecting appropriate motor targets when designing TMS based therapies.

4.3 Introduction

Transcranial magnetic stimulation (TMS) techniques have received increased attention in recent years as potential treatments for neurological disorders via manipulating cortical excitability, such as traumatic brain injury, stroke, spinal cord injury, and movement disorders [199]–[202]. Intermittent

theta burst stimulation (iTBS) is a form of repetitive transcranial magnetic stimulation (rTMS) that can facilitate corticomotor excitability [6], [38], [39], [54], [203]. Motor targets investigated in iTBS studies include the biceps brachii [204] and the first dorsal interosseous (FDI) [6], [38], [39], [54], [203] due to their roles in rehabilitation and activities of daily living (ADLs). iTBS has been evaluated in individuals with spinal cord injury (SCI), showing variable effects [69]. Other work has noted that although TMS techniques are therapeutically promising, considerable work remains to be done in determining the driving factors behind treatment response variability [199].

High variability has been reported in changes in corticomotor excitability both within and across individuals in TMS studies [38], [56], [57], [70]–[72], [78]. This is seen regarding response to TMS as measured by motor thresholds (MT) [56], [205], and response to iTBS as measured by motor evoked potentials (MEPs) [56], [72], [73], [77], [206]. Factors contributing to TMS motor threshold variability include individual differences of synaptic plasticity [56], [173], use of medication, clinical pathology, age, and gender [205]. Factors contributing to the variability [39] of iTBS effects include genetics [66], age [207], motor target [8], cortical organization [77], [78], alertness [208], neurotransmitter and receptor variation [49], [50], and brain anatomy [80]. Individual neuroanatomy can also contribute to variability [79]. Distinct motor regions in the brain have unique characteristics, such as surface area [8], neuron density [73], or orientation of neurons with respect to the skull [209]. However, the effects of these individual level differences are not well characterized.

Individual neuroanatomy would be expected to affect responsiveness to iTBS because the conduction of the induced current from TMS is dependent on the morphology and material properties of the stimulated medium, and individual brains have unique anatomical features. Furthermore, anatomical complexities of cortical motor regions and their corresponding fiber tracts determine TMS induced electric fields in the brain, which are the mechanistic impetus for TMS activation and more specifically rTMS paradigms [54], [75]. Depolarization of the neurons in the motor cortex elicits responses to TMS, and as a result, brain anatomy and related morphology features likely impact the effectiveness of iTBS even for different motor targets of the same individual [8], [76]–[80]. For example, brain scalp distance (BSD) has been associated with TMS response [79], [81]. However, BSD is limited as it is a one dimensional parameter as opposed to induced electric field which is a three dimensional parameter that takes into account the composition of tissue between the scalp and cortex [80].

The objectives of this preliminary study were to determine the effects of individual brain neuroanatomy as measured by simulated induced electric fields from TMS over motor cortical regions of the biceps and FDI on: a) resting motor threshold (RMT), and b) MEPs after iTBS. Healthy individuals underwent iTBS for empirical data collection and magnetic resonance imaging (MRI), from which we developed anatomically accurate computational head models with relevant neuroanatomy [79], [80]. Induced electric fields were computed in head models using finite element analysis across individual brain morphology; fiber tract geometry was determined based on surface area and fiber count. The neurophysiological effects of single pulse TMS and iTBS in the form of RMT and MEPs, respectively, were

recorded in the same participants. Our central hypothesis was that brain anatomy evidenced by the simulated induced electric field would influence corticomotor excitability. First, we hypothesized that empirically derived RMT would negatively correlate with the magnitude of the simulated induced electric field and with fiber tract size, regardless of the motor target. The basis of this hypothesis was that a greater responsiveness to TMS (as indicated by lower RMT) would relate to a larger induced cortical current (and corresponding white matter tract). This would establish a relationship between model-derived parameters and empirical single pulse TMS response. Second, we hypothesized that individuals with greater simulated electric field strength would exhibit a larger change in corticomotor excitability (as measured by increased MEP amplitude) after iTBS in both motor targets. Lastly, we hypothesized that the specific factors such as electric field strength and fiber tract geometry would differently influence the response from the two motor targets (biceps and FDI) due to differences in cortical architecture. Overall, we sought to elucidate whether MRI-based measures of neuroanatomy can predict whether an individual is likely to respond to iTBS-based therapies.

4.4 Methods

4.4.1 Participants

Ten healthy individuals (7 females, 3 males, 23.5 ± 5 years) participated in this study (Tables 4.1 & 4.2). The inclusion criteria required participants to be between the ages of 18 and 65 years old. Exclusion criteria were presence of severe medical illness and sequelae, existing infection, cardiovascular disease, significant osteoporosis, metal implanted devices, personal or family history of seizure activity, and any acute or current history of neuromuscular or motor dysfunction. All participants were screened to ensure safety of the TMS and MRI protocols and provided informed consent. This study was approved by the Virginia Commonwealth University Institutional Review Board.

Table 4.1: Motor thresholds and maximum voluntary contraction (MVC) prior to first dorsal interosseus (FDI) iTBS presented as mean \pm one standard deviation.

<i>Participant</i>	Age	Prior to Sham iTBS				Prior to Active iTBS		
		FDI MVC EMG ^a (mV)	FDI RMT ^b	FDI AMT ^c	Average Baseline nMEPs ^d	FDI RMT	FDI AMT	Average Baseline nMEPs
01	21	238.3	46	38	0.353	49	35	0.660
02	24	472.4	41	48	0.211	41	47	0.295
03	19	170.1	68	31	0.735	55	36	0.351
04	20	130.7	64	43	0.713	64	50	0.727
05	23	504.7	72	28	0.034	78	40	0.369
06	19	750.4	70	36	0.250	50	50	0.045
07	32	263.3	43	37	0.134	43	44	0.113
08	26	370.6	41	33	0.404	33	42	0.320
09	29	887.9	54	30	0.136	51	39	0.399
10	27	740.9	70	39	0.170	68	47	0.502
<i>Mean \pm SD</i>	23.5 \pm 5	452.93 \pm 265.9	56.9 \pm 13	36.3 \pm 6	0.2941 \pm 0.269	53.2 \pm 14	43.0 \pm 5	0.3891 \pm 0.314

a) MVC: maximum voluntary contraction; b) RMT: resting motor threshold as percent of maximum stimulator output (%MSO) measured with monophasic stimulation inducing an AP current in the brain; c) AMT: active motor threshold as %MSO measured with biphasic PA/AP stimulation; d) nMEP: normalized motor evoked potential (%MVC) measured with monophasic AP stimulation, presented as mean \pm one standard deviation.

Table 4.2: Motor thresholds and maximum voluntary contraction (MVC) prior to biceps iTBS presented as mean \pm one standard deviation.

<i>Participant</i>	Age	Biceps MVC EMG ^a (mV)	Prior to Sham iTBS			Prior to Active iTBS		
			Biceps RMT ^b	Biceps AMT ^c	Average Baseline nMEPs ^d	Biceps RMT	Biceps AMT	Average Baseline nMEPs
01	21	411.0	57	68	0.066	61	68	0.059
02	24	118.0	62	60	0.067	67	58	0.112
03	19	183.2	100	70	0.011	100	74	0.011
04	20	144.6	49	67	0.024	65	74	0.032
05	23	185.2	86	72	0.041	87	73	0.025
06	19	453.2	61	70	0.136	85	48	0.102
07	32	184.1	100	72	0.023	100	73	0.012
08	26	128.9	69	57	0.078	78	52	0.12
09	29	256.0	44	44	0.093	47	46	0.292
10	27	112.2	100	62	0.065	100	65	0.055
<i>Mean \pm SD</i>	23.5 \pm 5	217.63 \pm 121.1	72.8 \pm 22	64.2 \pm 9	0.0602 \pm 0.049	79.0 \pm 19	63.1 \pm 11	0.0820 \pm 0.084

a) MVC: maximum voluntary contraction; b) RMT: resting motor threshold as percent of maximum stimulator output (%MSO) measured with monophasic stimulation inducing an AP current in the brain; c) AMT: active motor threshold as %MSO measured with biphasic PA/AP stimulation; d) nMEP: normalized motor evoked potential (%MVC) measured with monophasic AP stimulation, presented as mean \pm one standard deviation.

4.4.2 Experiment Overview

Each participant completed one FDI targeted iTBS session, one biceps targeted iTBS session, and an MRI session of the head on three separate days. The iTBS sessions were separated by a minimum of three days to prevent carry over effects [57]. Sessions were scheduled for the same time of day for each participant to control for diurnal effects. MRI data were used to generate head models for neuroanatomical parameters. The experimental steps can be seen in Fig 4.1.

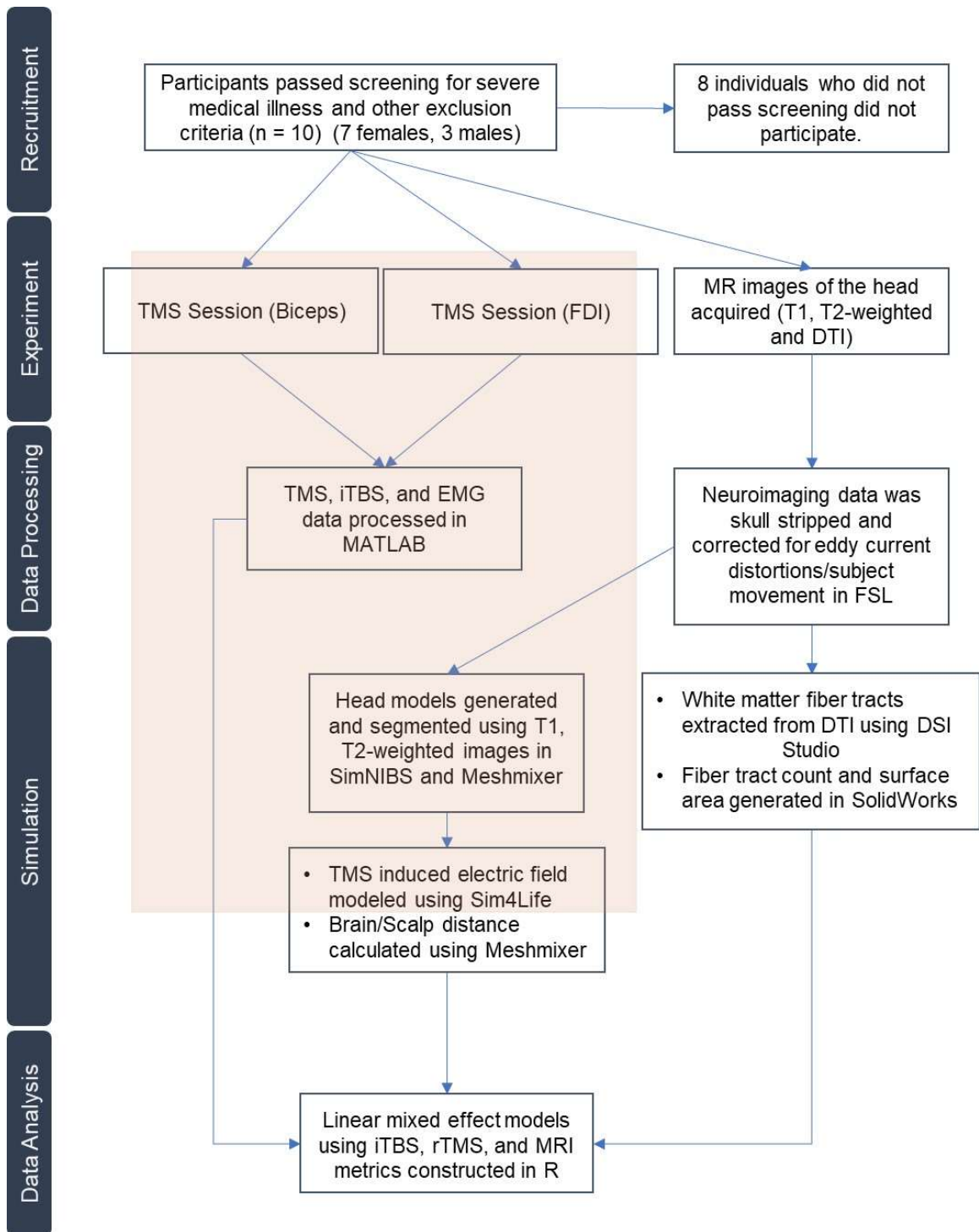


Fig 4.1: Experimental Design. Participants underwent two sessions of TMS for empirical measurements (FDI and biceps), and one MRI to develop individualized, neuroanatomically accurate simulations. MRI head images were used to establish neuroanatomical parameters for each participant. These were evaluated for their influence on empirical TMS data. The shaded region represents empirical and simulated TMS data.

4.4.3 Transcranial Magnetic Stimulation Experiments

Electromyography (EMG) data were recorded using a Trigno™ Wireless System (Delsys, Natick, MA). EMG signals were recorded with Spike 2 software (Cambridge Electron Design, Cambridge, UK). The FDI and first palmer interosseus (FPI) for FDI sessions, and long head of the biceps and the lateral head of the triceps for biceps sessions were instrumented with surface electrodes on the skin, verified by functional muscle testing (Fig 4.2). FPI and triceps were instrumented for monitoring purposes. EMG signals were amplified (x1000), bandpass-filtered (20-450 Hz) prior to A/D conversion (Micro 1401 MkII, Cambridge Electron Design, Cambridge, UK), and sampled at 2000 Hz.

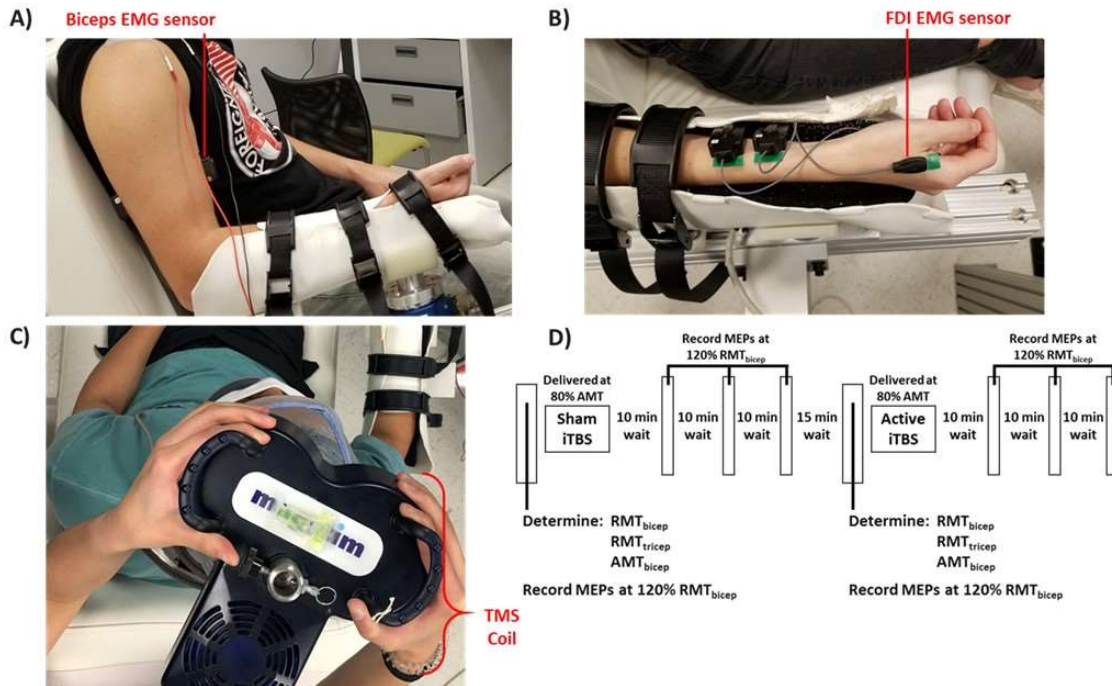


Fig 4.2: Experimental setup and structure of TMS sessions. (A,B) Participants' forearms were supported horizontally with EMG sensors placed on their biceps (A) or first dorsal interosseus (FDI) (B). (C) The TMS coil was placed tangentially over the scalp above motor cortex, oriented to induce a posterior-anterior current within in the motor cortex. (D) Sessions began with motor threshold and baseline MEP measurements before performing iTBS. MEPs were collected post-iTBS at 120% RMT in 10-minute intervals. Sham iTBS did not deliver stimulation.

Single pulse TMS was delivered as a monophasic posterior-anterior current to the primary motor cortex contralateral to the resting arm using a Magstim BiStim² stimulator via a 70 mm figure-of-eight coil (P/N 4150-00), while iTBS was performed using a Magstim Super Rapid² Plus¹ stimulator (Magstim, Whitland, UK) via a 70 mm figure-of-eight air film coil (P/N 3910-00) that delivered high frequency biphasic pulses with currents in the posterior-anterior then anterior- posterior directions. The vertex at the intersection of theinion-nasion and inter-aural lines were marked on a cap fitted on the participant's head and used to orient the coil near the cortical target. The coil was held tangentially on the scalp via a support stand with the coil center rotated to induce a posterior-to-anterior cortical

current across the central sulcus (Figure 2C). The hotspot for the target muscle was identified as the location evoking the largest peak-to-peak amplitude MEP using the lowest stimulation intensity [210], [211].

RMT was defined as the lowest stimulus intensity that induced MEPs of $\geq 50 \mu\text{V}$ in at least 5 of 10 consecutive stimuli with the target muscle fully relaxed [150]. AMT was defined as the stimulus intensity that elicited a MEP of $\geq 200 \mu\text{V}$ in at least 5 of 10 consecutive stimuli recorded during sustained isometric contraction of $10 \pm 5\%$ of the participant's maximum effort [38], [150]. Maximum effort was measured by the average EMG in the highest 0.5 s period of a 5 s isometric maximum voluntary contraction (MVC), averaged across 3 trials. Stimulus intensity was determined using an adaptive parameter estimation by sequential testing software [150]. Evoked potential operant conditioning software (EPOCS) developed by the Evoked Potential Operant Conditioning Core at the National Center of Neuromodulation for Rehabilitation was used to record motor thresholds and display effort levels for participants.

iTBS was applied using a Magstim Super Rapid² Plus¹ stimulator and a 70 mm double air film coil following the common protocol presented by Huang et al. applied to motor areas [54] (Figure 2D). iTBS applied to the motor target cortical hotspot consisted of three pulses presented at 50 Hz, every 200 ms for 2 s, for 8 s, at a subthreshold intensity of 80% of the participant's AMT resulting in 600 pulses [39], [54]. During sham iTBS, a Magstim 70 mm figure-of-eight air film sham coil (P/N: 3950-00) (Magstim, Whitland, UK) was used which looked identical to the active coil and made similar noises without delivering any stimulation [204], [212], [213]. Throughout each session participants were blinded to the type of stimulation they were receiving.

Participants received single pulse TMS to elicit MEPs before iTBS and in ten-minute intervals after for thirty minutes (Fig 4.3). During each time interval, no more than 20 stimulations were delivered.

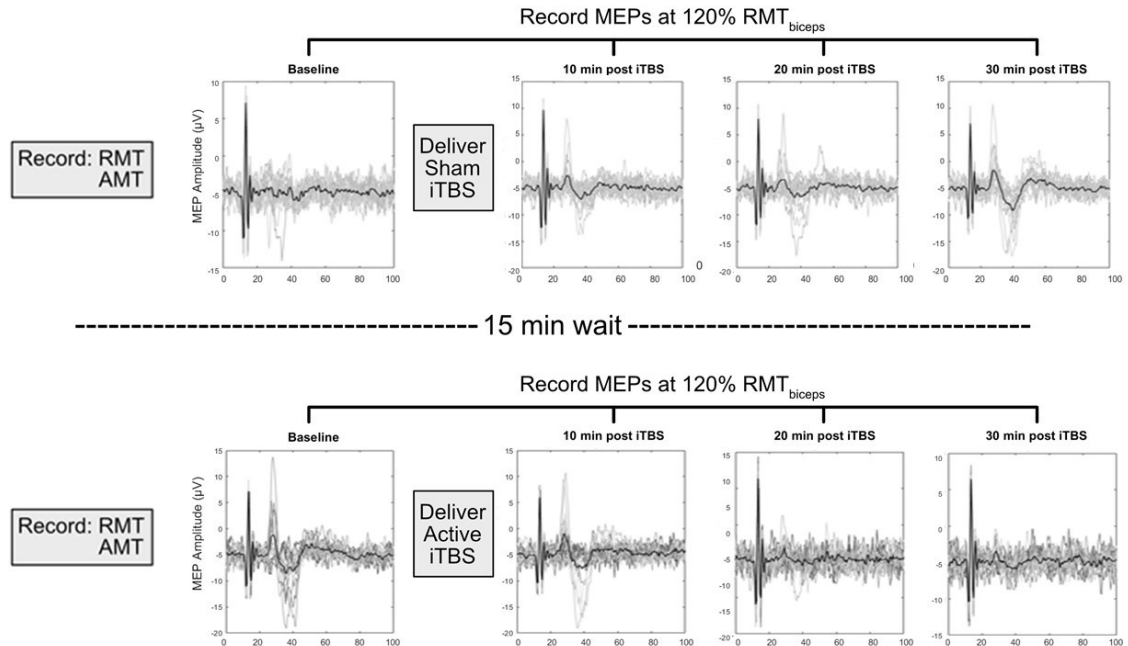


Fig 4.3: TMS Sessions and Empirical Data. Before application of iTBS, single pulse TMS was used to determine RMT, AMT, and collect baseline MEPs for the motor target. iTBS was delivered at an intensity of 80% of AMT. Single pulse TMS elicited MEPs at 10-minute intervals following iTBS, at 120% RMT. Data shown represent processed and collected raw MEPs of a single session from a representative participant. Grey lines represent individual MEPs and the black line represents the average MEP. Horizontal axis depicts time (ms), with the TMS pulse delivered at time 0.

4.4.4 TMS Data Processing

Using purpose-written code in MATLAB (MathWorks, MATLAB v 9.7.0.1190202), peak-to-peak MEP amplitudes were calculated from the motor target EMG data of each session. The root mean square (RMS) amplitude was calculated for the evoked response over a 50 ms window (12–62 ms post TMS pulse), and for a 50 ms window prior to the TMS pulse (pre-stimulus). Instances where the pre-stimulus RMS exceeded the evoked response RMS were excluded [73]. MEPs were then normalized by and presented as a percentage of the MVC EMG [214]. Normalized MEPs (nMEPs) served as our measure of corticomotor excitability, with the average of nMEPs collected prior to iTBS serving as the baseline.

4.4.5 Neuroimaging Acquisition

Structural T1- and T2-weighted images were acquired using a Philips 3.0T Ingenia system with a 32-channel receive head coil (Philips Medical Systems, Best, Netherlands). T1-weighted images were acquired using a 3D MPRAGE sequence with the following parameters: repetition time (TR) = 8 ms, echo time (TE) = 3.7 ms, acquired sagittally with a 1.0x1.0x1.0 mm resolution at a flip angle of 8°, echo train length (ETL) = 256, matrix=256x240). T2-weighted images were acquired using a 3D multishot turbo spin

echo sequence (TE/TR=245/2500 ms acquired sagittally with a matching resolution of the T1-weighted images, two averages, flip angle=90°, ETL=117, matrix=256x256).

Whole brain diffusion weighted images were acquired in the transverse plane using a single shot diffusion sensitized spin echo planar imaging sequence [215] with the following parameters: b-factors = 1000 s/mm² and 0 s/mm², SENSE in-plane acceleration factor = 2.75, repetition time (TR) = 6.05 seconds, echo time (TE) = 96ms, half-scan factor = 0.602, 60 diffusion directions, 6 repetitions of b-factor = 0, field of view = 256x256, acquisition matrix = 140x141, slice thickness = 1.7mm, 80 slices, flip angle = 90°, and a voxel resolution of 1.7mm x 1.7mm x 1.7mm. The diffusion tensor imaging (DTI) acquisition time was approximately 10 minutes per subject.

4.4.6 *Neuroimaging Preprocessing*

DTI images were transformed to Neuroimaging Informatics Technology Initiative format using dcm2niix [216]. DTI images were then pre-processed using the FMIRB Software Library (FSL, version 6.0) [217]. Images were corrected for eddy current-induced and head motion-induced distortions using a variant of the eddy command [218] called eddy_cuda8.0, which uses Compute Unified Device Architecture, an accelerated computing platform on NVIDIA graphics processor units, to parallelize analyses. Brain tissue was extracted and an exclusion mask generated using FSL's Brain Extraction Tool through the bet2 command [219]. These corrected and extracted images were then used in subsequent head model generation. The workflow for MRI images and subsequent model derivations can be seen in Fig 4.3.

Using the extracted T1- and T2-weighted images from all the subjects, a SimNIBS pipeline (SimNIBS Developers 2019, v2.0.1) [76], [79] was used to create seven separate segments (white matter, grey matter, cerebrospinal fluid, skin, skull, ventricles, and cerebellum) as separate 3D modeled files. Abnormalities were smoothed using Meshmixer (AutoDesk, Inc. v11.2.37) (Fig 4.4A).

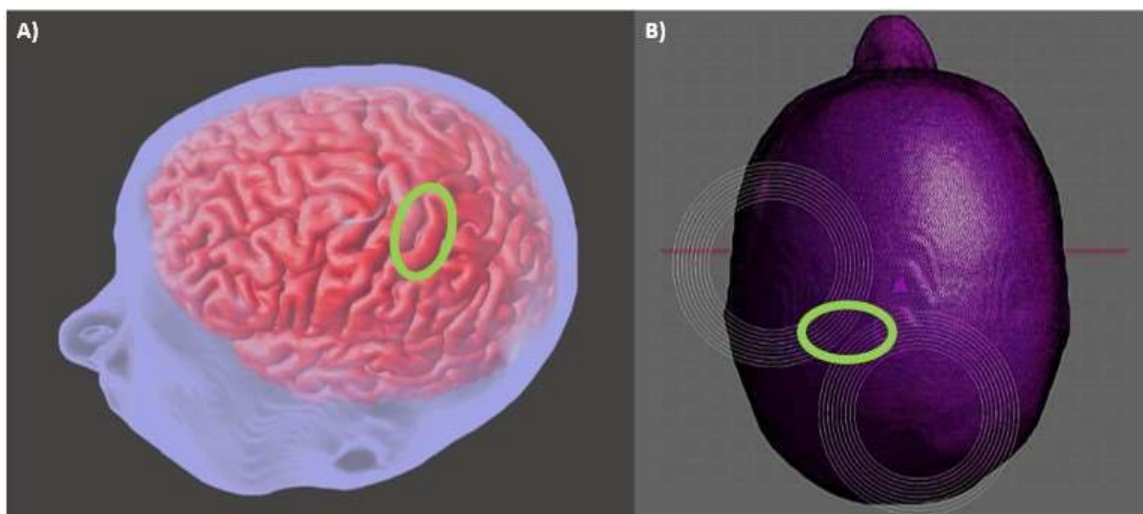


Fig 4.4: MRI-derived individual anatomically accurate head models. (A) Head models integrated seven segments derived from MRI: skin (blue), bone (transparent), cerebrospinal fluid (transparent), ventricular space (below the visible grey matter), cerebellum (below the visible grey matter), grey matter (pink), and white matter (below the visible grey matter). The grey matter can be seen as the surface of the cortex in this image. (B) Head models then underwent finite element simulation of TMS. White concentric circles represent the modeled coil. The green circle (A, B) encompasses the hand knob representative of upper limb control of the motor cortex.

4.4.7 Induced Electric Field Modeling

Induced electric field from peak intensity stimulation at the upper limb control region of the primary motor cortex, was computed using Sim4Life finite element analysis software (Zurich Med Tech, v6.2.1.4972) [220], on the generated head models [79], [81]. Head model segments were imported into Sim4Life [220]. The simulated coil was defined to match dimensions and function of the Magstim 70mm figure-of-8 coil [82]. The coil was oriented with the center directly over the region of stimulation interest with 45° orientation to the coronal plane to match the empirical test setup (Fig 4.4B). The target region of stimulation was identified as the precentral gyrus posterior to the superior frontal sulcus, within the “knob” as defined by Yousry and consistent with approximations from motor homunculi [221].

The stimulation current strength was set to 5000 A, corresponding to 100% MSO, at 2,500 Hz [80] and the seven segments of the head model as well as the air were assigned their respective material properties based on the IT’IS LF database (IT’IS Foundation, v4.0). The magnetic stimulation induced electric field strength (EFS) at the surface of the cortex at the point of interest, specifically of the grey matter segment, was determined (Fig 4.5). EFS was used in analyses to represent the simulated cortical current across the MRI-derived anatomy for each individual.

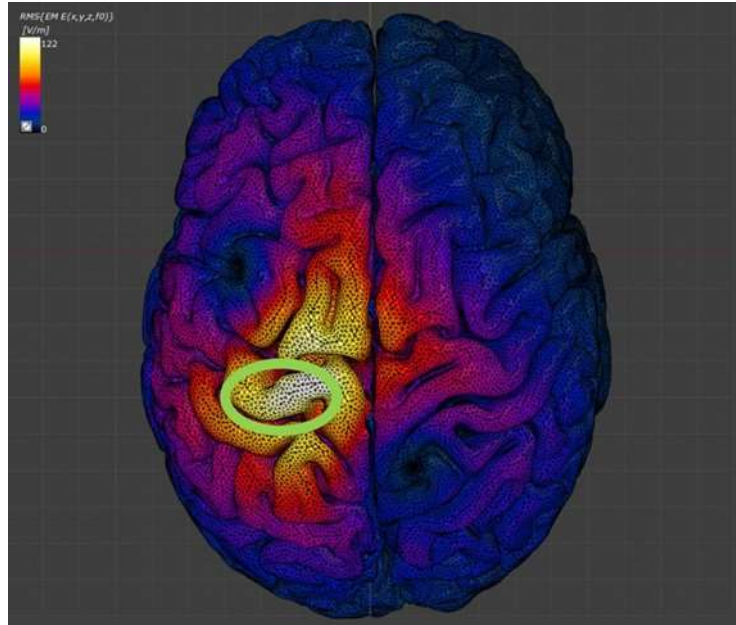


Fig 4.5: Induced electric field strength. Finite element simulations of the individual head models were performed to calculate the induced electric field strength of magnetic stimulation of the motor cortex for each head model. Maximal stimulation was confirmed to be over the primary motor cortex in the region of upper limb control. Color bar represents induced electric field intensity (V/m), ranging from maximal (white) to minimal (dark blue). The green circle encompasses the hand knob representative of upper limb control of the motor cortex.

Brain scalp distance (BSD) calculations were made using the grey matter and skin files from each subject in Meshmixer (Fig 4.4A). Calculations were made from identification of the surface of both segments using the same location that was designated as the target for the induced electric field simulations. BSD was used in analyses as a representation of magnetic field attenuation, due to the distance between the cortex and the coil surface.

Fiber tracts were extracted from DTI data using DSI Studio (Feh, Y., Zenodo, April 2020). The left side of the brain was located, and the anatomical landmarks to the “knob” of the primary motor cortex (superior frontal sulcus, precentral sulcus, central sulcus, and precentral gyrus), were identified [221]. The region of interest was drawn using the circle tool with a 6 mm diameter to ensure gyrus coverage without extending beyond the precentral gyrus. The FDI region was drawn between the landmark sulci, centered on the precentral gyrus, and in line with the superior frontal sulcus along the “knob” region [221]. The biceps region was drawn medially to the FDI region, within the automated left corticospinal tract from DSI Studio. After the regions of interest were drawn, the fibers in the respective regions were extracted and trimmed following the automated corticospinal tract [83] (Fig 4.6). Fiber coordinates were then imported into SolidWorks (BIOVIA, Dassault Systèmes, SolidWorks, SP3.0, San Diego: Dassault Systèmes, 2017) and used to generate tract fiber counts (TFC) and fiber tract surface areas (FTSA) for each individual fiber tract. FTSA and TFC were used in analyses as representations of fiber tract size.

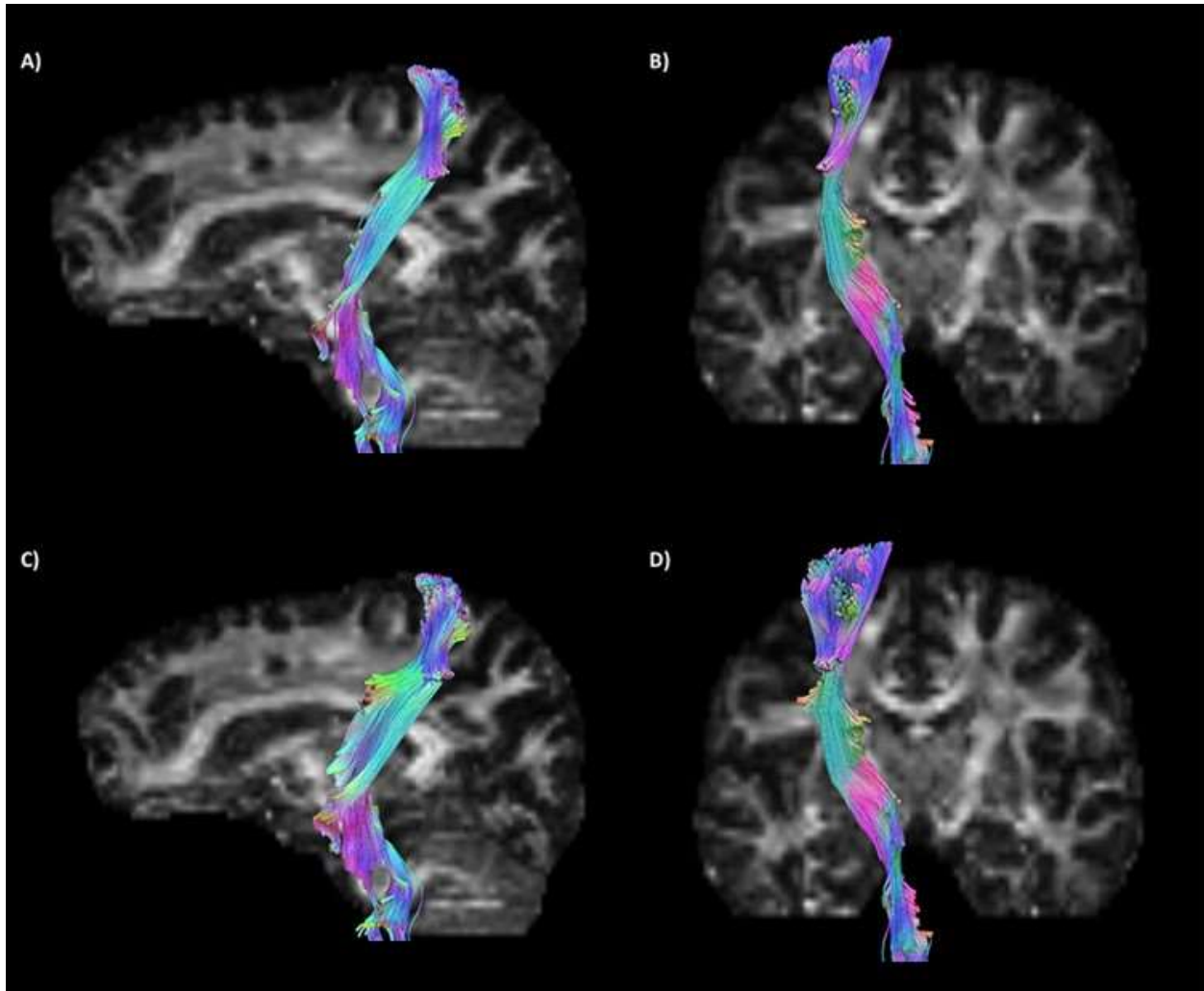


Fig 4.6: Fiber Tractography. Regions of interest in the primary motor cortex representing the biceps (A, B) and (C, D) FDI (C, D) were used to extract fiber tracts for upper limb motor control. Colorized tracts represent the pathways included after trimming for non-corticospinal and recursive connections. (A) Biceps, sagittal section. (B) Biceps, coronal section. (C) FDI, sagittal section. (D) FDI, coronal section.

4.4.8 Statistical Analysis

Linear mixed effects models were analyzed to test the effect of neuroanatomy on the empirical response to single pulse TMS, as measured by RMT. RMT served as the dependent variable, with model fixed effects of induced electric field, fiber tract surface area, tract fiber count, and BSD. Participants were included in the statistical model as a random effect because each TMS session collected two RMT values, one for MEP elicitation to study sham iTBS and one for active iTBS. Interactions between electric field and fiber tract geometry were considered. Linear mixed effects models were created and analyzed using purpose-written R (The R Foundation, 2018) code based on the LME4 package [153], [154].

Linear mixed effects models were also analyzed to test the effect of neuroanatomy on nMEPs recorded after iTBS. The change from baseline and effect of stimulation type, sham or active, was used to assess effect of iTBS by the interaction between these parameters, and RMT was used as an input to represent empirical responsiveness to TMS. This assessment was performed separately for biceps and FDI motor targets.

4.5 Results

For all participants, baseline measurements taken from TMS sessions are presented in Tables 1 & 2. Data supporting our results can be found through the Open Science Framework – https://osf.io/qtxn4/?view_only=54a0e81eeb3e44f8a90971cbbd07c433.

4.5.1 *Effect of neuroanatomy on empirically measured RMT of the FDI*

The FDI RMT correlated with the interaction between EFS and FTSA ($\chi^2 = 4.41$, $p = 0.036$). The FDI RMT also correlated with the interaction between EFS and TFC in the FDI ($\chi^2 = 8.14$, $p = 0.004$). BSD did not affect FDI RMT ($\chi^2 = 0.64$, $p = 0.423$). Significant relationships are shown in Figures 4.7 and 4.8.

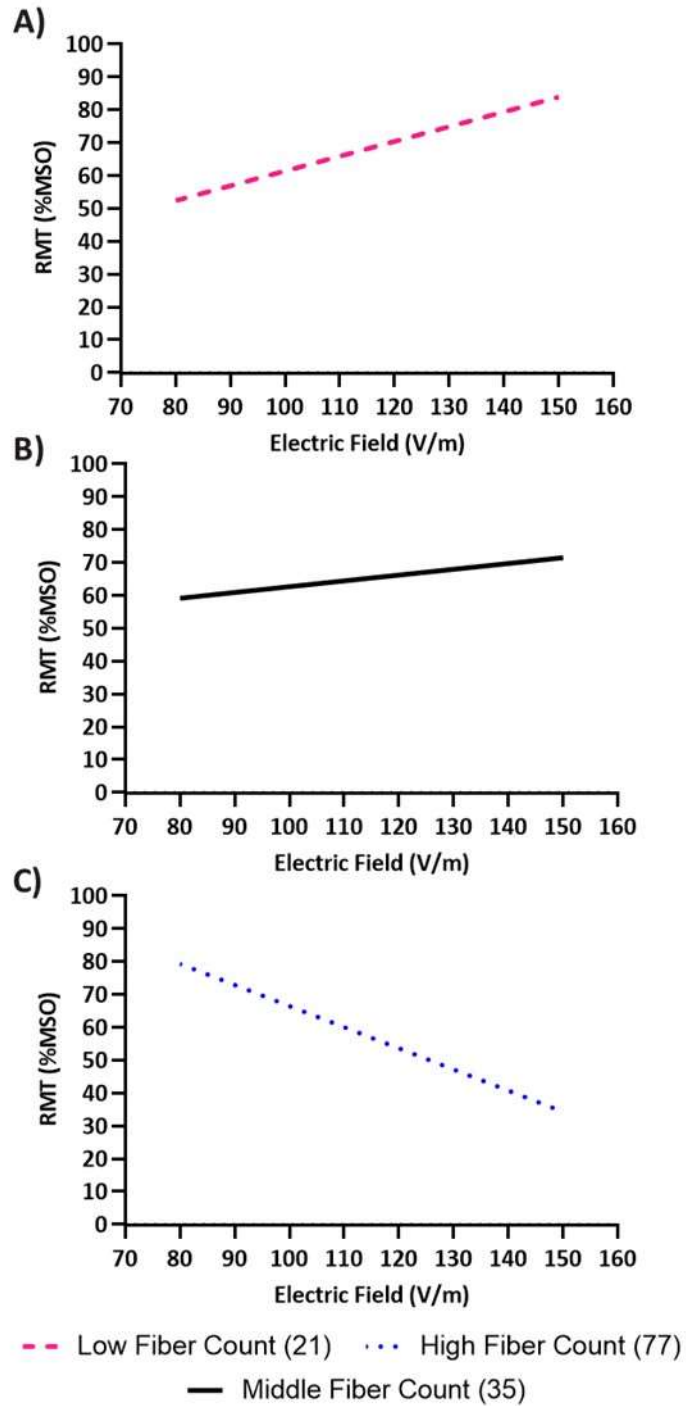


Fig 4.7: Effect of tract fiber count (TFC) on empirically measured RMT of the FDI. (A) At lower TFC, and (B) as TFC increased, RMT was positively correlated with electric field strength (EFS). (C) At higher TFC, RMT was less affected by EFS, evidenced by a simulated reversal of the relationship.

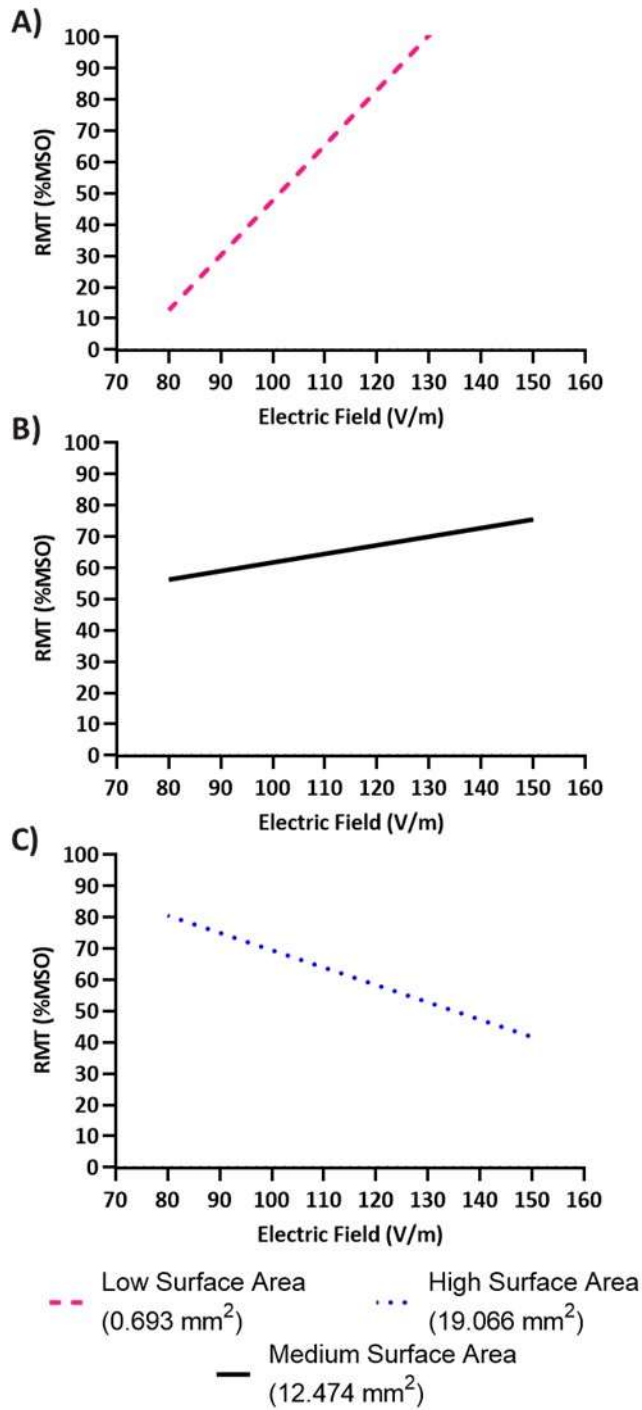


Fig 4.8: Effect of fiber tract surface area (FTSA) on empirically measured RMT of the FDI. (A) At lower FTSA, and (B) as FTSA increased, RMT was positively correlated with electric field strength (EFS). (C) At higher FTSA, RMT was less affected by EFS, evidenced by a simulated reversal of the relationship.

4.5.2 *Effect of neuroanatomy on empirically measured RMT of the biceps*

The biceps RMT correlated with the interaction between EFS and FTSA. ($\chi^2 = 5.24$, $p = 0.022$). The biceps RMT also correlated with the interaction between EFS and BSD ($\chi^2 = 6.68$, $p = 0.010$), but there was no significant effect of TFC ($\chi^2 = 0.14$, $p = 0.712$). Significant relationships are shown in Figures 4.9 and 4.10.

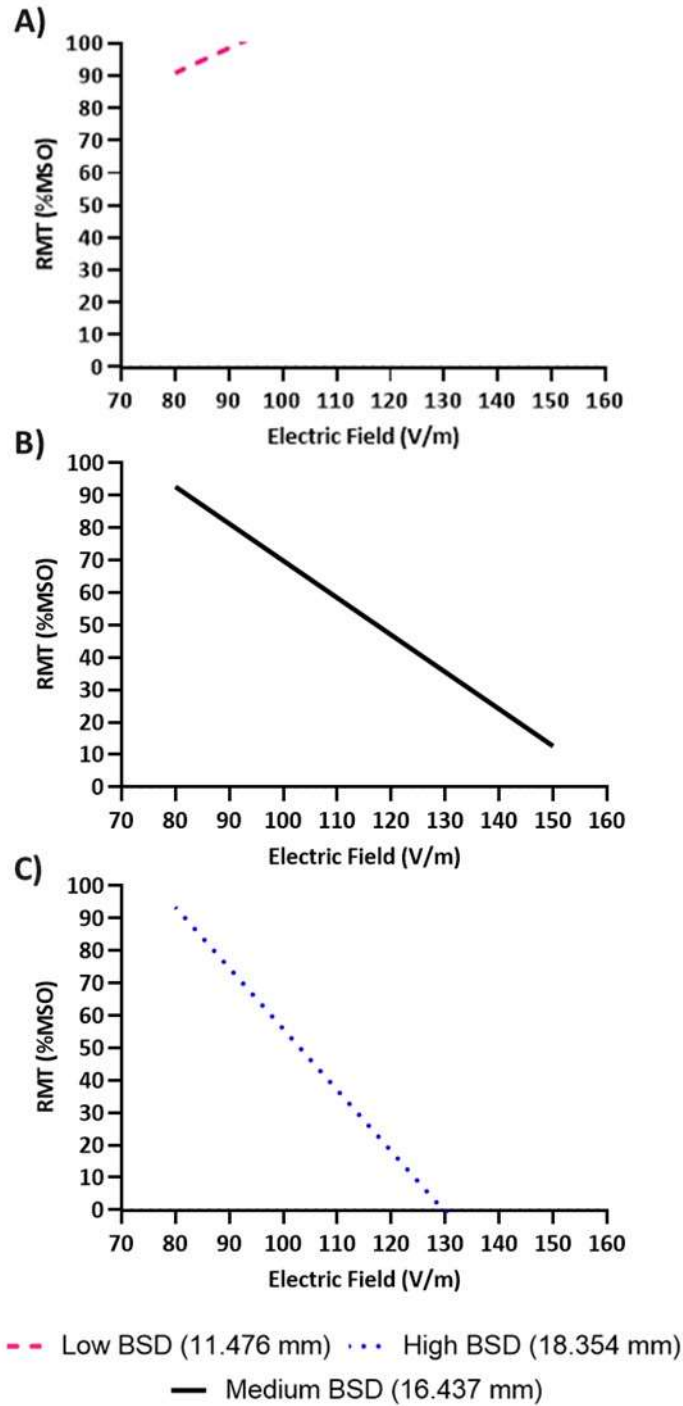


Fig 4.9: Effect of brain scalp distance (BSD) on empirically measured RMT of the biceps. (A) At lower BSD, RMT was not dependent on electric field strength (EFS), as evidenced by the reversal of the simulated relationship seen at other BSD magnitudes and calculated RMT's greater than 100% MSO. (B) As BSD increased and ultimately (C) at high BSD, RMT was increasingly negatively correlated with EFS.

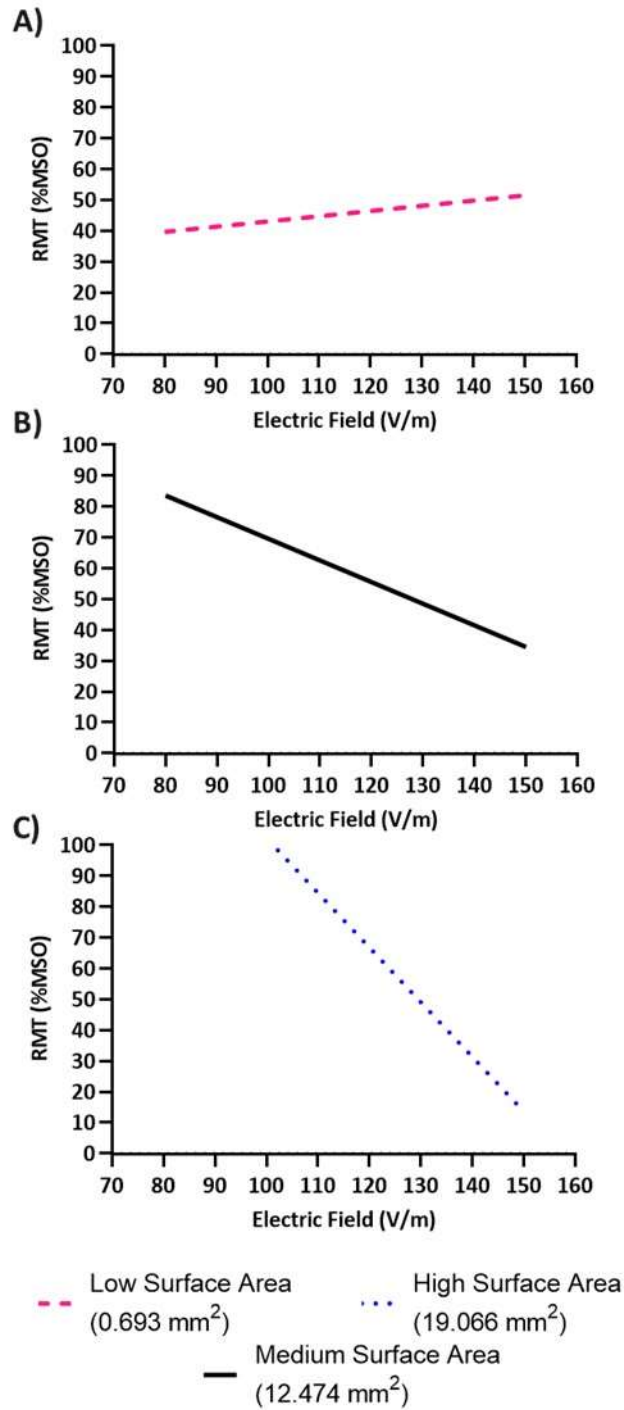


Fig 4.10: Effect of fiber tract surface area (FTSA) on empirically measured RMT of the biceps. (A) At lower FTSA, RMT was not strongly dependent on electric field strength (EFS). (B) As FTSA increased and ultimately (C) at high FTSA, RMT was increasingly negatively correlated with EFS.

4.5.3 Effect of neuroanatomy on empirically measured change in nMEPs of the FDI after iTBS

There was no groupwise effect of iTBS on the FDI in this cohort ($\chi^2 = 1.48$, $p = 0.223$) (Figure 11). Post-iTBS change in FDI nMEPs correlated with the interaction between stimulation type (sham or active iTBS) and the following: RMT ($\chi^2 = 24.79$, $p < 0.001$); EFS ($\chi^2 = 11.21$, $p = 0.001$); BSD ($\chi^2 = 8.13$, $p = 0.004$); and FTSA ($\chi^2 = 6.48$, $p = 0.011$) (Fig 4.11). There was no effect of TFC ($\chi^2 = 1.26$, $p = 0.262$).

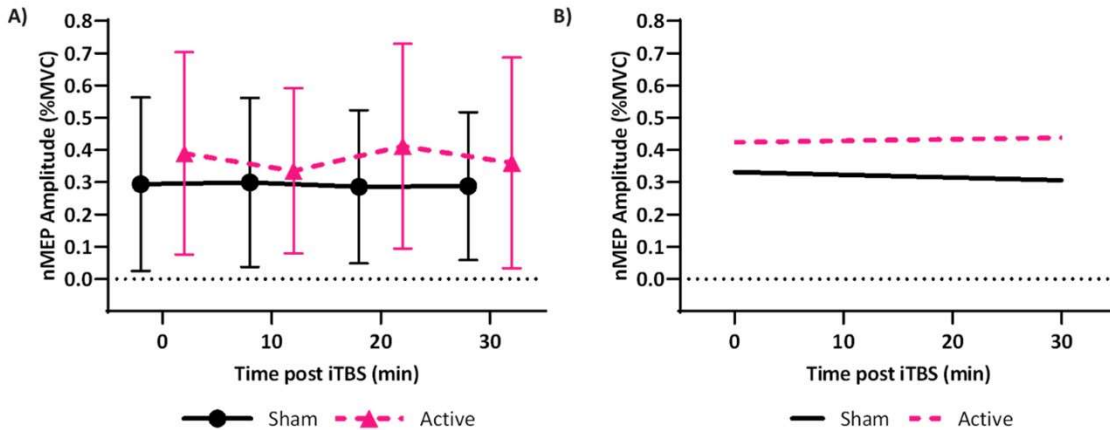


Fig 4.11: Effect of neuroanatomy on empirically measured change in nMEPs of the FDI after iTBS. (A) Mean FDI nMEP across the cohort is shown for each time point (error bars represent 1 standard deviation, 0 minutes represents the baseline). (B) Simulated nMEP are shown, from the linear mixed effects model containing significant interactions between iTBS stimulation type (active or sham) and neuroanatomical parameters. nMEP amplitude after iTBS positively correlated with RMT, EFS, FTSA, and negatively with BSD.

4.5.4 Effect of neuroanatomy on empirically measured change in nMEPs of the biceps after iTBS

iTBS had a facilitatory effect on the biceps ($\chi^2 = 6.12$, $p = 0.013$) (Fig 4.12). Post-iTBS change in biceps nMEPs correlated with the interaction between stimulation type (sham or active iTBS) and the following: RMT ($\chi^2 = 180.27$, $p < 0.001$); FTSA ($\chi^2 = 19.11$, $p < 0.001$); and TFC ($\chi^2 = 52.18$, $p < 0.001$) (Figure 12). There was no effect of EFS ($\chi^2 = 0.08$, $p = 0.784$) or BSD ($\chi^2 = 1.49$, $p = 0.223$).

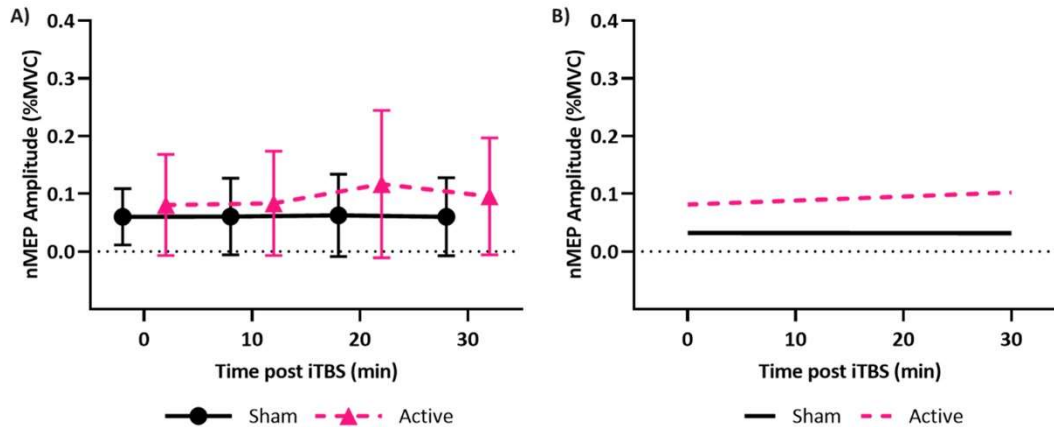


Fig 4.12: Effect of neuroanatomy on empirically measured change in nMEPs of the biceps after iTBS. (A) Mean biceps nMEP across the cohort is shown for each time point (error bars represent 1 standard deviation, 0 minutes represents the baseline). (B) Simulated nMEP are shown, from the linear mixed effects model containing significant interactions between iTBS stimulation type (active or sham) and neuroanatomical parameters. nMEP amplitude after iTBS positively correlated with FTSA and TFC, and negatively with RMT

4.6 Discussion

The aim of this preliminary study was to determine how individual neuroanatomy would affect the response of motor targets (FDI and biceps brachii) to single pulse TMS and iTBS paradigms. Identifying individual neuroanatomical characteristics that influence treatment response has the potential to inform future studies implementing iTBS techniques as a clinical treatment. Overall, response to both single pulse TMS and iTBS, of both the FDI and the biceps, depended on individualized neuroanatomical MRI-derived parameters: EFS, FTSA, TFC, and BSD.

First, we hypothesized that RMT in the biceps and FDI would negatively correlate with the magnitude of the induced electric field, with fiber tract geometry affecting this relationship. This hypothesis was partially supported for both FDI and the biceps. The TMS response (RMT) of the FDI was dependent on fiber tract size and simulated induced electric field, whereas the biceps RMT was independent of fiber tract size. This suggests that tract organization plays a more important role than tract density in differentiating these two motor targets and their stimulation response to TMS.

The second hypothesis, that a greater field strength would correlate to a more excitatory effect of iTBS, was also partially supported. In the biceps, iTBS had a facilitatory effect, but this response was independent of induced electric field and BSD which represent cortical current. Instead, the excitatory effect of iTBS on the biceps correlated negatively with RMT, thus scaled with target sensitivity to TMS. Excitation was also greater in the presence of larger fiber tracts. In the FDI, however, there was no groupwide facilitation of iTBS. The FDI response was inversely related to the strength of current and correlated positively with higher RMTs whereas higher induced electric field and greater TMS

responsiveness correlated negatively with the iTBS response. Larger tracts and less stimulation attenuation also contributed to the iTBS changes for the FDI.

Our final hypothesis that specific factors such as electric field strength and fiber tract geometry would differently influence the response from the two motor targets (biceps and FDI) due to differences in cortical architecture, was also supported. The responses of the motor targets were variable, and response to TMS was not described sufficiently by BSD alone. iTBS of the biceps was more dependent on fiber tract parameters, while the smaller effect on the FDI was dependent on induced electric field. BSD was an influencing factor in some cases, negatively correlating with biceps RMT and with increase in corticomotor excitability after iTBS in the FDI, but less consistently so than the model-derived parameters of electric field and fiber tract geometry. In the biceps, the effect of increasing BSD was to decrease RMT, contrary to expectation and to the electric field intensity, which highlights the limitations of using a single dimensional distance-based metric to represent the complex tissue mediums through which the stimulation passes. Electric field intensity based on accurate head and brain anatomy provides further nuance for the calculation and therefore is more consistent with the empirical effect of TMS.

These results suggest that MRI-based measures of neuroanatomy have predictive value in the selection of TMS targets and confirm that cortical architecture is fundamentally influential in the motor system's response to neuromodulation paradigms. The parameters presented are predictive both in a homogeneously responsive group (biceps target) and a heterogeneously responsive group (FDI target) with regards to empirical response to both single pulse TMS and iTBS. This supports the proposition that individual anatomy plays a prominent role in TMS mechanisms.

The value of MRI-based measures of neuroanatomy has numerous clinical implications. TMS and iTBS have seen increased use in recent years, especially in patients presenting with a variety of neurological and neuropsychiatric disorders [222], [223]. Our findings regarding the importance of individual neuroanatomy in treatment response address treatment response variability and provide a path forward for future work [223]. Neuroimaging techniques have been proposed [224] to assist in the identification of motor targets or potential patients who, based on individual brain anatomy, are most likely to benefit from iTBS based therapies [79], [80]. Diffusion-weighted methods like DTI, provide an avenue through which to control for the individual differences that may underlie previous inconsistent evidence [225]–[227]. Although this work is a preliminary investigation, these findings support the use of neuroimaging-derived techniques to inform the application of TMS treatment in clinical populations beyond the scope of neuronavigation. Furthermore, emerging neuroimaging techniques, such as Neurite Orientation Dispersion and Density Imaging (NODDI), also have great potential to further address variability that may be arising from individual differences. NODDI is a relatively new in-vivo diffusion MRI-based analysis technique that allows for the estimation of microstructural complexity of dendrites and axons [228]. NODDI is one method for avoiding the well-documented issues in diffusivity estimations that arise when DTI-based estimation techniques are used on complex white matter structures [228], [229]. Given our previously noted results indicating the importance of fiber tract count

in RMT, it is possible that techniques (e.g., NODDI) that account for the microstructural complexity of white matter tracts could further shed light on this issue.

Other analysis techniques might also offer a unique perspective on the issue of individual variability in TMS treatment response. Fiber based analysis (FBA) is a new analytical technique that uses diffusion-weighted MRI data to assess white matter micro- and macrostructure. FBA generates three primary metrics: fiber density (microstructure), fiber/bundle cross-section (macrostructure), and a combination of the two (fiber density and fiber/bundle cross-section) [230]. Given the similarity between FBA and the measures generated in the present work, it is worth investigating whether a FBA-based pipeline would produce similar results to those reported here.

4.7 Limitations

This preliminary study included no clinical population as participants. The addition of clinical diagnoses to a proof-of-concept study, such as this, would make it difficult to assess whether findings were being driven by individual differences in neuroanatomy or by clinical disorders. Future work should consider applying these techniques in clinical populations. Regarding the TMS sessions, while the sham stimulation was delivered prior to active iTBS in each session to prevent any potential response to active iTBS from influencing the sham response, it is possible this decision resulted in an order effect. It is also possible that immediate effects of iTBS were not captured, as the first 10 minutes after stimulation were not evaluated. Post-iTBS time points replicated previous work and were more focused on the time frame most realistic to application in rehabilitation protocols. These would take place most likely at least with some delay after iTBS priming [38], [56], [177]. The use of MEPs to capture changes due to iTBS could be considered a limitation, even though they remain a conventional approach to measuring corticomotor excitability at the time of stimulation. iTBS promotes long-term potentiation of cortical neurons [39], [54], and multiple circuits contribute to individual MEPs making interpretation of changing amplitudes difficult [176]. With respect to the simulations, the electric field was calculated using a magneto-quasistatic solver to calculate what should be a time varying parameter in the finite element analysis. This simplification was made to account for reasonable approximation respective to available computing power. Furthermore, the simulated induced electric field was a single pulse TMS product, as we are currently unable to simulate time effects and repetitive stimulation so iTBS was not modeled. Future studies of iTBS responsiveness would benefit from simulations of cortical effects of iTBS stimulation itself.

4.8 Conclusion

This preliminary study evaluated the effects of individual neuroanatomy on RMT and corticomotor excitability after iTBS. Neuroimaging and modeling techniques were used to determine the brain scalp distance, simulated induced electrical field strength, fiber tract surface area, and tract fiber count, uniquely accurate to each participant. Our results demonstrate that these neuroanatomy-based

measures are predictive of RMT and iTBS outcomes for the biceps and FDI, albeit differently. One of the contributing factors to these differences could be the variability in the RMT and MEP data for the two muscles. Overall, individual anatomy is a driver of TMS response and MRI-based modeling can be used to select responsive TMS motor targets based on brain scalp distance, electrical field strength, fiber tract surface area and tract fiber count

5 Effect of Fiber Tracts and Depolarized Brain Volume on Resting Motor Thresholds during Transcranial Magnetic Stimulation

5.1 Authors and Submission Details

N. Mittal, C Lewis, Y Cho, CL Peterson, RL Hadimani, “Effect of Fiber Tracts and Depolarized Brain Volume on Resting Motor Thresholds during Transcranial Magnetic Stimulation”, Submitted to *Transactions on Magnetics* 10-29-2021. Submission ID: MAGCON-21-10-0644, linked to 2022 MMM-INTERMAG Conference Abstract IOH-14.

IRB Approval: VCU IRB HM20018505

Clinical Trials Registration: clinicaltrials.gov NCT04586387

5.2 Abstract

Transcranial magnetic stimulation (TMS) is a treatment procedure for some neuropsychiatric disorders, and has been used for brain mapping, as well as diagnosis and treatment of neuromuscular dysfunctions. There is a disconnect between TMS modeling and clinical data: several groups have reported the simulated induced electric field and measured resting motor threshold (RMT) with inconsistent results in the relationship between RMT and brain scalp distance (BSD). This necessitates the use of simulation parameters that further account for individual differences in neuroanatomy. We recruited 10 healthy subjects and obtained empirical RMT, magnetic resonance images (MRI), and diffusion tensor images (DTI). We developed anatomically accurate brain models from MRI and simulated TMS to determine the percent depolarized grey matter volume (DVG) from TMS induced electric fields. Corticospinal fiber tracts were extracted from the primary motor cortex from DTI to obtain fiber tract surface areas (FTSA) for each participant. Linear mixed effects models were used to evaluate the effect of DVG and FTSA on RMT. We report that DVG correlates with RMT when accounting for corticospinal FTSA.

5.3 Introduction

Finite Element Modeling (FEM) simulations of transcranial magnetic stimulation (TMS) using complex head models and coils have been used to better understand neuromodulation strategies. TMS is a promising neuromodulation paradigm for brain mapping, diagnostics, and treatment of neurological and psychiatric disorders [6], [200]–[202], [224]. However, it is limited by high intra- and inter-subject variability in its effects [38], [56], [57], [70]–[72], [78], [204], [205], [224]. Methods of modeling derived from magnetic resonance imaging (MRI) have been used with TMS to tailor stimulation protocols [224], and to connect individual neuroanatomy to variations in response by measurement of the brain scalp distance (BSD) [79], [81]. BSD however, as a single dimensional measurement, fails to account for the composition of tissue between the scalp and cortex. Induced electric field strength (EFS) from the

magnetic field generated by the TMS coil, however, is a 3-dimensional parameter and accounts for greater complexity of tissue organization [80].

Individual differences in neuroanatomy will influence TMS response as the induced electric field is dependent on the brain morphology, and communication along a pathway is dependent on the fiber tracts leading from cortex to spine [8], [54], [77]–[80], [137], [183]. TMS responses from the motor cortex can be characterized by the resting motor threshold (RMT), which has two definitions. From the perspective of neuron depolarization, RMT is the stimulation intensity in % of maximum stimulator output required to induce cortical EFS of at least 100 V/m [231]. From a motor response perspective, in a clinical setting, RMT is defined as the stimulus intensity, also in % maximum stimulator output, that elicits a motor evoked potential of at least 50 microvolts in at least five out of ten consecutive stimuli [149], [150]. These definitions are linked because an EFS of at least 100 V/m is the threshold of consistent depolarization of neurons, which would lead to the motor evoked potentials. However, current simulation work has not investigated simulated EFS and RMT in the context of individual level anatomical variation while considering inter-subject fiber tracts for differences in corticospinal communication, and simultaneously compared to empirical response to TMS.

The purpose of this study was to investigate the effect of neuroanatomy on response to TMS. Specifically, RMT was recorded from human subjects to establish TMS motor response, while simulated TMS was applied to individualized, anatomically accurate head models derived from MRI of the same human participants. EFS and head models were used to calculate the percent of depolarized volume of grey matter (DVG), to incorporate cortical interconnectivity into the anatomical metric of EFS. Fiber tractography was performed to calculate fiber tract surface area (FTSA), representing the neural communication architecture along the motor pathway of interest. DVG and FTSA were compared to the empirically collected RMT. We hypothesized that RMT would negatively correlate with DVG, indicating greater TMS response with more brain volume depolarization. Furthermore, we hypothesized that the relationship between DVG and RMT would depend on FTSA.

5.4 Methods

5.4.1 Participants and Empirical TMS Sessions

Ten individuals (7 females, 3 males, 23.5 ± 5 years) participated after screening to ensure safety of the TMS and MRI protocols, and provided informed consent. Eligible participants were between the ages of 18 and 65 years old. Severe medical illness and sequelae, existing infection, cardiovascular disease, significant osteoporosis, metal implanted devices, personal or family history of seizure activity, and any acute or current history of neuromuscular or motor dysfunction were exclusionary. Participants underwent TMS sessions targeting the motor hotspot of the first dorsal interosseous (FDI) as described by Mittal et al. [204]. Each participant had 2 RMT measurements in their session, to account for intra-subject variability (see *Statistical Analysis*). This study was approved by the Virginia Commonwealth

University Institutional Review Board (Study ID: HM20018505). Clinical Trial Registration: ClinicalTrials.gov: NCT04586387.

5.4.2 MRI-Derived TMS Simulations and Modeled Parameters

Structural T1- and T2-weighted images and whole brain diffusion weighted images were acquired for head model generation and fiber tractography from diffusion tensor imaging (DTI) respectively. Extracted T1- and T2-weighted images from all the subjects passed a SimNIBS pipeline (SimNIBS Developers 2019, v2.0.1) [76], [79] to create individual segments. Abnormalities were smoothed using Meshmixer (AutoDesk, Inc. v11.2.37) (Fig 5.1).

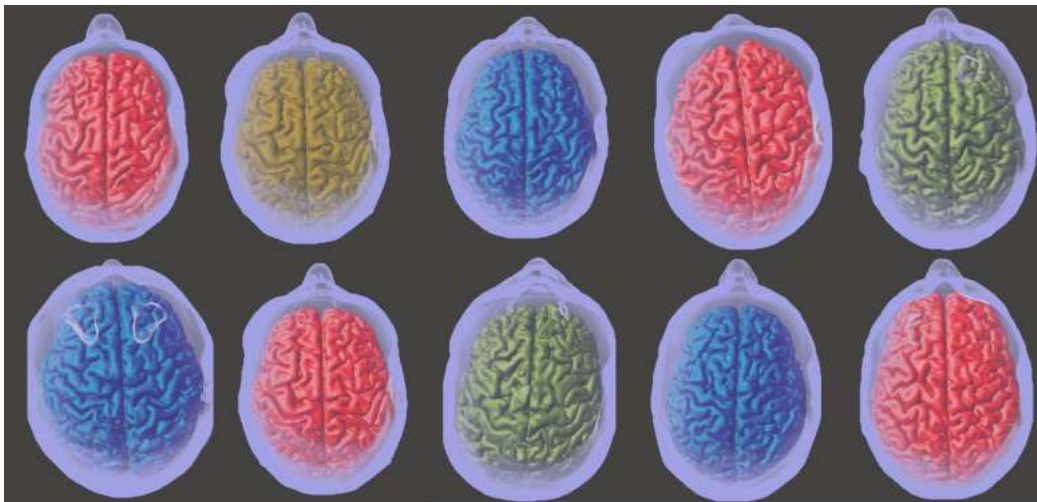


Fig 5.1: Anatomical Variation. Head models from each participant are visualized (participant ID. 1-10, from top left, across, then to bottom left and across). Each head model is distinct and made to the MRI of an individual participant.

Sim4Life finite element analysis software (Zurich Med Tech, v6.2.1.4972) was used to compute magnetic field, B , and induced electric field, E on the generated head models from peak intensity stimulation of the primary motor cortex [79]–[81], [220]. The simulated coil matched dimensions of the Magstim 70mm figure-of-8 coil [82], oriented to match the empirical setup (Fig 5.2), targeting the precentral gyrus posterior to the superior frontal sulcus, within the “knob” as defined by Yousry et al. [221].

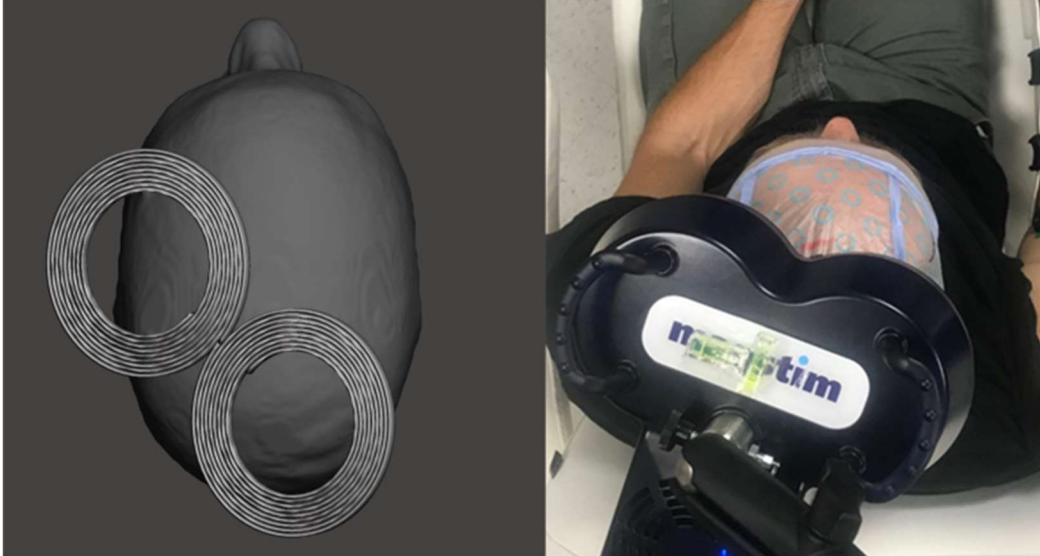


Fig 5.2: Coil Positioning. Left: The simulated coil is placed to induce a monophasic anterior-to-posterior current on the cortex, maximally over the region of upper motor control in the primary motor cortex. Right: TMS session setup for coil placement after adjustments to find the optimal empirical point of target.

The stimulation current strength was set to 5000 A, corresponding to 100% MSO, at 2,500 Hz [80] and the segments of the head model and air were assigned material properties based on the IT'IS LF database (IT'IS Foundation, v4.0). Electrical conductivity of grey matter, white matter and cerebrospinal fluid were 0.24 S/m, 0.27 S/m and 1.78 S/m respectively. The relative permeability of all the materials (to air) was 1. The magnetic stimulation was calculated based on stimulator and model material parameters (Fig 5.3). Induced electric field strength (EFS) at the surface of the cortex, specifically of the grey matter segment, was interpolated (Fig 5.4), and the grey matter electrical field vectors for each voxel were extracted [80]. The root mean square (RMS) was calculated to find the EFS at each individual voxel for the grey matter. DVG was found by calculating the percent of voxels above the threshold of 100 V/m using MATLAB (MathWorks, MATLAB v 9.7.0.1190202).

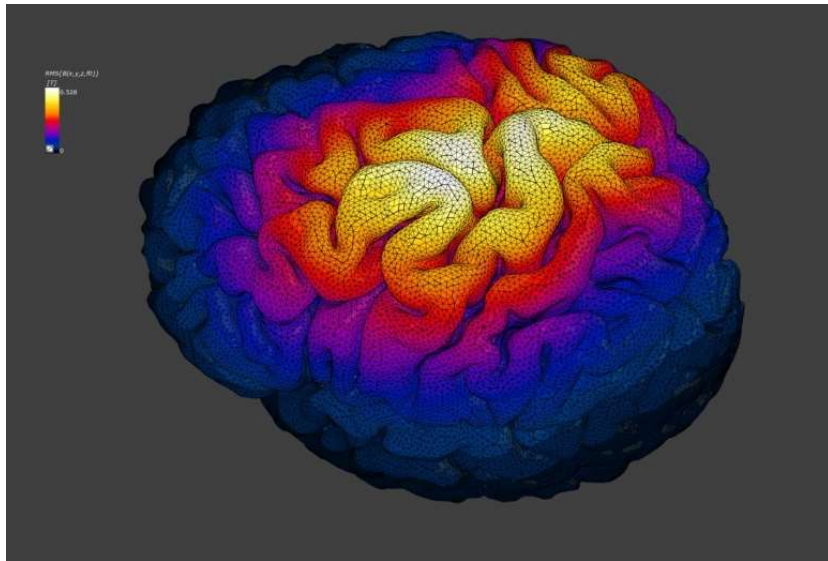


Fig 5.3: Simulated Magnetic Field on Cortex (Sagittal Plane). The magnetic field generated by the TMS coil was generated within the head model. Magnetic field strength (B-field) was determined based on the coil parameters, positioning, and material mediums in the head models. Maximal stimulation was located over the upper limb motor control region of the primary motor cortex. White is maximum B-field, 0.528 T, to dark blue, 0 T.

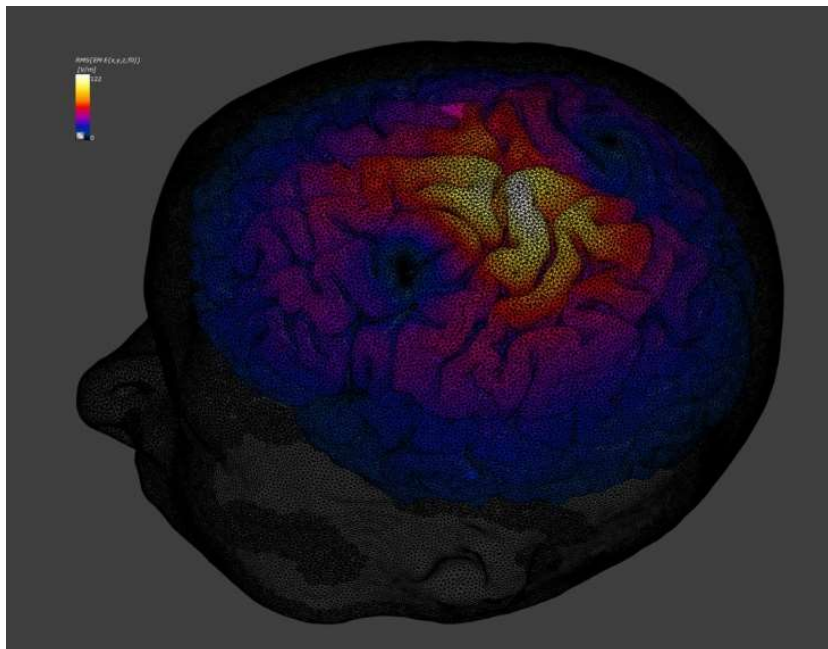


Fig 5.4: Induced Electric Field Strength on Cortex (Sagittal Plane). Finite element simulations of magnetic stimulation delivered to individual head models were performed to calculate electric field strength (EFS) based on the magnetic field. Maximal stimulation was located over the upper limb motor control region of the primary motor cortex. White is maximum EFS, 122 V/m to dark blue, 0 V/m.

Fiber tracts were extracted from DTI using DSI Studio (Feh, DSI Studio, 2020) based on the anatomical landmarks (superior frontal sulcus, precentral sulcus, central sulcus, and precentral gyrus) to

the “knob” of the primary motor cortex [221]. A 6 mm diameter region of interest seeded extraction of fibers [83] (Fig 5.5). Fiber coordinates were then imported into SolidWorks (BIOVIA, Dassault Systèmes, SolidWorks, SP3.0, San Diego: Dassault Systèmes, 2017) to calculate FTSA for each model’s fiber tract.

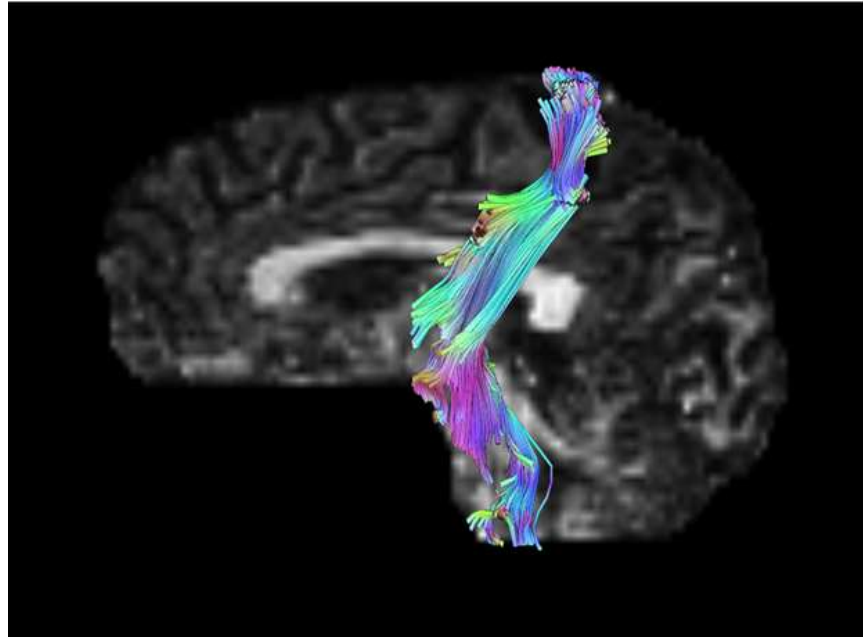


Fig 5.5: Fiber Tractography. Corticospinal fiber tracts were extracted from DTI beginning from a region of interest that encompassed upper limb motor control in the primary motor cortex.

5.4.3 Statistical Analysis

Spearman’s correlation tested for simple relationships between either DVG or FTSA and RMT. Linear mixed effects models tested for relationships between DVG and FTSA and their effects on RMT in R (The R Foundation, v3.4.3) [153], [154]. Participants were included in the statistical model due to having two measurements for each, as a random effect to account for intra-session, intra-subject variability between multiple RMT measurements in a single session and from a single individual.

5.5 Results

5.5.1 Magnetic field, B and induced electric field E

Magnetic field, B and electric fields, E were calculated in all the regions of the brain of the 10 subjects. The peak fields in all subjects were determined below the figure of eight coil on the upper limb control area of the motor cortex where we intended to target. Table 5.1 below shows the variation of B and E fields of all ten subjects. These values are similar to the reported B and E field values reported in the literature by other researchers [82], [232]–[234].

Table 5.1: Simulation parameters for each participant.

Participant	B^a	E^b	DVG^c	FTSA^d
01	0.528	122	0.18	12.5
02	0.412	90.5	0.00	2.7
03	0.442	112	0.07	18.2
04	0.435	122	0.11	19.1
05	0.519	147	0.27	11.0
06	0.415	87.8	0.00	11.0
07	0.425	92.2	0.00	0.7
08	0.512	110	0.26	19.9
09	0.471	116	0.12	15.6
10	0.501	113	0.11	14.2
Mean ± SD	0.4660 ± 0.045	111.3 ± 17	0.110 ± 0.00	12.48 ± 6.5

a) B: magnetic (B) field strength, presented in T; b) E: electric (E) field strength, presented in V/m; c) DVG: depolarized volume of grey matter, presented as percent total volume grey matter; d) FTSA: fiber tract surface area, presented in mm².

5.5.2 TMS Response (RMT)

Table 5.2 shows the FDI RMT of ten subjects along with their age, and both RMTs for each session. Maximum RMT recorded was 78% of the maximum stimulator output/power. Minimum RMT recorded was 33% of the maximum stimulator output/power. There was no correlation between RMT and DVG alone ($p = 0.17$). There was no correlation between RMT and FTSA alone ($p = 0.9$).

Table 5.2: Resting motor threshold (RMT) for each participant.

Participant	Age	FDI RMT^a	
01	21	46	49
02	24	41	41
03	19	68	55
04	20	64	64
05	23	72	78
06	19	70	50
07	32	43	43
08	26	41	33
09	29	54	51
10	27	70	68
Mean ± SD	23.5 ± 5	56.9 ± 13	53.2 ± 14

a) RMT: resting motor threshold, presented as percent of maximum stimulator output. Both values were taken during the same session, spaced approximately one hour apart.

5.5.3 Effect of DVG or FTSA on RMT

DVG and FTSA values can be found in Table 5.1. There was no correlation between RMT and DVG alone ($p = 0.17$). There was no correlation between RMT and FTSA alone ($p = 0.9$). DVG and FTSA values can be found in Table 1.

5.5.4 Interaction between DVG and FTSA

Interactions with FTSA revealed a correlation between RMT and DVG ($p < 0.001$). RMT negatively correlated with DVG, but only at high FTSA. The correlation became less negative as FTSA decreased, until a positive correlation was observed at the lowest FTSA range. These relationships can be seen in Fig 5.6.

DVG and FTSA were positively correlated ($p = 0.013$).

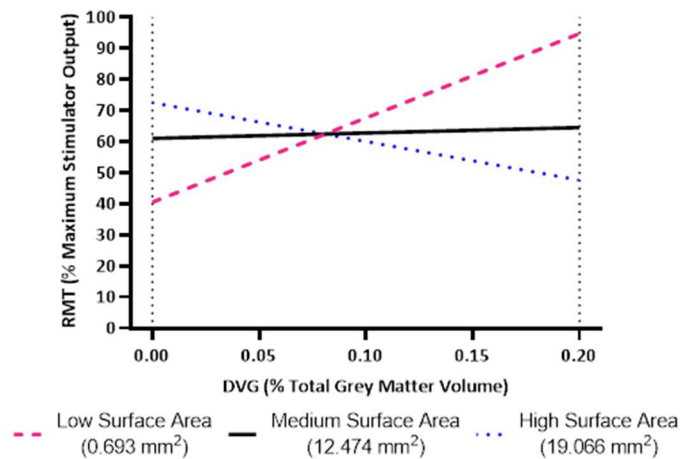


Fig 5.6: Effect of depolarized volume of grey matter (DVG) on RMT. RMT was found to correlate with DVG when accounting for fiber tract geometry in the form of fiber tract surface area (FTSA). Larger tracts exhibited the expected negative correlation between RMT and DVG given the equation: $RMT_{V/m} = -124.52 * DVG_{\% \text{ bra volume}} + 72.45$.

5.6 Discussion

The objective of this preliminary study was to investigate the relationship between modeled brain depolarization volume above a threshold electric field (DVG), and empirical TMS responsiveness (RMT). A secondary objective was to determine the influence of fiber tract geometry (FTSA) on the empirical TMS responsiveness to brain depolarization. The hypothesis that RMT would correlate negatively with DVG was partially supported; this relationship was found with a negative correlation between RMT and DVG, but only when accounting for fiber tract geometry, with larger fiber tracts (high FTSA).

This interaction suggests that the expected relationship between brain depolarization and TMS evoked motor response is dependent on the connectivity within the cortex. That is, more depolarized brain results in more motor activity, under the right condition (which is large FTSA). High DVG and low RMT both would be expected in a more responsive anatomical architecture, while larger fiber tracts would be expected to effectively transmit this from the cortex. The correlation between DVG and FTSA support this: both parameters would indicate aspects of neural connectivity. Thus when both the DVG and FTSA are large, RMT is decreased. RMT depends on DVG in a predictively linear fashion, as long as FTSA is taken into account, but when fiber tracts are smaller, the relationship between brain depolarization and motor output requires further investigation.

This was a preliminary study with some limitations, and future work is needed. This study is limited by a small sample size that included no subjects with brain disorders. The effects of neuropathology on the relationships investigated would be essential to ascertain before developing treatment paradigms. However, the addition of diagnostic variables to a proof-of-concept study would make it difficult to characterize the interaction of these parameters at baseline. Furthermore, electric field strength is a time-varying parameter, but was evaluated using a quasi-static solver for finite element analysis, due to computational limitations. Lastly, DTI was used for proof-of-concept, but future study with more sophisticated methods, such as neurite orientation dispersion and density imaging [228] or fixel based analysis [230] would allow for greater insights of effects of individual variability in neuroanatomy.

Our results show that the effects of TMS are governed by cortical organization due to anatomy and fiber tract geometry. Further investigation is needed to understand the mechanistic drivers of the relationship between depolarized brain volume and RMT at different fiber tract sizes.

6 Motor Neural Circuit Simulated Response to iTBS

6.1 Script Repository

Function Library: Open Science Framework –

https://osf.io/6mxcd/?view_only=5479c48acfa542888e1f4741c32e80f1

This library is being updated as further work is done on the model.

6.2 Context Overview: Existing Simulation in Neural Circuits and TMS

Mechanistic understanding of TMS-based paradigms such as iTBS is incomplete [63], [84]. While individual neuroplastic changes, either LTP-like plasticity or disinhibition, have been modeled on their own or in disorganized connection clouds of neurons, they have not been combined or expressed within the context of organized cortical communication [63], [84], [98], [99]. Existing iTBS models that do address synaptic plasticity are limited to a single mechanism which would fail to capture both the excitation effects of LTP and the interneuron inhibition of disinhibition regardless of the cellular organization. Furthermore, when simulations have attempted increasing complexity or scope with regards to the size of the neuron population being studied, the organization is population-based, and statistically weighted with simple excitation/inhibition connections in a cloud, and lacking relevance to physiological cortical organization [99], [100]. As a whole, these studies have done little to address how iTBS would affect a fundamental neural unit of motor control.

A neural circuit represents the simplest building block of complex cortical networks, and the smallest subunit of a discrete neural activity; this has not been used as a framework for studying TMS-induced neuroplasticity [98], [99], [135].

6.3 Specific Examples of Simulation Work and Theory: TMS, Neural Circuits, Hodgkin Huxley

6.3.1 Hodgkin Huxley Simulations and the Relationship to Neural Circuits and TMS

Hodgkin Huxley style membrane models of cellular membrane potentials have contributed to understanding neuron function. Wang, et al. presented an ionic conductance model of neocortex to show the physiological relevance of these constructs and how membrane ion channel parameters governed unique neuron spike patterns [235]. The presentation of neurons in general was done with greater complexity, albeit in a crustacean cardiac pacing neuron, by Ball, et al. to show that individual neuron compartments and unique individual cell parameters could be used to accurately model a network of autonomically spiking cells [97].

From the work of Ball, et al. to the formation of neural circuits via Hodgkin Huxley membrane models was an obvious step [119]. As stated by Catterall, et al., this framework shows the conditions governing cellular level activity with regards to action potentials, making it highly relevant to the design and study of neural circuit models. Static cortical circuits were studied in isolation by Konstantoudaki, et

al., whereby a complex network was constructed using unique excitatory cell types to represent different pyramidal cells, and 3 different types of interneurons, each with unique parameters [135]. This network was able to provide insights on network inhibition, with the researchers concluding that somatic inhibition provided valuable pacemaker timing to the output of complex networks. This model was static, with hardwired behavior for each cell in the network and not meant for scaling or tuning applications.

TMS motor thresholds were modeled using a coarse representation of the head as a mesh of Hodgkin Huxley axons [236]. This model provided evidence of a strong relationship between Hodgkin Huxley membrane behavior and TMS response, though without any context of synaptic function and neuroplasticity.

6.3.2 Neural Circuits and Specific Ties to Motor Learning Neuroplasticity

Neural circuits have been applied to explaining the function of behavior and learning. Lerner, et al. expressed motor learning as a function of change in striatal circuits [126]. These effects have been linked to changes in the structure of motor cortex synapses in rodent models, which Xu, et al. presented was due to motor cortex circuitry changes [237]. Papale & Hooks showed that neural circuits of the motor cortex specifically changed during skill acquisition in a rodent model [91]. They related the outcomes of motor training to structural changes in both local and long-range circuitry.

6.3.3 Large Scale Cellular Network Modeling

Presenting the complexity of neural populations as large volumes of interconnected and nonuniform cells has followed two primary routes. First, weighted mass models represent populations as aggregates. Bhattacharya, et al. modified a kinetic representation of neurotransmitter function to capture neurotransmission dynamics that may differ in populations [117]. Specifics in mass models differ, but the goal is to use a single representation for an ensemble of identical neurons, due to their proximity in space, function, and timescale of action. This approach is effective for capturing neurotransmitter governed firing rates of simple neuron populations and regional level organization but does not effectively capture synaptic level effects. Alternatively, cloud models of population-based connections, such as that used by Wilson, et al., capture the unique relationships between excitatory and inhibitory neurons [238]. These models specifically define the behavior of the individual neuron types and use large clouds of interconnected networks that are determined based on the desired levels of neuron interconnectivity and relative populations of inhibitory and excitatory neurons. These models effectively capture general population behavior, but they lack uniform organization and are ultimately limited by their randomized interconnectivity. While they have captured the effects of LTP, for example, there is no functional subunit of relevance that can be studied to determine the most discrete level of neuromodulation effect or any imposed structure for testing a specific cortical organization.

6.3.4 TMS Cellular Mechanisms

The effects of TMS at a cellular level have long been studied, with simulation playing a critical role. These efforts have provided a starting point for understanding or quantifying the mechanistic effects of neuromodulation, that empirical studies of cell and cortex have illuminated. For example, Huang, et al. proposed a cellular level model of theta burst stimulation response, based on the role of intracellular calcium on cellular excitation [63]. However, this purely mathematical construct used simple exponentials as a placeholder for the many series of calcium mediated reactions and optimized numerically with parameters that lacked specific physiological meaning. This model however was based on accepted theory that such reaction behavior could be fit to exponential equations. Li, et al. expanded on this framework to account for the growing understanding that disinhibition also plays a role in the neuroplastic effects [84]. Li's work, however, provided no proposed mathematical framework or testing of the schematic, which closely resembled a canonical circuit. Other models have expanded on these principles, though not necessarily with appropriate cortical organization [238].

6.3.5 Other TMS Modeling

Non-cellular simulation of TMS is also prevalent, as looking at the entire system provides another set of insights. Syeda, et al. used simulation of TMS induced electric fields to study the effect of TMS on deep brain stimulation probes, as the electric field effects would be different in scope to that of synaptic changes [239]. Geeter, et al. combined fiber tractography with simulation of TMS induced electric fields on head models [240]. This allowed for the study of current effects along communication pathways in the brain, though without correlation to clinical measures.

6.3.6 Targeted Contributions of the Presented Model

The model defined in this project aims to continue building these tools by integrating the structure of a canonical neural circuit in a motor cortex [84] to mathematical representation of membrane potentials across multiple neurons [97] representing relevant motor cortical intercellular communication neuroplastic mechanisms [84], [135], [238]. Furthermore, the development of a discrete subunit relevant to motor learning [91] will allow for organized scaling up by the running of multiple subunits in parallel [238], which can be modified based on the balance in neurotransmitter permeabilities which results in change in cellular behavior [135]. Doing so in a MATLAB suite with an organized function library and possibly a graphical interface will enable for *in silico* testing of patterned stimulation effects such as iTBS on tailored cortical regions, represented by populations of neurons, to ultimately provide cheap and rapid exploration into treatment optimization or target selection.

6.4 Description of Completed Work

6.4.1 Approach

A conductance-based model based on the Hodgkin-Huxley model was used to convert neuron neurons into circuit diagram representations. This allowed for calculation of action potentials through a canonical neural circuit representative of motor cortex subunit output. Permeability of the membrane to unique ionic species was defined by individualized equations and published values. In the future, this network will be enabled for adaptation based on LTP and disinhibition, guided by the mechanisms of iTBS.

It was hypothesized that a canonical circuit using realistic cellular parameters can be constructed using a simple MATLAB function library, and present physiologically relevant spiking patterns, tunable by excitation of the inputter or inhibitor cells. At this time, spontaneous spiking behavior and manipulation of firing rates have been programmed, pre-neuroplastic mechanisms, supporting this hypothesis with a tunable output simple circuit.

6.4.2 Baseline Hodgkin & Huxley – Derived Functionality of a Canonical Neural Circuit

A proof-of-concept model has been generated to show the feasibility of describing unique cellular constituents in MATLAB and connecting them with response to an exogenous current. The circuit comprises one superficial excitatory pyramidal neuron (layer 2/3, L23), one fast-spiking parvalbumin expressing interneuron (IN), and one deep excitatory pyramidal neuron (layer 5, L5) (Fig 6.1).

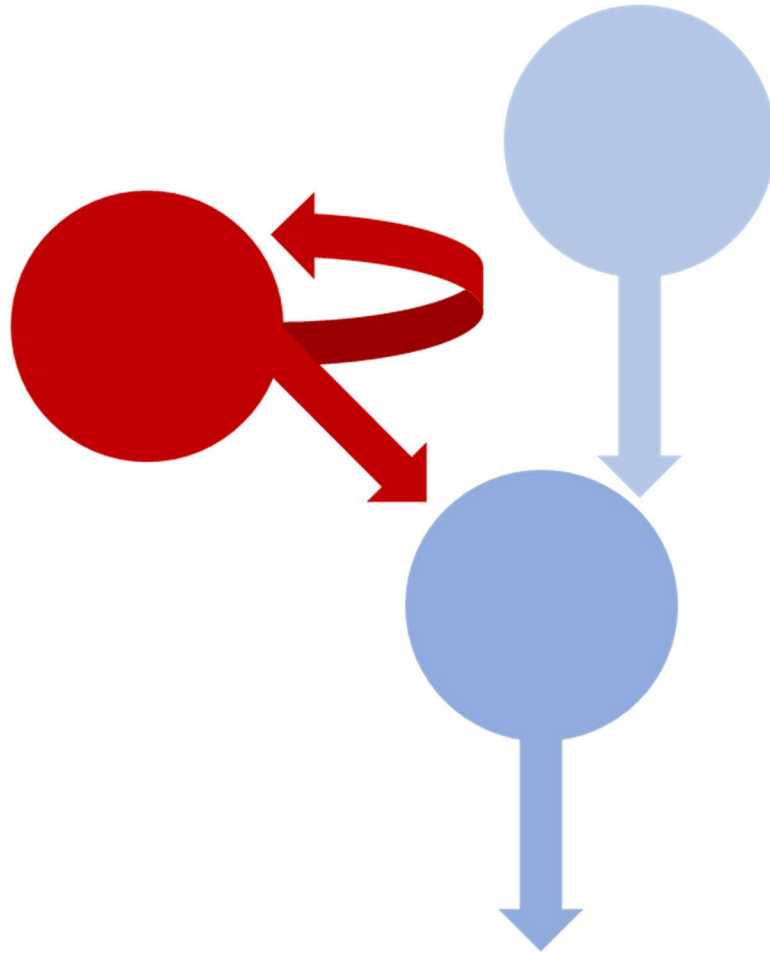


Fig 6.1: Schematic, Cell Circuit Organization. Blue represents excitatory cells, red represents inhibitory. Axons are presented as arrows directed from their cell of origin to their target. A canonical neural circuit contains an initiator (top right, light blue), an outputter (bottom, blue), and an inhibitor (left, red). In this circuit, the inhibitor directs an axon back toward itself to represent the connections of disinhibition, where an autapse represents the self-directed inhibitory signal. Both the initiator and inhibitor project axons to the outputter.

Cell membranes are treated as capacitors, and Kirchoff's law is used to express the current across the membrane as the sum of the ionic and exogenic currents. Resistance to ionic current is the inverse of permeability to ionic flow (G), thus each ion current is a function of its permeability. A voltage gradient is generated for each ion based on the current membrane voltage and each ion's Nernst (equilibrium, E) potential. Equations governing the behavior of membrane currents are shown in Table 6.1, with specific values for channel subunit probabilities and equation parameters taken from literature [97], [106], [116]. A circuit diagram of the neural circuit is shown in Fig 6.2.

Table 6.1: Equations for Membrane Modeling.

(1)	$I_{ion} = G_{ion} * (V_{ion} - E_{ion})$
(2)	$\frac{dx}{dt} = \frac{x_{\infty}(V) - x}{\tau(V)}$
(3)	$I_{Axon} = I_{inject} - \sum_i (I_{ion})$
(4)	$I_{ion} = S_{neurotransmitter} * (V_{neurotransmitter} - E_{neurotransmitter})$
(5)	$\frac{ds}{dt} = k_f \frac{1}{1 + e^{\left(\frac{V_{spre}}{2}\right)}} (1 - s) - k_r s$
(6)	$I_{NMDA} = g_{NMDA} \left(\sum_i s_i \right) \frac{V_d - E_{NMDA}}{1 + 0.15e^{(-0.08(V_d - E_{NMDA}))}}$
(7)	$\frac{ds}{dt} = k_f \frac{1}{1 + e^{\left(\frac{-V_{spre}}{2}\right)}} (1 - s) - k_r s$
(8)	$I_{cell} = C_{Membrane} * \frac{dV_{Membrane}}{dt} = (I_{inject} - I_{Axon} - \sum_i (I_{neurotransmitter}))$

(1) – General Current Equation; (2) – Calculation of Ionic Channel Subunit Activation State; (3) – Axonal Current, Independent of Dendritic Channels; (4) – Neurotransmitter Channel Current (AMPA, GABA); (5) – Calculation of Gating Fraction for AMPA and GABA; (6) – NMDA Channel Current; (7) – Calculation of Gating Fraction for NMDA; (8) – Total Cell Membrane Current at Axon; k_f , k_r – Rate Constants; x : Ionic Channel Subunit; x_{∞} : Equilibrium State of x ; V_{spre} : Presynaptic Membrane Voltage

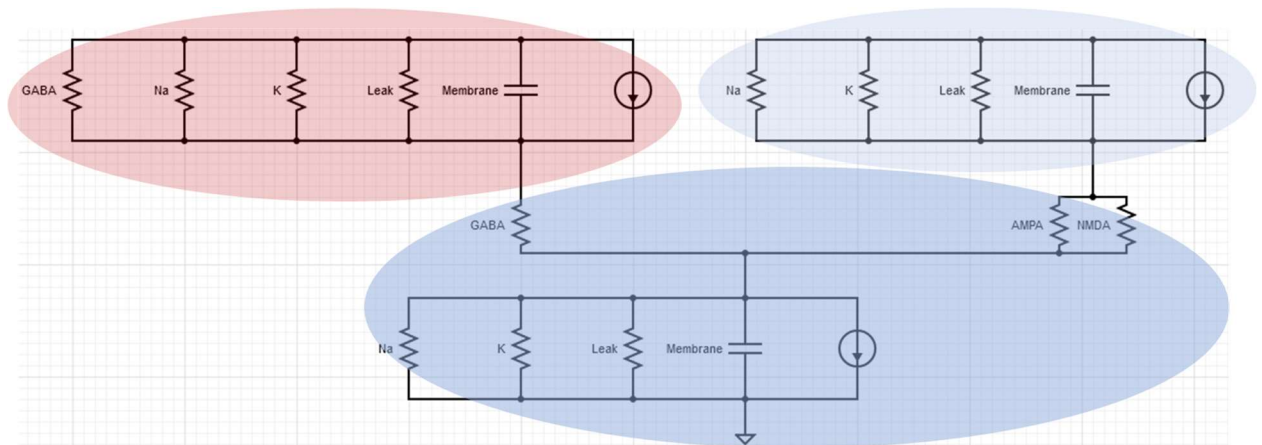


Fig 6.2: Schematic, Circuit Diagram. The three cells are represented as circuit diagrams for their respective ion or neurotransmitter channel mediated currents: initiator (top right, light blue), outputter (bottom, blue), and inhibitor (left, red). Excitatory synapses are represented postsynaptically as AMPA and NMDA channels while inhibitory synapses are postsynaptically represented as GABA channels.

The instantaneous permeability of the membrane to each ion is a voltage dependent probability distribution, that when taken across the population of receptors, can be used to calculate the approximate percentage of open channels at a given voltage. The current across the capacitor is the output current for the compartment (Table 6.1) [97], [106].

Neurotransmitter equations for glutamate and gamma aminobutyric acid (GABA) are more complex, relying on a gating probability rather than subunit activation. They share the same general form, with a gating parameter (s) in the current equation. The gating parameter, s , is a function of presynaptic voltage, thus linking the presynaptic and postsynaptic membranes. To capture the hyperpolarization/depolarization characteristics of NMDA channels, they have further expressions in a denominator, or a scaling factor (Table 6.1) [116], [117].

At this time, all cells have been scripted and linked, with appropriate subunit equations. The result is a membrane that accepts an exogenous current and generates an axonal output, for each cell, networked by synaptic equations. This network displays basic physiological function of a spiking network of cells, where the outputting cell's spike rate can be tuned by the excitation or inhibition of upstream signals. See Figures 6.3, 6.4, 6.5.

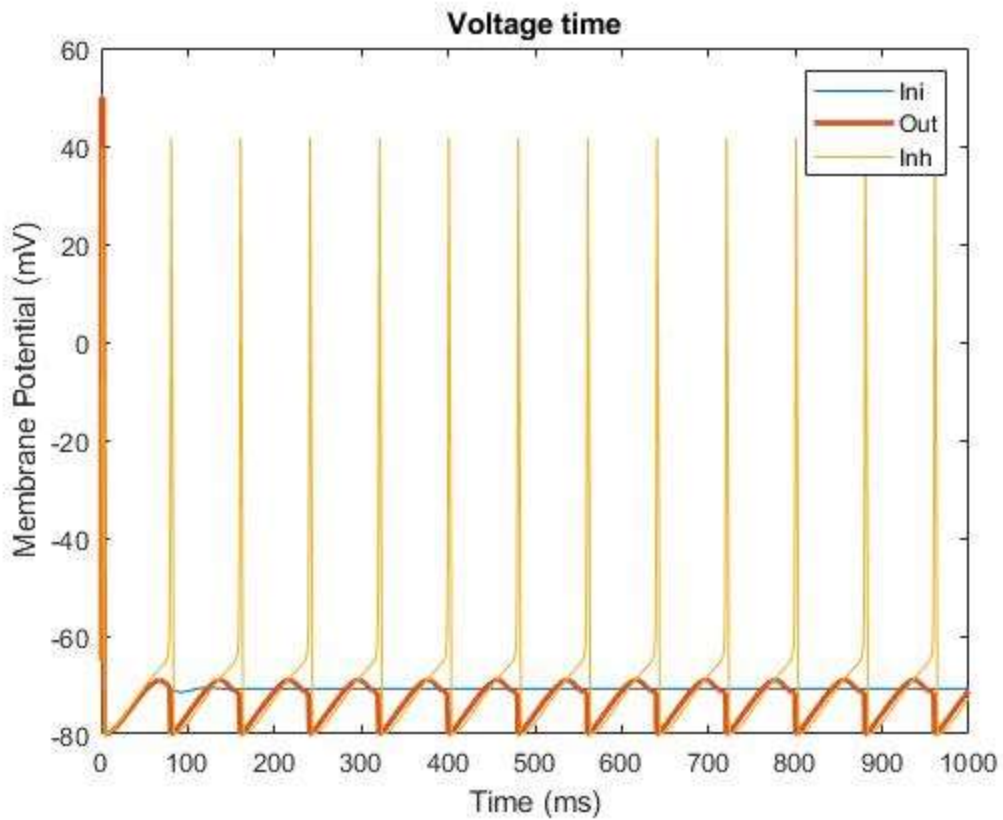


Fig 6.3: No initiator spiking. No spiking from the initiating cell results in no autonomous spiking behavior: a group of physiologically inert cell. The lack of initiator input yields no output from the outputting cell. Inhibitor cell spike pattern is unaffected, starting at a sample rate of 12 Hz. Ini: Initiator; Out: Outputter; Inh: Inhibitor.

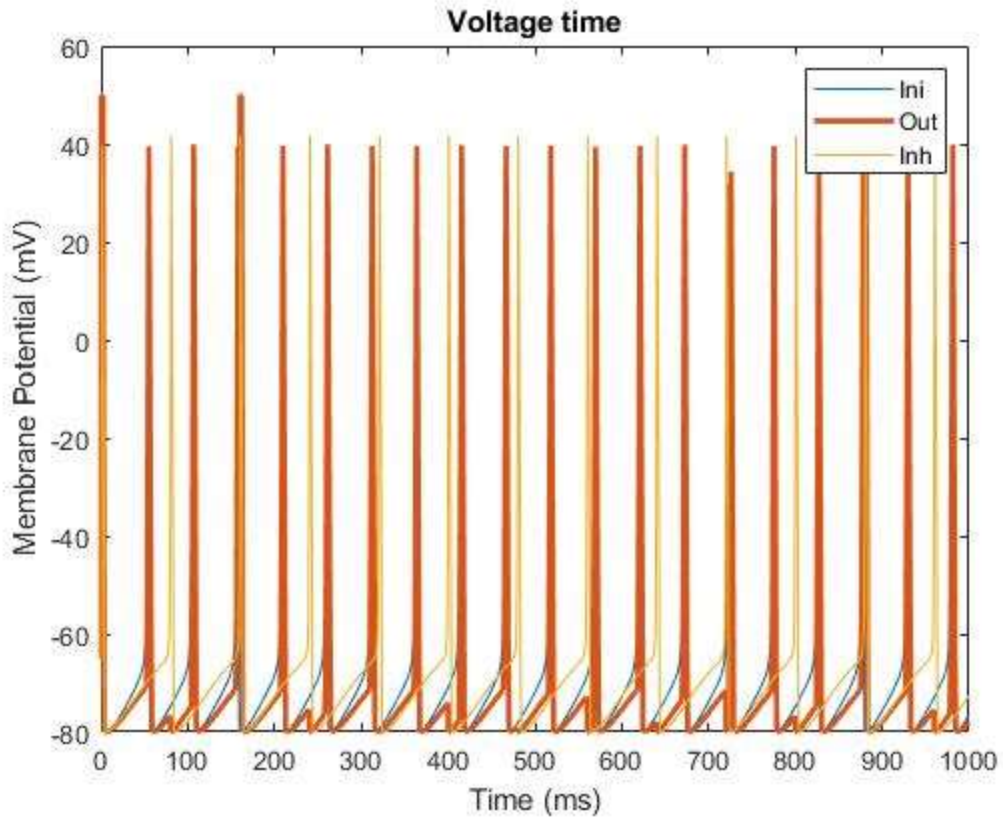


Fig 6.4: Initiator spiking. A steady spike pattern from the initiating cell results in fidelity in output cell spiking behavior: a circuit that generates an output, starting sample rate of 19 Hz. Inhibitor cell with a slow spike pattern does not slow the output spike pattern. Ini: Initiator; Out: Outputter; Inh: Inhibitor.

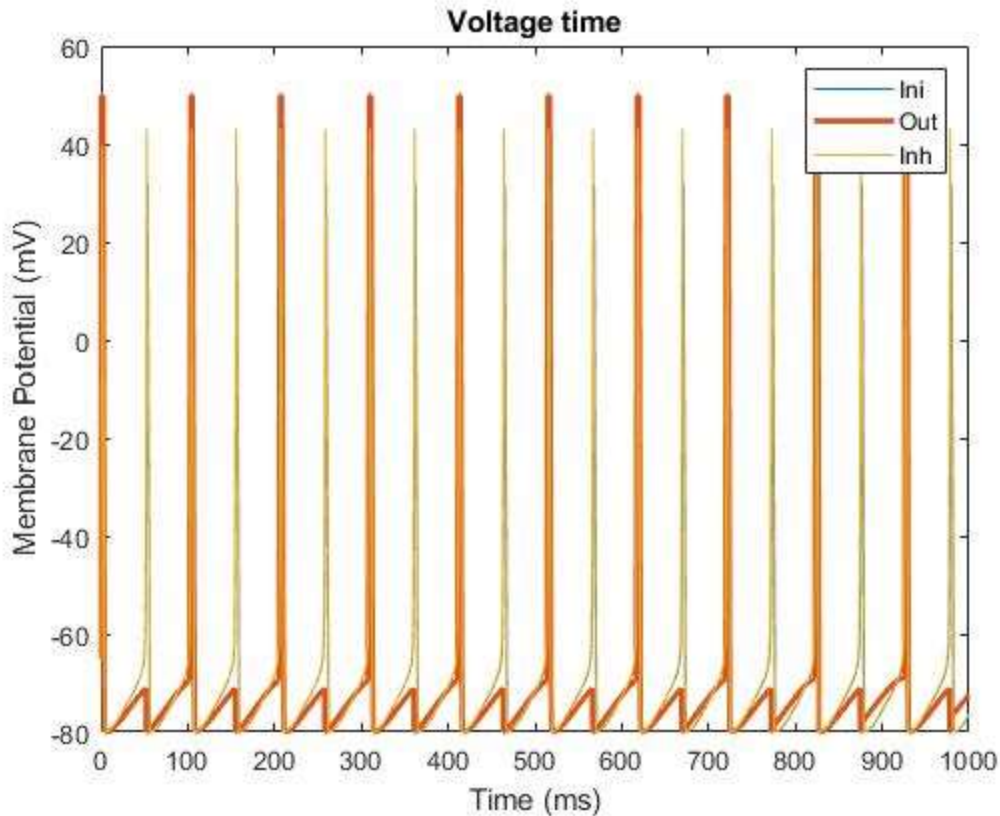


Fig 6.5: Initiator spiking, inhibitor rate increased. A steady spike pattern from the initiating cell results in fidelity in output cell spiking behavior: a circuit that generates an output. Inhibitor cell with a faster 19 Hz spike pattern slows the output spike pattern down to 9 Hz. Ini: Initiator; Out: Outputter; Inh: Inhibitor.

6.5 Future Work

Theoretically, this network could be capable of exhibiting disinhibition, but patterned stimulations have not yet been applied and there is no coded function for changes in channel permeability due to patterned ionic bursting. LTP has not yet been added but should be simulated by linking permeability of AMPA channels to NMDA currents in form with literature-derived relationships. After this step, the synaptic response to iTBS would be able to be observed for a single, nonvarying circuit. The Gillespie approach could be used to introduce stochasticity inherent in chemistry of biological systems for generating population-based outputs to model the behavior of a cortical region, beyond a single circuit [241], [242]. This would be dependent on obtaining time constants (τ) for each channel type, which allow for variable but smaller time steps with a probabilistic decision as to which channels exhibit change at each iteration, ensuring no two simulation runs will be identical. Furthermore, the inclusion of a noise current could provide more physiological variability [90].

This project initiates the path to complete a circuit that accurately presents physiological response to iTBS and can be run in series to represent a full cortical target region. That circuit, run in

parallel, would represent the aggregate behavior of a cortical target. Corticomotor excitability changes, as measured by change in output voltage response to input stimuli, should be compared to empirical MEP data.

Ultimately the function of this model is to illustrate how the neuroplastic effects of iTBS can be captured at the synaptic level in a scalable subunit for further application. Testing iTBS optimizations in a physiologically relevant *in silico* medium would enable individualized therapies and testing of multimodal neuromodulative therapies, to better identify how to improve response. Validation by *in vitro* cell assay-based studies to identify changes in synaptic markers that resemble what is modeled. *In vitro* and *in vivo* studies of individually tailored or combinatorial neuromodulation therapies would be required before application in conjunction with physical training and rehabilitation. Such validation and application work would require extensive collaborations with wet lab based and physical therapy facilities and expertise and would represent a new project. The goal of these follow-up projects would be to either improve neuromodulation techniques by optimizations or combinations, or to better determine when to apply them as they exist now. Either direction would reduce the variability and unpredictable nature of TMS as evidenced by the presented data.

7 Conclusion

This work in iTBS response characterization provides valuable answers regarding appropriate targets both in somatic site, population, and individual section, all. The study of iTBS in nonimpaired biceps showed that despite the variability inherent in the technique and measurement method, a rehabilitation relevant target exhibited corticomotor excitability. The study of iTBS in individuals with SCI further showed that populations in need of rehabilitative efforts had potential to directly benefit from the neuroplastic priming effects. The linking of individual neuroanatomical markers to iTBS response for different motor targets, along with the establishment of a predictive metric in the motor threshold ratio, or corticomotor conductance potential, provides a framework to determine prior to neuromodulation whether an individual or specific target site will respond, even on a session-by-session basis.

The neural circuit paradigm combines the elements from earlier simulation work in the field of TMS, pairing empirically established system behavior and mechanisms to a well-defined mathematical construct (Hodgkin Huxley membrane behavior) and in a widely accepted organizational structure (neural circuit). This is a flexible paradigm that can be tuned to represent specific cortical or circuit conditions for the use of tailoring neuromodulation protocols or selecting the most appropriate targets.

These results can be the start of research into optimized rehabilitation efforts, by investigating the effects of iTBS paired with motor training, effects of iTBS on other potential appropriate targets, and deeper studies into the mechanistic drivers of neuromodulation-induced neuroplasticity. The neural circuit can serve to validate existing theory as well as expand upon it, especially when paired with clinical data to train and support programmed function. Furthermore, with enough sophistication, a neural circuit population, as an *in silico* cortical subregion, can serve to test optimizations of neuromodulation techniques by simulation, dramatically reducing the cost in time, money, resources, and participant difficulty, to improve individualized therapies.

The combination of predictive measures and simulation-based tools to test technique optimizations address the limitations of iTBS as stated: high variability in response, poor predictability in outcomes, and limited mechanistic understanding to optimize methods.

7.1.1 Future Work Recommendations

This project was entirely composed of pilot studies, and there are multiple avenues of follow-up to further potential use of iTBS. Expanded projects with larger sample sizes, more clinical populations, and more motor targets, could further improve our understanding of population-based response to iTBS. Furthermore, fiber tract geometry was collected but never incorporated into head models that underwent simulated TMS, while simulated TMS was limited to single pulse paradigms. The next step would be to combine the fiber tracts with head models to determine the induced electric fields at the

fiber tract level, while also incorporating time varying simulated magnetic fields to model the cortical currents of and after iTBS. Lastly, as previously stated, there is still the need to add neuroplastic relationships and biological variability to the neural circuit. As it stands, this tool is organized and physiologically relevant, but does not capture the TMS effects as they pertain to synaptic change. Implementing mechanisms of disinhibition and LTP, as well as variation and parallel-in-population, would allow for rigorous testing of iTBS and related stimulation paradigms.

8 Scientific Communications

8.1 Papers

8.1.1 Published

N Mittal, BC Majdic, A Sima and CL Peterson, "The effect of intermittent theta burst stimulation on corticomotor excitability of the biceps brachii in nonimpaired individuals", *Neuroscience Letters*, vol. 764, p. 136220, 2021. Available: 10.1016/j.neulet.2021.136220.

8.1.2 Submitted

N Mittal, BC Majdic and CL Peterson, "Intermittent Theta Burst Stimulation Modulates Biceps Brachii Corticomotor Excitability in Individuals with Tetraplegia", Submitted to *The Journal of NeuroEngineering and Rehabilitation*, 9-20-2021. Available (Preliminary Preprint): 10.21203/rs.3.rs-907901/v1. Submission ID: JNER-D-21-00301.

N Mittal, B Thakkar, C Hodges, C Lewis, Y Cho, RL Hadimani, CL Peterson, "Effect of Neuroanatomy on Corticomotor Excitability During and After Transcranial Magnetic Stimulation and Intermittent Theta Burst Stimulation", Submitted to *Human Brain Mapping*, 10-25-2021. Submission ID: HBM-21-1017.

N Mittal, C Lewis, Y Cho, CL Peterson, RL Hadimani, "Effect of Fiber Tracts and Depolarized Brain Volume on Resting Motor Thresholds during Transcranial Magnetic Stimulation", Submitted to *Transactions on Magnetics*, 10-29-2021. Submission ID: MAGCON-21-10-0644, linked to 2022 MMM-INTERMAG Conference Abstract IOH-14.

8.1.3 Other Journal Contributions

C Lynch, T Roumengous, N. Mittal, CL Peterson, "Effects of Stimulus Waveform on Transcranial Magnetic Stimulation Metrics in Proximal and Distal Arm Muscles", Submitted to *Neurophysiologie Clinique*, 09-28-2021. Submission ID: NEUCLI-D-21-00139.

8.2 Conference Posters and Presentations

8.2.1 Posters

"Effect of Intermittent Theta Burst Stimulation Parameters on Biceps Corticomotor Excitability". Poster by Majdic BC, Dr Mittal N, Dr Peterson CL. Biomedical Engineering Society, Atlanta, GA; 2018.

"The Effect of Intermittent Theta Burst Stimulation on Biceps Corticomotor Excitability in Nonimpaired Individuals and Individuals with Tetraplegia". Poster by Dr Mittal N, Majdic BC, Dr Peterson CL. Summer Biomechanics, Bioengineering, & Biotransport Conference (SB3C), Seven Springs, PA; 2019.

“Effect of Fiber Tract Surface Area on Resting Motor Thresholds during Transcranial Magnetic Stimulation”. (Abstract REU 137-3023) Poster by Lewis C, Dr Mittal N, Dr Hodges C, Thakkar B, Cho Y, Andrade A, Nevadomski B, Li K, Dr Peterson CL, Dr Hadimani RL. Biomedical Engineering Society, Orlando, FL; 2021.

“Effect of Neuroanatomy on the Response to Neuromodulation in the Biceps Brachii”. (Abstract REU 137-2807) Poster by Cho Y, Dr Mittal N, Dr Hodges C, Thakkar B, Lewis C, Andrade A, Nevadomski B, Li K, Dr Hadimani RL, Dr Peterson CL. Biomedical Engineering Society, Orlando, FL; 2021.

“Effect of Neuroanatomy on Transcranial Magnetic Stimulation Resting Motor Thresholds”. Poster by Thakkar B, Dr Mittal N, Dr Hodges C, Cho Y, Lewis C, Dr Hadimani RL, Dr Peterson CL. American Congress of Rehabilitation Medicine 98th Annual VIRTUAL Conference; 2021.

“Effect of Neuroanatomy on Intermittent Theta Burst Stimulation Motor Evoked Potentials”. Poster by Dr Hodges C, Dr Mittal N, Thakkar B, Cho Y, Lewis C, Dr Hadimani RL, Dr Peterson CL. American Congress of Rehabilitation Medicine 98th Annual VIRTUAL Conference; 2021.

“Effect of Neuroanatomy on Intermittent Theta Burst Stimulation Motor Evoked Potentials”. (Poster, P1.042) Poster by Dr Mittal N, Thakkar B, Dr Hodges C, Cho Y, Lewis C, Andrade A, Nevadomski B, Li K, Dr Hadimani RL, Dr Peterson CL. 4th International Brain Stimulation Conference, Charleston, SC; 2021.

“Effect of Neuroanatomy on Transcranial Magnetic Stimulation Resting Motor Thresholds”. (Poster, P3.082) Poster by Thakkar B, Dr Mittal N, Dr Hodges C, Cho Y, Lewis C, Andrade A, Nevadomski B, Li K, Dr Hadimani RL, Dr Peterson CL. 4th International Brain Stimulation Conference, Charleston, SC; 2021.

“Effect of Fiber Tract Surface Area on Resting Motor Thresholds during Transcranial Magnetic Stimulation”. (Poster, IPE-07) Poster by Lewis C, Dr Mittal N, Dr Hodges C, Thakkar B, Cho Y, Andrade A, Nevadomski B, Li K, Dr Peterson CL, Dr Hadimani RL. Joint MMM-INTERMAG Conference, New Orleans, LA; 2022.

8.2.2 Presentations

“Excitatory Effect of Intermittent Theta Burst Stimulation on Corticomotor Excitability of the Biceps in Individuals with Tetraplegia”. Presentation by Majdic BC, Dr Mittal N (Presenter), Dr Peterson CL. International Society of Biomechanics/American Society of Biomechanics, Calgary, CA; 2019.

“Effect of Neuroanatomy on Motor Evoked Potentials after Intermittent Theta Burst Stimulation”. (Presentation, IOH-14) Presentation by Dr Mittal N (Presenter), Thakkar B, Dr Hodges C, Cho Y, Lewis C, Andrade A, Nevadomski B, Li K, Dr Hadimani RL, Dr Peterson CL. 2022 Joint MMM-INTERMAG Conference, New Orleans, SC; 2022.

9 Acknowledgements

First, thanks to my advisor, Carrie Peterson, for her mentorship, offering me a place in her lab, giving me the support to pursue topics of interest, and most of all giving her respect. Similarly, thanks to the other members of my committee, Christopher Lemmon, Ravi Hadimani, Dean Krusienski, and George Gitchel, for their availability, responsiveness, attention to my work, flexibility, and guidance. Thanks to REAL Lab co-investigators, Blaize Majdic, Yeajin Cho, Bhushan Thakkar, Keith Li, Abigail Andrade, and Brent Nevadomski. Thanks to co-investigators outside the REAL Lab: Connor Lewis from Biomagnetics Lab, and Cooper Hodges, from the VCU CARI Center. Also thanks to Joshua Arenas, Emily Cheng, Rob Cadrain, Joel Steinberg, James Bjork, Adam Sima, and Brian Taylor. The work presented here would not be possible without each of these individuals supporting it.

Funding for the various studies presented was provided through the NIH, VCU CERSE grants, The CCI, and VCU's DURi program, without which the completed and proposed research would not be possible.

10 Abbreviated Curriculum Vitae

10.1.1 Professional Experience

2021: Patent Examiner for USPTO (Alexandria, VA)

2015: Ensign (O1) Engineer for USPHS (JRCOSTEP Internship), IHS Great Plains (Pierre, SD)

2013-2015: Engineering Assistant for Exponent (Philadelphia, PA)

2010-2013: Research Assistant for Cooper University Hospital Emergency Department

2011-2011: Extern, Guest Lecturer for Cooper University Hospital Psychiatry and LaSalle University Psychology Doctoral Program (Camden, NJ)

2010-2011: House Officer at A.G. Holley (Lantana, FL)

10.1.2 Education

2017-2021: Virginia Commonwealth University (Richmond, VA): PhD in Biomedical Engineering, REAL Lab, Dr. C. L. Peterson – *“Intermittent Theta Burst Stimulation: Application to Spinal Cord Injury Rehabilitation and Computational Modeling”*

2015-2017: Drexel University (Philadelphia, PA): BS & MS in Biomedical Engineering, Dr. Y. Zhong – *“Model Driven Optimization of Drug Delivery for Spinal Cord Injury”*

2003-2009: Medical University of Silesia (Katowice, Poland): MD, ECFMG certified; USMLE Steps 1, 2CS, 2CK, 3 passed

10.1.3 Select Work: Contributor

“Arterial blood pressure and neurological outcome after resuscitation from cardiac arrest.” *Critical Care Medicine*. 2014; DOI: 10.1097/CCM.0000000000000406

“Multiple organ dysfunction after return of spontaneous circulation in postcardiac arrest syndrome.” *Critical Care Medicine*. 2013; DOI: 10.1097/CCM.0b013e31828a39e9

"Association between postresuscitation partial pressure of arterial carbon dioxide and neurological outcome in patients with post-cardiac arrest syndrome". *Circulation*. 2013; DOI: 10.1161/CIRCULATIONAHA.112.000168

“Emergency Department inter-hospital transfer for post-cardiac arrest care: Initial experience with implementation of a regional cardiac resuscitation center in the United States.” *Resuscitation*. 2013; DOI:10.1016/j.resuscitation.2012.09.018

11 References

- [1] K. H. Herrmann, I. Kirchberger, F. Biering-Sørensen, and A. Cieza, "Differences in functioning of individuals with tetraplegia and paraplegia according to the International Classification of Functioning, Disability and Health (ICF)," *Spinal Cord*, vol. 49, no. 4, pp. 534–543, Apr. 2011, doi: 10.1038/sc.2010.156.
- [2] National Spinal Cord Injury Statistical Center, "Spinal Cord Injury Facts and Figures at a Glance, 2020 SCI Data Sheet," 2020. [Online]. Available: [https://www.nscisc.uab.edu/Public/Facts and Figures 2020.pdf](https://www.nscisc.uab.edu/Public/Facts%20and%20Figures%202020.pdf).
- [3] K. D. Anderson, J. Fridén, and R. L. Lieber, "Acceptable benefits and risks associated with surgically improving arm function in individuals living with cervical spinal cord injury," *Spinal Cord*, vol. 47, no. 4, pp. 334–338, 2009, doi: 10.1038/sc.2008.148.
- [4] J. Benito *et al.*, "Motor and gait improvement in patients with incomplete spinal cord injury induced by high-frequency repetitive transcranial magnetic stimulation," in *Topics in Spinal Cord Injury Rehabilitation*, 2012, vol. 18, no. 2, pp. 106–112, doi: 10.1310/sci1802-106.
- [5] M. Belci, M. Catley, M. Husain, H. L. Frankel, and N. J. Davey, "Magnetic brain stimulation can improve clinical outcome in incomplete spinal cord injured patients," *Spinal Cord*, vol. 42, no. 7, pp. 417–419, 2004, doi: 10.1038/sj.sc.3101613.
- [6] W. Klomjai, R. Katz, and A. Lackmy-Vallée, "Basic principles of transcranial magnetic stimulation (TMS) and repetitive TMS (rTMS)," *Ann. Phys. Rehabil. Med.*, vol. 58, no. 4, pp. 208–213, Sep. 2015, doi: 10.1016/J.REHAB.2015.05.005.
- [7] P. Bawa, J. D. Hamm, P. Dhillon, and P. A. Gross, "Bilateral responses of upper limb muscles to transcranial magnetic stimulation in human subjects," *Exp. Brain Res.*, vol. 158, no. 3, pp. 385–390, 2004, doi: 10.1007/s00221-004-2031-x.
- [8] M. P. Malcolm, W. J. Triggs, K. E. Light, O. Shechtman, G. Khandekar, and L. J. Gonzalez Rothi, "Reliability of motor cortex transcranial magnetic stimulation in four muscle representations," *Clin. Neurophysiol.*, vol. 117, no. 5, pp. 1037–1046, 2006, doi: 10.1016/j.clinph.2006.02.005.
- [9] C. Neige, H. Massé-Alarie, M. Gagné, L. J. Bouyer, and C. Mercier, "Modulation of corticospinal output in agonist and antagonist proximal arm muscles during motor preparation," *PLoS One*, vol. 12, no. 11, pp. 1–14, 2017, doi: 10.1371/journal.pone.0188801.
- [10] M. S. A. Graziano, C. S. R. Taylor, T. Moore, and D. F. Cooke, "The cortical control of movement revisited," *Neuron*, vol. 36, no. 3, Cell Press, pp. 349–362, 24-Oct-2002, doi: 10.1016/S0896-6273(02)01003-6.
- [11] A. Pascual-Leone, A. Cammarota, E. M. Wassermann, J. P. Brasil-Neto, L. G. Cohen, and M. Hallett, "Modulation of motor cortical outputs to the reading hand of braille readers," *Ann. Neurol.*, vol. 34, no. 1, pp. 33–37, Jul. 1993, doi: 10.1002/ana.410340108.

- [12] A. Pascual-Leone, A. Amedi, F. Fregni, and L. B. Merabet, "The plastic human brain cortex," *Annual Review of Neuroscience*, vol. 28. Annu Rev Neurosci, pp. 377–401, 2005, doi: 10.1146/annurev.neuro.27.070203.144216.
- [13] M. Bruehlmeier, V. Dietz, K. L. Leenders, U. Roelcke, J. Missimer, and A. Curt, "How does the human brain deal with a spinal cord injury?," *Eur. J. Neurosci.*, vol. 10, no. 12, pp. 3918–3922, Dec. 1998, doi: 10.1046/j.1460-9568.1998.00454.x.
- [14] W. J. Levy, V. E. Amassian, M. Traad, and J. Cadwell, "Focal magnetic coil stimulation reveals motor cortical system reorganized in humans after traumatic quadriplegia," *Brain Res.*, 1990, doi: 10.1016/0006-8993(90)90738-W.
- [15] H. Topka, L. G. Cohen, R. A. Cole, and M. Hallett, "Reorganization of corticospinal pathways following spinal cord injury.," *Neurology*, vol. 41, no. 8, pp. 1276–83, Aug. 1991, doi: 10.1212/WNL.41.8.1276.
- [16] J. H. Kaas, "Functional plasticity in adult cortex," in *Seminars in the Neurosciences*, 1997, vol. 9, no. 1–2, p. 1, doi: 10.1006/smns.1997.0100.
- [17] S. C. Cramer *et al.*, "Harnessing neuroplasticity for clinical applications," *Brain*, vol. 134, no. 6. Brain, pp. 1591–1609, Jun-2011, doi: 10.1093/brain/awr039.
- [18] L. A. Simpson, J. J. Eng, J. T. C. Hsieh, and D. L. Wolfe, "The health and life priorities of individuals with spinal cord injury: A systematic review," *J. Neurotrauma*, vol. 29, no. 8, pp. 1548–1555, May 2012, doi: 10.1089/neu.2011.2226.
- [19] N. Z. Hampton, "Subjective Well-Being Among People with Spinal Cord Injuries," *Rehabil. Couns. Bull.*, vol. 48, no. 1, pp. 31–37, Oct. 2004, doi: 10.1177/00343552040480010401.
- [20] C. M. Van Leeuwen *et al.*, "Trajectories in the course of life satisfaction after spinal cord injury: Identification and predictors," *Arch. Phys. Med. Rehabil.*, vol. 92, no. 2, pp. 207–213, Feb. 2011, doi: 10.1016/j.apmr.2010.10.011.
- [21] G. Scivoletto, F. Tamburella, L. Laurenza, and M. Molinari, "The spinal cord independence measure: How much change is clinically significant for spinal cord injury subjects," *Disabil. Rehabil.*, vol. 35, no. 21, pp. 1808–1813, Oct. 2013, doi: 10.3109/09638288.2012.756942.
- [22] C. M. C. Van Leeuwen *et al.*, "Life satisfaction in people with spinal cord injury during the first five years after discharge from inpatient rehabilitation," *Disabil. Rehabil.*, vol. 34, no. 1, pp. 76–83, 2012, doi: 10.3109/09638288.2011.587089.
- [23] M. A. Nosek, M. J. Fuhrer, and C. Potter, "Life Satisfaction of People With Physical Disabilities. Relationship to Personal Assistance, Disability Status, and Handicap," *Rehabil. Psychol.*, vol. 40, no. 3, pp. 191–202, Sep. 1995, doi: 10.1037/0090-5550.40.3.191.
- [24] R. Schulz and S. Decker, "Long-Term Adjustment to Physical Disability. The Role of Social Support,

- Perceived Control, and Self-Blame," *J. Pers. Soc. Psychol.*, vol. 48, no. 5, pp. 1162–1172, May 1985, doi: 10.1037/0022-3514.48.5.1162.
- [25] R. K. Bode and A. W. Heinemann, "Course of functional improvement after stroke, spinal cord injury, and traumatic brain injury," *Arch. Phys. Med. Rehabil.*, vol. 83, no. 1, pp. 100–106, 2002, doi: 10.1053/apmr.2002.26073.
- [26] J. Von Meyenburg, C. Brösamle, G. A. S. Metz, and M. E. Schwab, "Regeneration and sprouting of chronically injured corticospinal tract fibers in adult rats promoted by NT-3 and the mAb IN-1, which neutralizes myelin-associated neurite growth inhibitors," *Exp. Neurol.*, vol. 154, no. 2, pp. 583–594, 1998, doi: 10.1006/exnr.1998.6912.
- [27] B. H. Dobkin, "Confounders in rehabilitation trials of task-oriented training: Lessons from the designs of the EXCITE and SCILT multicenter trials," *Neurorehabilitation and Neural Repair*, vol. 21, no. 1. Neurorehabil Neural Repair, pp. 3–13, Mar-2007, doi: 10.1177/1545968306297329.
- [28] R. Martin and J. Silvestri, "Current Trends in the Management of the Upper Limb in Spinal Cord Injury," *Curr. Phys. Med. Rehabil. Reports*, vol. 1, no. 3, pp. 178–186, Sep. 2013, doi: 10.1007/s40141-013-0020-3.
- [29] Paralyzed-Veterans-of-America-Consortium-for-Spinal-Cord-Medicine, "Preservation of upper limb function following spinal cord injury: a clinical practice guideline for health-care professionals," *J. Spinal Cord Med.*, vol. 28, no. 5, pp. 434–470, 2005, doi: 10.1080/10790268.2005.11753844.
- [30] S. Kalsi-Ryan and M. C. Verrier, "A synthesis of best evidence for the restoration of upper-extremity function in people with tetraplegia," *Physiotherapy Canada*, vol. 63, no. 4. Canadian Physiotherapy Association, pp. 474–489, 2011, doi: 10.3138/ptc.2009-46.
- [31] V. R. Edgerton *et al.*, "Retraining the injured spinal cord," *J. Physiol.*, vol. 533, no. 1, pp. 15–22, 2001, doi: 10.1111/j.1469-7793.2001.0015b.x.
- [32] A. Wernig, S. Muller, A. Nanassy, and E. Cago, "Laufband Therapy Based on 'Rules of Spinal Locomotion' is Effective in Spinal Cord Injured Persons," *Eur. J. Neurosci.*, vol. 7, pp. 823–829, 1995.
- [33] A. A. Freehafer, "Tendon transfers in tetraplegic patients : The Cleveland experience," *Spinal Cord*, vol. 36, pp. 315–319, 1998.
- [34] B. R. Johnstone, C. J. Jordan, and J. A. Buntine, "A review of surgical rehabilitation of the upper limb in quadriplegia," *Paraplegia*, vol. 26, no. 5, pp. 317–339, 1988, doi: 10.1038/sc.1988.47.
- [35] M. E. Johanson, "Rehabilitation after surgical reconstruction to restore function to the upper limb in tetraplegia: A changing landscape," *Archives of Physical Medicine and Rehabilitation*, vol. 97, no. 6. W.B. Saunders, pp. S71–S74, 01-Jun-2016, doi: 10.1016/j.apmr.2016.03.015.

- [36] D. Becker, C. L. Sadowsky, and J. W. McDonald, "Restoring function after spinal cord injury," *Neurologist*, vol. 9, no. 1. Lippincott Williams and Wilkins, pp. 1–15, Jan-2003, doi: 10.1097/01.nrl.0000038587.58012.05.
- [37] J. Fridén and A. Gohritz, "Novel Concepts Integrated in Neuromuscular Assessments for Surgical Restoration of Arm and Hand Function in Tetraplegia," *Phys. Med. Rehabil. Clin. N. Am.*, vol. 23, no. 1, pp. 33–50, 2012, doi: 10.1016/j.pmr.2011.11.002.
- [38] M. R. Hinder *et al.*, "Inter- and Intra-individual Variability Following Intermittent Theta Burst Stimulation: Implications for Rehabilitation and Recovery," *Brain Stimul.*, vol. 7, no. 3, pp. 365–371, May 2014, doi: 10.1016/J.BRS.2014.01.004.
- [39] A. Suppa *et al.*, "Ten Years of Theta Burst Stimulation in Humans: Established Knowledge, Unknowns and Prospects," *Brain Stimul.*, vol. 9, no. 3, pp. 323–335, May 2016, doi: 10.1016/J.BRS.2016.01.006.
- [40] S. J. Ackerley, W. D. Byblow, P. A. Barber, H. MacDonald, A. McIntyre-Robinson, and C. M. Stinear, "Primed physical therapy enhances recovery of upper limb function in chronic stroke patients," *Neurorehabil. Neural Repair*, vol. 30, no. 4, pp. 319–348, May 2016, doi: 10.1177/1545968315595285.
- [41] J. Gomes-Osman, J. A. Tibbett, B. P. Poe, and E. C. Field-Fote, "Priming for improved hand strength in persons with chronic tetraplegia: A comparison of priming-augmented functional task practice, priming alone, and conventional exercise training," *Front. Neurol.*, vol. 7, no. JAN, 2017, doi: 10.3389/fneur.2016.00242.
- [42] M. E. Stoykov and S. Madhavan, "Motor priming in neurorehabilitation," *J. Neurol. Phys. Ther.*, vol. 39, no. 1, pp. 33–42, 2015, doi: 10.1097/NPT.0000000000000065.
- [43] A. Pascual-Leone, N. Dang, L. G. Cohen, J. P. Brasil-Neto, A. Cammarota, and M. Hallett, "Modulation of muscle responses evoked by transcranial magnetic stimulation during the acquisition of new fine motor skills," *J. Neurophysiol.*, vol. 74, no. 3, pp. 1037–1045, 1995, doi: 10.1152/jn.1995.74.3.1037.
- [44] Y. Z. Huang, M. J. Edwards, E. Rounis, K. P. Bhatia, and J. C. Rothwell, "Theta burst stimulation of the human motor cortex," *Neuron*, vol. 45, no. 2, pp. 201–206, Jan. 2005, doi: 10.1016/j.neuron.2004.12.033.
- [45] M. S. George *et al.*, "Daily repetitive transcranial magnetic stimulation (rTMS) improves mood in depression," *Neuroreport*, vol. 6, no. 14, pp. 1853–1856, 1995, doi: 10.1097/00001756-199510020-00008.
- [46] A. B. Mendlowitz *et al.*, "Implementation of intermittent theta burst stimulation compared to conventional repetitive transcranial magnetic stimulation in patients with treatment resistant depression: A cost analysis," *PLoS One*, vol. 14, no. 9, Sep. 2019, doi: 10.1371/journal.pone.0222546.

- [47] F. Mawase, S. Uehara, A. J. Bastian, and P. Celnik, "Motor learning enhances use-dependent plasticity," *J. Neurosci.*, vol. 37, no. 10, pp. 2673–2685, Mar. 2017, doi: 10.1523/JNEUROSCI.3303-16.2017.
- [48] U. Ziemann, W. Muellbacher, M. Hallett, and L. G. Cohen, "Modulation of practice-dependent plasticity in human motor cortex," *Brain*, vol. 124, no. 6, pp. 1171–1181, 2001, doi: 10.1093/brain/124.6.1171.
- [49] U. Ziemann, S. Lönnecker, B. J. Steinhoff, and W. Paulus, "Effects of antiepileptic drugs on motor cortex excitability in humans: A transcranial magnetic stimulation study," *Ann. Neurol.*, vol. 40, no. 3, pp. 367–378, Sep. 1996, doi: 10.1002/ana.410400306.
- [50] U. Ziemann *et al.*, "TMS and drugs revisited 2014," *Clinical Neurophysiology*, vol. 126, no. 10. Elsevier Ireland Ltd, pp. 1847–1868, 01-Oct-2015, doi: 10.1016/j.clinph.2014.08.028.
- [51] N. A. Noh, G. Fuggetta, and P. Manganotti, "Theta-burst transcranial magnetic stimulation alters the functional topography of the cortical motor network," *Malaysian J. Med. Sci.*, vol. 22, no. Spec Issue, pp. 35–43, Dec. 2015.
- [52] C. L. Peterson *et al.*, "Posture-Dependent Corticomotor Excitability Differs between the Transferred Biceps in Individuals with Tetraplegia and the Biceps of Nonimpaired Individuals," *Neurorehabil. Neural Repair*, vol. 31, no. 4, pp. 354–363, Apr. 2017, doi: 10.1177/1545968316680488.
- [53] N. Smaby, M. E. Johanson, B. Baker, D. E. Kenney, W. M. Murray, and V. R. Hentz, "Identification of key pinch forces required to complete functional tasks," *J. Rehabil. Res. Dev.*, vol. 41, no. 2, p. 215, Mar. 2004, doi: 10.1682/JRRD.2004.02.0215.
- [54] Y. Huang, M. Edwards, E. Rounis, K. Bhatia, and J. Rothwell, "Theta burst stimulation of the human motor cortex," *Neuron*, vol. 45, no. 2, pp. 201–206, Jan. 2005, doi: 10.1016/j.neuron.2004.12.033.
- [55] A. Priori, M. Hallett, and J. C. Rothwell, "Repetitive transcranial magnetic stimulation or transcranial direct current stimulation?," *Brain Stimul.*, vol. 2, no. 4, pp. 241–245, Oct. 2009, doi: 10.1016/j.brs.2009.02.004.
- [56] R. Perellón-Alfonso *et al.*, "Similar effect of intermittent theta burst and sham stimulation on corticospinal excitability: A 5-day repeated sessions study," *Eur. J. Neurosci.*, vol. 48, no. 4, pp. 1990–2000, 2018, doi: 10.1111/ejn.14077.
- [57] Y. Z. Huang *et al.*, "Plasticity induced by non-invasive transcranial brain stimulation: A position paper," *Clinical Neurophysiology*, vol. 128, no. 11. Elsevier Ireland Ltd, pp. 2318–2329, 01-Nov-2017, doi: 10.1016/j.clinph.2017.09.007.
- [58] P. M. Rossini *et al.*, "Non-invasive electrical and magnetic stimulation of the brain, spinal cord, roots and peripheral nerves: Basic principles and procedures for routine clinical and research

- application: An updated report from an I.F.C.N. Committee," *Clinical Neurophysiology*, vol. 126, no. 6. Elsevier Ireland Ltd, pp. 1071–1107, 01-Jun-2015, doi: 10.1016/j.clinph.2015.02.001.
- [59] S. Groppa *et al.*, "A practical guide to diagnostic transcranial magnetic stimulation: Report of an IFCN committee," *Clinical Neurophysiology*. 2012, doi: 10.1016/j.clinph.2012.01.010.
- [60] P. M. Rossini *et al.*, *Non-invasive electrical and magnetic stimulation of the brain, spinal cord, roots and peripheral nerves: Basic principles and procedures for routine clinical and research application: An updated report from an I.F.C.N. Committee*, vol. 126, no. 6. Elsevier Ireland Ltd, 2015, pp. 1071–1107.
- [61] M. R. Ljubisavljevic *et al.*, "The Effects of Different Repetitive Transcranial Magnetic Stimulation (rTMS) Protocols on Cortical Gene Expression in a Rat Model of Cerebral Ischemic-Reperfusion Injury," *PLoS One*, vol. 10, no. 10, p. e0139892, Oct. 2015, doi: 10.1371/journal.pone.0139892.
- [62] W. A Stateman, "Repetitive Transcranial Magnetic Stimulation (Rtms) increases Plasma Calcium both in-vivo and in-vitro," *J. Clin. Exp. Pathol.*, vol. 04, no. 04, pp. 1–6, Aug. 2014, doi: 10.4172/2161-0681.1000187.
- [63] Y. Z. Huang, J. C. Rothwell, R. S. Chen, C. S. Lu, and W. L. Chuang, "The theoretical model of theta burst form of repetitive transcranial magnetic stimulation," *Clin. Neurophysiol.*, vol. 122, no. 5, pp. 1011–1018, May 2011, doi: 10.1016/j.clinph.2010.08.016.
- [64] J. Medina, A. Marcos-García, I. Jiménez, G. Muratore, and J. L. Méndez-Suárez, "Biceps to Triceps Transfer in Tetraplegic Patients: Our Experience and Review of the Literature.," *Hand (N. Y.)*, vol. 12, no. 1, pp. 85–90, 2017, doi: 10.1177/1558944716646764.
- [65] E. M. ter Braack, A. A. de Goede, and M. J. A. M. van Putten, "Resting Motor Threshold, MEP and TEP Variability During Daytime," *Brain Topogr.*, vol. 32, no. 1, pp. 17–27, Jan. 2019, doi: 10.1007/s10548-018-0662-7.
- [66] A. Jannati, G. Block, L. M. Oberman, A. Rotenberg, and A. Pascual-Leone, "Interindividual variability in response to continuous theta-burst stimulation in healthy adults," *Clin. Neurophysiol.*, vol. 128, no. 11, pp. 2268–2278, Nov. 2017, doi: 10.1016/j.clinph.2017.08.023.
- [67] A. Jannati, P. J. Fried, G. Block, L. M. Oberman, A. Rotenberg, and A. Pascual-Leone, "Test-retest reliability of the effects of continuous theta-burst stimulation," *Front. Neurosci.*, vol. 13, no. MAY, 2019, doi: 10.3389/fnins.2019.00447.
- [68] P. G. Martin, S. C. Gandevia, and J. L. Taylor, "Theta burst stimulation does not reliably depress all regions of the human motor cortex," *Clin. Neurophysiol.*, vol. 117, no. 12, pp. 2684–2690, Dec. 2006, doi: 10.1016/j.clinph.2006.08.008.
- [69] H. J. Fassett *et al.*, "Transcranial Magnetic Stimulation with Intermittent Theta Burst Stimulation Alters Corticospinal Output in Patients with Chronic Incomplete Spinal Cord Injury.," *Front. Neurol.*, vol. 8, p. 380, 2017, doi: 10.3389/fneur.2017.00380.

- [70] C. Nettekoven *et al.*, “Inter-individual variability in cortical excitability and motor network connectivity following multiple blocks of rTMS,” *Neuroimage*, vol. 118, pp. 209–18, Sep. 2015, doi: 10.1016/j.neuroimage.2015.06.004.
- [71] A. Guerra, V. López-Alonso, B. Cheeran, and A. Suppa, “Variability in non-invasive brain stimulation studies: Reasons and results,” *Neurosci. Lett.*, no. December, p. 133330, 2018, doi: 10.1016/j.neulet.2017.12.058.
- [72] V. López-Alonso, B. Cheeran, D. Río-Rodríguez, and M. Fernández-Del-Olmo, “Inter-individual variability in response to non-invasive brain stimulation paradigms,” *Brain Stimul.*, vol. 7, no. 3, pp. 372–380, 2014, doi: 10.1016/j.brs.2014.02.004.
- [73] W. G. Darling, S. L. Wolf, and A. J. Butler, “Variability of motor potentials evoked by transcranial magnetic stimulation depends on muscle activation,” *Exp. Brain Res.*, vol. 174, no. 2, pp. 376–385, 2006, doi: 10.1007/s00221-006-0468-9.
- [74] M. Pellegrini, M. Zoghi, and S. Jaberzadeh, “Biological and anatomical factors influencing interindividual variability to noninvasive brain stimulation of the primary motor cortex: a systematic review and meta-analysis,” *Rev. Neurosci.*, vol. 29, no. 2, pp. 199–222, Feb. 2018, doi: 10.1515/revneuro-2017-0048.
- [75] V. Di Lazzaro *et al.*, “The physiological basis of the effects of intermittent theta burst stimulation of the human motor cortex,” vol. 16, pp. 3871–3879, 2008, doi: 10.1113/jphysiol.2008.152736.
- [76] E. Lee, P. Rastogi, R. Hadimani, D. Jiles, and J. Camprodon, “Impact of non-brain anatomy and coil orientation on inter- and intra-subject variability in TMS at midline,” *Clin. Neurophysiol.*, vol. 129, no. 9, pp. 1873–1883, Sep. 2018, doi: 10.1016/j.clinph.2018.04.749.
- [77] L. Cárdenas-Morales *et al.*, “Network connectivity and individual responses to brain stimulation in the human motor system,” *Cereb. Cortex*, vol. 24, no. 7, pp. 1697–1707, Jul. 2014, doi: 10.1093/cercor/bht023.
- [78] M. Hamada, N. Murase, A. Hasan, M. Balaratnam, and J. C. Rothwell, “The role of interneuron networks in driving human motor cortical plasticity,” *Cereb. Cortex*, vol. 23, no. 7, pp. 1593–1605, Jul. 2013, doi: 10.1093/cercor/bhs147.
- [79] E. Lee *et al.*, “Investigational Effect of Brain-Scalp Distance on the Efficacy of Transcranial Magnetic Stimulation Treatment in Depression,” *IEEE Trans. Magn.*, vol. 52, no. 7, Jul. 2016, doi: 10.1109/TMAG.2015.2514158.
- [80] F. Syeda, H. Magsood, E. G. Lee, A. A. El-Gendy, D. C. Jiles, and R. L. Hadimani, “Effect of anatomical variability in brain on transcranial magnetic stimulation treatment,” *AIP Adv.*, vol. 7, no. 5, May 2017, doi: 10.1063/1.4974981.
- [81] L. J. Crowther, R. L. Hadimani, and D. C. Jiles, “Effect of anatomical brain development on induced electric fields during transcranial magnetic stimulation,” *IEEE Trans. Magn.*, vol. 50, no. 11, Nov.

- 2014, doi: 10.1109/TMAG.2014.2326819.
- [82] Z. De Deng, S. H. Lisanby, and A. V. Peterchev, "Electric field depth-focality tradeoff in transcranial magnetic stimulation: Simulation comparison of 50 coil designs," *Brain Stimul.*, vol. 6, no. 1, pp. 1–13, Jan. 2013, doi: 10.1016/j.brs.2012.02.005.
- [83] J. Mak, F. Syeda, and R. L. Hadimani, "3D Modeling of Diffusion Tensor Imaging Tractography Data for Finite Element Analysis," in *IEEE International Symposium on Biomedical Imaging*, 2018, p. Apr. 2018, vol. Paper FrP2O-01.11, pp. 2O–01.11.
- [84] C. T. Li, Y. Z. Huang, Y. M. Bai, S. J. Tsai, T. P. Su, and C. M. Cheng, "Critical role of glutamatergic and GABAergic neurotransmission in the central mechanisms of theta-burst stimulation," *Human Brain Mapping*, vol. 40, no. 6. John Wiley and Sons Inc., pp. 2001–2009, 15-Apr-2019, doi: 10.1002/hbm.24485.
- [85] M. D. Humphries, R. D. Stewart, and K. N. Gurney, "A physiologically plausible model of action selection and oscillatory activity in the basal ganglia," *J. Neurosci.*, vol. 26, no. 50, pp. 12921–12942, Dec. 2006, doi: 10.1523/JNEUROSCI.3486-06.2006.
- [86] C. Cali, T. K. Berger, M. Pignatelli, A. Carleton, H. Markram, and M. Giugliano, "Inferring connection proximity in networks of electrically coupled cells by subthreshold frequency response analysis," *J. Comput. Neurosci.*, vol. 24, no. 3, pp. 330–345, Jun. 2008, doi: 10.1007/s10827-007-0058-2.
- [87] J. Heinze, K. Hepp, and K. A. C. Martin, "A microcircuit model of the frontal eye fields," *J. Neurosci.*, vol. 27, no. 35, pp. 9341–9353, Aug. 2007, doi: 10.1523/JNEUROSCI.0974-07.2007.
- [88] Y. X. Li, R. Bertram, and J. Rinzel, "Modeling N-methyl-D-aspartate-induced bursting in dopamine neurons," *Neuroscience*, vol. 71, no. 2, pp. 397–410, 1996, doi: 10.1016/0306-4522(95)00483-1.
- [89] V. Di Lazzaro and U. Ziemann, "The contribution of transcranial magnetic stimulation in the functional evaluation of microcircuits in human motor cortex," *Front. Neural Circuits*, vol. 7, no. JAN, p. 18, Jan. 2013, doi: 10.3389/fncir.2013.00018.
- [90] D. V. Raman, A. P. Rotondo, and T. O'Leary, "Fundamental bounds on learning performance in neural circuits," *Proc. Natl. Acad. Sci. U. S. A.*, vol. 116, no. 21, pp. 10537–10546, May 2019, doi: 10.1073/pnas.1813416116.
- [91] A. E. Papale and B. M. Hooks, "Circuit changes in motor cortex during motor skill learning," *Neuroscience*, vol. 368. Elsevier Ltd, pp. 283–297, 01-Jan-2018, doi: 10.1016/j.neuroscience.2017.09.010.
- [92] D. Purves *et al.*, *Neuroscience: Ch. 2 Neural Circuits*. Sinauer Associates, 2001.
- [93] R. J. Douglas and K. A. Martin, "A functional microcircuit for cat visual cortex.," *J. Physiol.*, vol. 440, no. 1, pp. 735–769, Aug. 1991, doi: 10.1113/jphysiol.1991.sp018733.

- [94] R. J. Douglas and K. A. C. Martin, "NEURONAL CIRCUITS OF THE NEOCORTEX," *Annu. Rev. Neurosci.*, vol. 27, no. 1, pp. 419–451, 2004, doi: 10.1146/annurev.neuro.27.070203.144152.
- [95] A. M. Bastos, W. M. Usrey, R. A. Adams, G. R. Mangun, P. Fries, and K. J. Friston, "Canonical Microcircuits for Predictive Coding," *Neuron*, vol. 76, no. 4. NIH Public Access, pp. 695–711, 21-Nov-2012, doi: 10.1016/j.neuron.2012.10.038.
- [96] E. Hernández-Balaguera, H. Vara, and J. L. Polo, "Identification of Capacitance Distribution in Neuronal Membranes from a Fractional-Order Electrical Circuit and Whole-Cell Patch-Clamped Cells," *J. Electrochem. Soc.*, vol. 165, no. 12, pp. G3104–G3111, Aug. 2018, doi: 10.1149/2.0161812jes.
- [97] J. M. Ball, C. C. Franklin, A. E. Tobin, D. J. Schulz, and S. S. Nair, "Coregulation of ion channel conductances preserves output in a computational model of a crustacean cardiac motor neuron," *J. Neurosci.*, vol. 30, no. 25, pp. 8637–8649, Jun. 2010, doi: 10.1523/JNEUROSCI.6435-09.2010.
- [98] M. Ferrante, M. Migliore, and G. A. Ascoli, "Feed-forward inhibition as a buffer of the neuronal input-output relation," *Proc. Natl. Acad. Sci. U. S. A.*, vol. 106, no. 42, pp. 18004–18009, Oct. 2009, doi: 10.1073/pnas.0904784106.
- [99] G. L. Chadderton *et al.*, "Motor cortex microcircuit simulation based on brain activity mapping," *Neural Comput.*, vol. 26, no. 7, pp. 1239–1262, 2014, doi: 10.1162/NECO_a_00602.
- [100] S. Dura-Bernal *et al.*, "Evolutionary algorithm optimization of biological learning parameters in a biomimetic neuroprosthesis," *IBM J. Res. Dev.*, vol. 61, no. 2–3, p. 6.1, 2017, doi: 10.1147/JRD.2017.2656758.
- [101] P. Sah and R. F. Westbrook, "Behavioural neuroscience: The circuit of fear," *Nature*, vol. 454, no. 7204. Nature Publishing Group, pp. 589–590, 31-Jul-2008, doi: 10.1038/454589a.
- [102] P. Tovote, J. P. Fadok, and A. Lüthi, "Neuronal circuits for fear and anxiety," *Nature Reviews Neuroscience*, vol. 16, no. 6. Nature Publishing Group, pp. 317–331, 26-Jun-2015, doi: 10.1038/nrn3945.
- [103] H. Liu, Y. Temel, J. Boonstra, and S. Hescham, "The effect of fornix deep brain stimulation in brain diseases," *Cellular and Molecular Life Sciences*, vol. 77, no. 17. Springer, pp. 3279–3291, 01-Sep-2020, doi: 10.1007/s00018-020-03456-4.
- [104] D. Yu, H. Yan, J. Zhou, X. Yang, Y. Lu, and Y. Han, "A circuit view of deep brain stimulation in Alzheimer's disease and the possible mechanisms," *Molecular Neurodegeneration*, vol. 14, no. 1. BioMed Central Ltd., pp. 1–12, 08-Aug-2019, doi: 10.1186/s13024-019-0334-4.
- [105] I. Escobar, J. Xu, C. W. Jackson, M. A. Perez-Pinzon, and K. S. Jagannatha Rao, "Altered neural networks in the papez circuit: Implications for cognitive dysfunction after cerebral ischemia," *Journal of Alzheimer's Disease*, vol. 67, no. 2. IOS Press, pp. 425–446, 2019, doi: 10.3233/JAD-180875.

- [106] A. L. Hodgkin and A. F. Huxley, "A quantitative description of membrane current and its application to conduction and excitation in nerve," *J. Physiol.*, vol. 117, no. 4, pp. 500–544, Aug. 1952, doi: 10.1113/jphysiol.1952.sp004764.
- [107] M. A. Van Der Vlag, G. Smaragdous, Z. Al-Ars, and C. Strydis, "Exploring complex brain-simulation workloads on multi-GPU deployments," *ACM Trans. Archit. Code Optim.*, vol. 16, no. 4, Dec. 2019, doi: 10.1145/3371235.
- [108] M. E. Tagluk and R. Tekin, "The influence of ion concentrations on the dynamic behavior of the Hodgkin-Huxley model-based cortical network," *Cogn. Neurodyn.*, vol. 8, no. 4, pp. 287–298, 2014, doi: 10.1007/s11571-014-9281-5.
- [109] C. L. Lei, M. Clerx, D. G. Whittaker, D. J. Gavaghan, T. P. De Boer, and G. R. Mirams, "Accounting for variability in ion current recordings using a mathematical model of artefacts in voltage-clamp experiments: Modelling patch clamp artefacts," *Philos. Trans. R. Soc. A Math. Phys. Eng. Sci.*, vol. 378, no. 2173, Jun. 2020, doi: 10.1098/rsta.2019.0348.
- [110] J. A. Bauer, K. M. Lambert, and J. A. White, "The past, present, and future of real-time control in cellular electrophysiology," *IEEE Trans. Biomed. Eng.*, vol. 61, no. 5, pp. 1448–1456, 2014, doi: 10.1109/TBME.2014.2314619.
- [111] D. L. Armstrong, C. Erxleben, and J. A. White, *Patch clamp methods for studying calcium channels*, vol. 99, no. C. Academic Press, 2010.
- [112] J. W. Lynch, Y. Zhang, S. Talwar, and A. Estrada-Mondragon, "Glycine Receptor Drug Discovery," in *Advances in Pharmacology*, vol. 79, Academic Press Inc., 2017, pp. 225–253.
- [113] T. Rahman and C. W. Taylor, *Nuclear patch-clamp recording from inositol 1,4,5-trisphosphate receptors*, vol. 99, no. C. Academic Press Inc., 2010.
- [114] J. H. Byrne, "Postsynaptic Potentials and Synaptic Integration," in *From Molecules to Networks: An Introduction to Cellular and Molecular Neuroscience: Third Edition*, Elsevier Inc., 2014, pp. 489–507.
- [115] C. C. Chen *et al.*, "Patch-clamp technique to characterize ion channels in enlarged individual endolysosomes," *Nat. Protoc.*, vol. 12, no. 8, pp. 1639–1658, Aug. 2017, doi: 10.1038/nprot.2017.036.
- [116] H. Sanders, M. Berends, G. Major, M. S. Goldman, and J. E. Lisman, "NMDA and GABAB (KIR) conductances: The 'perfect couple' for bistability," *J. Neurosci.*, vol. 33, no. 2, pp. 424–429, Jan. 2013, doi: 10.1523/JNEUROSCI.1854-12.2013.
- [117] B. S. Bhattacharya, "Implementing the cellular mechanisms of synaptic transmission in a neural mass model of the thalamo-cortical circuitry," *Front. Comput. Neurosci.*, vol. 7, no. JUN, pp. 1–17, Jul. 2013, doi: 10.3389/fncom.2013.00081.

- [118] T. V. P. Bliss and T. Lømo, "Long-lasting potentiation of synaptic transmission in the dentate area of the anaesthetized rabbit following stimulation of the perforant path," *J. Physiol.*, vol. 232, no. 2, pp. 331–356, Jul. 1973, doi: 10.1113/jphysiol.1973.sp010273.
- [119] W. A. Catterall, I. M. Raman, H. P. C. Robison, T. J. Sejnowski, and O. Paulsen, "The hodgkin-huxley heritage: From channels to circuits," *J. Neurosci.*, vol. 32, no. 41, pp. 14064–14073, Oct. 2012, doi: 10.1523/JNEUROSCI.3403-12.2012.
- [120] R. Brette *et al.*, "Simulation of networks of spiking neurons: A review of tools and strategies," *Journal of Computational Neuroscience*, vol. 23, no. 3. J Comput Neurosci, pp. 349–398, Dec-2007, doi: 10.1007/s10827-007-0038-6.
- [121] G. Cao, J. Platisa, V. A. Pieribone, D. Raccuglia, M. Kunst, and M. N. Nitabach, "Genetically targeted optical electrophysiology in intact neural circuits," *Cell*, vol. 154, no. 4, pp. 904–913, Aug. 2013, doi: 10.1016/j.cell.2013.07.027.
- [122] S. Delcasso, S. Denagamage, Z. Britton, and A. M. Graybiel, "HOPE: Hybrid-Drive Combining Optogenetics, Pharmacology and Electrophysiology," *Front. Neural Circuits*, vol. 12, p. 41, May 2018, doi: 10.3389/fncir.2018.00041.
- [123] T. N. Lerner, L. Ye, and K. Deisseroth, "Communication in Neural Circuits: Tools, Opportunities, and Challenges," *Cell*, vol. 164, no. 6. Cell Press, pp. 1136–1150, 10-Mar-2016, doi: 10.1016/j.cell.2016.02.027.
- [124] G. Z. Tau and B. S. Peterson, "Normal development of brain circuits," *Neuropsychopharmacology*, vol. 35, no. 1. Nature Publishing Group, pp. 147–168, 30-Jan-2010, doi: 10.1038/npp.2009.115.
- [125] J. F. Guzowski, J. A. Timlin, B. Roysam, B. L. McNaughton, P. F. Worley, and C. A. Barnes, "Mapping behaviorally relevant neural circuits with immediate-early gene expression," *Current Opinion in Neurobiology*, vol. 15, no. 5. Elsevier Current Trends, pp. 599–606, 01-Oct-2005, doi: 10.1016/j.conb.2005.08.018.
- [126] T. N. Lerner, "Interfacing behavioral and neural circuit models for habit formation," *J. Neurosci. Res.*, vol. 98, no. 6, pp. 1031–1045, Jun. 2020, doi: 10.1002/jnr.24581.
- [127] R. Nardone *et al.*, "Effects of intermittent theta burst stimulation on spasticity after spinal cord injury," *Restor. Neurol. Neurosci.*, vol. 35, no. 3, pp. 287–294, 2017, doi: 10.3233/RNN-160701.
- [128] A. A. Gharooni, K. P. S. Nair, D. Hawkins, I. Scivill, D. Hind, and R. Hariharan, "Intermittent theta-burst stimulation for upper-limb dysfunction and spasticity in spinal cord injury: a single-blind randomized feasibility study," *Spinal Cord*, vol. 56, no. 8, pp. 762–768, 2018, doi: 10.1038/s41393-018-0152-5.
- [129] W. Song, A. Amer, D. Ryan, and J. H. Martin, "Combined motor cortex and spinal cord neuromodulation promotes corticospinal system functional and structural plasticity and motor function after injury," *Exp. Neurol.*, vol. 277, pp. 46–57, Mar. 2016, doi:

10.1016/J.EXPNEUROL.2015.12.008.

- [130] D. T. Corp *et al.*, "Large-scale analysis of interindividual variability in theta-burst stimulation data: Results from the 'Big TMS Data Collaboration,'" *Brain Stimul.*, vol. 13, no. 5, pp. 1476–1488, Sep. 2020, doi: 10.1016/j.brs.2020.07.018.
- [131] E. G. Jones, "GABAergic Neurons and Their Role in Cortical Plasticity in Primates," *Cereb. Cortex*, vol. 3, no. 5, pp. 361–372, Sep. 1993, doi: 10.1093/cercor/3.5.361-a.
- [132] A. Berardelli *et al.*, "Facilitation of muscle evoked responses after repetitive cortical stimulation in man," *Exp. Brain Res.*, vol. 122, no. 1, pp. 79–84, 1998, doi: 10.1007/s002210050493.
- [133] M. A. Perez, B. K. S. Lungholt, and J. B. Nielsen, "Short-term adaptations in spinal cord circuits evoked by repetitive transcranial magnetic stimulation: Possible underlying mechanisms," *Exp. Brain Res.*, vol. 162, no. 2, pp. 202–212, Apr. 2005, doi: 10.1007/s00221-004-2144-2.
- [134] A. Valero-Cabré, M. Oliveri, M. Gangitano, and A. Pascual-Leone, "Modulation of spinal cord excitability by subthreshold repetitive transcranial magnetic stimulation of the primary motor cortex in humans," *Neuroreport*, vol. 12, no. 17, pp. 3845–3848, Dec. 2001, doi: 10.1097/00001756-200112040-00048.
- [135] X. Konstantoudaki, A. Papoutsis, K. Chalkiadaki, P. Poirazi, and K. Sidiropoulou, "Modulatory effects of inhibition on persistent activity in a cortical microcircuit model," *Front. Neural Circuits*, vol. 8, no. JAN, Jan. 2014, doi: 10.3389/fncir.2014.00007.
- [136] H. M. Schambra *et al.*, "Differential Poststroke Motor Recovery in an Arm Versus Hand Muscle in the Absence of Motor Evoked Potentials," *Neurorehabil. Neural Repair*, vol. 33, no. 7, pp. 568–580, Jul. 2019, doi: 10.1177/1545968319850138.
- [137] V. Di Lazzaro *et al.*, "The physiological basis of the effects of intermittent theta burst stimulation of the human motor cortex," *J. Physiol.*, vol. 586, no. 16, pp. 3871–9, Aug. 2008, doi: 10.1113/jphysiol.2008.152736.
- [138] S. Diekhoff-Krebs *et al.*, "Interindividual differences in motor network connectivity and behavioral response to iTBS in stroke patients," *NeuroImage Clin.*, vol. 15, pp. 559–571, Jan. 2017, doi: 10.1016/j.nicl.2017.06.006.
- [139] Y. F. Hsu *et al.*, "Intermittent theta burst stimulation over ipsilesional primary motor cortex of subacute ischemic stroke patients: A pilot study," *Brain Stimul.*, vol. 6, no. 2, pp. 166–174, Mar. 2013, doi: 10.1016/j.brs.2012.04.007.
- [140] P. Talelli, R. J. Greenwood, and J. C. Rothwell, "Exploring Theta Burst Stimulation as an intervention to improve motor recovery in chronic stroke," *Clin. Neurophysiol.*, vol. 118, no. 2, pp. 333–342, Feb. 2007, doi: 10.1016/j.clinph.2006.10.014.
- [141] A. Pascual, E. M. Wassermann, N. Sadato, and M. Hallett, "The role of reading activity on the

- modulation of motor cortical outputs to the reading hand in braille readers," *Ann. Neurol.*, vol. 38, no. 6, pp. 910–915, Dec. 1995, doi: 10.1002/ana.410380611.
- [142] J. P. Brasil-Neto, L. M. McShane, P. Fuhr, M. Hallett, and L. G. Cohen, "Topographic mapping of the human motor cortex with magnetic stimulation: factors affecting accuracy and reproducibility," *Electroencephalogr. Clin. Neurophysiol. Evoked Potentials*, vol. 85, no. 1, pp. 9–16, Feb. 1992, doi: 10.1016/0168-5597(92)90095-S.
- [143] C. Phillips and R. Porter, *Corticospinal Neurons : Their Role in Movement*. London: Academic Press, 1977.
- [144] E. M. Wassermann, L. M. McShane, M. Hallett, and L. G. Cohen, "Noninvasive mapping of muscle representations in human motor cortex," *Electroencephalogr. Clin. Neurophysiol. Evoked Potentials*, vol. 85, no. 1, pp. 1–8, Feb. 1992, doi: 10.1016/0168-5597(92)90094-R.
- [145] M. Sommer *et al.*, "TMS of primary motor cortex with a biphasic pulse activates two independent sets of excitable neurones," *Brain Stimul.*, vol. 11, no. 3, pp. 558–565, May 2018, doi: 10.1016/j.brs.2018.01.001.
- [146] G. M. Opie and J. G. Semmler, "Preferential Activation of Unique Motor Cortical Networks With Transcranial Magnetic Stimulation: A Review of the Physiological, Functional, and Clinical Evidence," *Neuromodulation*. Blackwell Publishing Inc., 2020, doi: 10.1111/ner.13314.
- [147] S. Rossi *et al.*, "Safety, ethical considerations, and application guidelines for the use of transcranial magnetic stimulation in clinical practice and research," *Clinical Neurophysiology*, vol. 120, no. 12. Elsevier, pp. 2008–2039, 01-Dec-2009, doi: 10.1016/j.clinph.2009.08.016.
- [148] P. M. Rossini *et al.*, "Non-invasive electrical and magnetic stimulation of the brain, spinal cord and roots: basic principles and procedures for routine clinical application. Report of an IFCN committee," *Electroencephalogr. Clin. Neurophysiol.*, vol. 91, no. 2, pp. 79–92, Aug. 1994, doi: 10.1016/0013-4694(94)90029-9.
- [149] P. Rossini and A. Berardelli, "Guidelines of the IFCN (2nd Ed): Chapter 3.5 Applications of magnetic cortical stimulation," 1999.
- [150] J. J. Borckardt, Z. Nahas, J. Koola, and M. S. George, "Estimating Resting Motor Thresholds in Transcranial Magnetic Stimulation Research and Practice," *J. ECT*, vol. 22, no. 3, pp. 169–175, Sep. 2006, doi: 10.1097/01.yct.0000235923.52741.72.
- [151] MATLAB, "MATLAB." The MathWorks Inc., Natick, Massachusetts, 2019.
- [152] D. Schoenfeld, "Statistical considerations for pilot studies," *Int. J. Radiat. Oncol. Biol. Phys.*, 1980, doi: 10.1016/0360-3016(80)90153-4.
- [153] D. Bates, M. Mächler, B. Bolker, and S. Walker, "Fitting Linear Mixed-Effects Models Using lme4 | Bates | Journal of Statistical Software," *J. Stat. Softw.*, vol. 67, no. 1, pp. 1–48, 2015, doi: doi:

10.18637/jss.v067.i01.

- [154] The R Foundation, "R: The R Project for Statistical Computing." Vienna, Austria, 2018.
- [155] G. Fitzmaurice, N. Laird, and J. Ware, "Applied longitudinal Analysis (2nd Edition)," *Wiley*, 2011, doi: 10.1080/10543406.2013.789817.
- [156] M. Friedman, "The Use of Ranks to Avoid the Assumption of Normality Implicit in the Analysis of Variance," *J. Am. Stat. Assoc.*, 1937, doi: 10.1080/01621459.1937.10503522.
- [157] N. C. Rogasch, Z. J. Daskalakis, and P. B. Fitzgerald, "Mechanisms underlying long-interval cortical inhibition in the human motor cortex: A TMS-EEG study," *J. Neurophysiol.*, vol. 109, no. 1, pp. 89–98, 2013, doi: 10.1152/jn.00762.2012.
- [158] P. J. Fried, A. Jannati, P. Davila-Pérez, and A. Pascual-Leone, "Reproducibility of single-pulse, paired-pulse, and intermittent theta-burst TMS measures in healthy aging, Type-2 diabetes, and Alzheimer's disease," *Front. Aging Neurosci.*, vol. 9, no. AUG, pp. 1–13, 2017, doi: 10.3389/fnagi.2017.00263.
- [159] T. Kammer, S. Beck, A. Thielscher, U. Laubis-Herrmann, and H. Topka, "Motor thresholds in humans: A transcranial magnetic stimulation study comparing different pulse waveforms, current directions and stimulator types," *Clin. Neurophysiol.*, vol. 112, no. 2, pp. 250–258, Feb. 2001, doi: 10.1016/S1388-2457(00)00513-7.
- [160] V. Di Lazzaro *et al.*, "Comparison of descending volleys evoked by monophasic and biphasic magnetic stimulation of the motor cortex in conscious humans," *Exp. Brain Res.*, vol. 141, no. 1, pp. 121–127, 2001, doi: 10.1007/s002210100863.
- [161] P. Davila-Pérez, A. Jannati, P. J. Fried, J. Cudeiro Mazaira, and A. Pascual-Leone, "The Effects of Waveform and Current Direction on the Efficacy and Test–Retest Reliability of Transcranial Magnetic Stimulation," *Neuroscience*, vol. 393, pp. 97–109, Nov. 2018, doi: 10.1016/j.neuroscience.2018.09.044.
- [162] D. Burke, R. Hicks, S. C. Gandevia, J. Stephen, I. Woodforth, and M. Crawford, "Direct comparison of corticospinal volleys in human subjects to transcranial magnetic and electrical stimulation.," *J. Physiol.*, vol. 470, no. 1, pp. 383–393, Oct. 1993, doi: 10.1113/jphysiol.1993.sp019864.
- [163] H. Devanne, B. A. Lavoie, and C. Capaday, "Input-output properties and gain changes in the human corticospinal pathway," *Exp. Brain Res.*, vol. 114, no. 2, pp. 329–338, 1997, doi: 10.1007/PL00005641.
- [164] K. Sakai, Y. Ugawa, Y. Terao, R. Hanajima, T. Furubayashi, and I. Kanazawa, "Preferential activation of different I waves by transcranial magnetic stimulation with a figure-of-eight-shaped coil," *Exp. Brain Res.*, vol. 113, no. 1, pp. 24–32, Jan. 1997, doi: 10.1007/BF02454139.
- [165] U. Ziemann, F. Tergau, E. M. Wassermann, S. Wischer, J. Hildebrandt, and W. Paulus,

- “Demonstration of facilitatory I wave interaction in the human motor cortex by paired transcranial magnetic stimulation,” *J. Physiol.*, vol. 511, no. 1, pp. 181–190, Aug. 1998, doi: 10.1111/j.1469-7793.1998.181bi.x.
- [166] R. Nardone *et al.*, “Descending motor pathways and cortical physiology after spinal cord injury assessed by transcranial magnetic stimulation: a systematic review,” *Brain Res.*, vol. 1619, pp. 139–154, Sep. 2015, doi: 10.1016/j.brainres.2014.09.036.
- [167] I. Delvendahl, N. Gattinger, T. Berger, B. Gleich, H. R. Siebner, and V. Mall, “The role of pulse shape in motor cortex transcranial magnetic stimulation using full-sine stimuli,” *PLoS One*, vol. 9, no. 12, p. e115247, Dec. 2014, doi: 10.1371/journal.pone.0115247.
- [168] N. Y. Tse *et al.*, “The effect of stimulation interval on plasticity following repeated blocks of intermittent theta burst stimulation,” *Sci. Rep.*, vol. 8, no. 1, p. 8526, Jun. 2018, doi: 10.1038/s41598-018-26791-w.
- [169] N. Zafar, W. Paulus, and M. Sommer, “Comparative assessment of best conventional with best theta burst repetitive transcranial magnetic stimulation protocols on human motor cortex excitability,” *Clin. Neurophysiol.*, vol. 119, no. 6, pp. 1393–1399, Jun. 2008, doi: 10.1016/j.clinph.2008.02.006.
- [170] V. Di Lazzaro *et al.*, “Theta-burst repetitive transcranial magnetic stimulation suppresses specific excitatory circuits in the human motor cortex,” *J. Physiol.*, vol. 565, no. 3, pp. 945–950, Jun. 2005, doi: 10.1113/jphysiol.2005.087288.
- [171] F. Hashemirad, M. Zoghi, P. B. Fitzgerald, and S. Jaberzadeh, “Reliability of motor evoked potentials induced by transcranial magnetic stimulation: The effects of initial motor evoked potentials removal,” *Basic Clin. Neurosci.*, vol. 8, no. 1, pp. 43–50, 2017, doi: 10.15412/J.BCN.03080106.
- [172] M. Hamada, N. Murase, A. Hasan, M. Balaratnam, and J. C. Rothwell, “The role of interneuron networks in driving human motor cortical plasticity,” *Cereb. Cortex*, vol. 23, no. 7, pp. 1593–1605, 2013, doi: 10.1093/cercor/bhs147.
- [173] M. C. Ridding and U. Ziemann, “Determinants of the induction of cortical plasticity by non-invasive brain stimulation in healthy subjects,” *J. Physiol.*, vol. 588, no. 13, pp. 2291–2304, Jul. 2010, doi: 10.1113/jphysiol.2010.190314.
- [174] B. L. Day *et al.*, “Electric and magnetic stimulation of human motor cortex: surface EMG and single motor unit responses,” *J. Physiol.*, vol. 412, no. 1, pp. 449–473, May 1989, doi: 10.1113/jphysiol.1989.sp017626.
- [175] W. Paulus *et al.*, “State of the art: Pharmacologic effects on cortical excitability measures tested by transcranial magnetic stimulation,” *Brain Stimulation*, vol. 1, no. 3. Elsevier Inc., pp. 151–163, 2008, doi: 10.1016/j.brs.2008.06.002.

- [176] S. Bestmann and J. W. Krakauer, "The uses and interpretations of the motor-evoked potential for understanding behaviour," *Experimental Brain Research*, vol. 233, no. 3. Springer Verlag, pp. 679–689, 01-Mar-2015, doi: 10.1007/s00221-014-4183-7.
- [177] T. Yamaguchi *et al.*, "Priming With Intermittent Theta Burst Transcranial Magnetic Stimulation Promotes Spinal Plasticity Induced by Peripheral Patterned Electrical Stimulation," *Front. Neurosci.*, vol. 12, no. JUL, p. 508, Jul. 2018, doi: 10.3389/fnins.2018.00508.
- [178] K. H. Herrmann, I. Kirchberger, F. Biering-Sørensen, and A. Cieza, "Differences in functioning of individuals with tetraplegia and paraplegia according to the International Classification of Functioning, Disability and Health (ICF)," *Spinal Cord*, vol. 49, no. 4, pp. 534–543, Apr. 2011, doi: 10.1038/sc.2010.156.
- [179] A. Kuppuswamy *et al.*, "Action of 5Hz repetitive transcranial magnetic stimulation on sensory, motor and autonomic function in human spinal cord injury," *Clin. Neurophysiol.*, vol. 122, no. 12, pp. 2452–2461, 2011, doi: 10.1016/j.clinph.2011.04.022.
- [180] T. Tazoe and M. A. Perez, "Effects of repetitive transcranial magnetic stimulation on recovery of function after spinal cord injury," *Arch. Phys. Med. Rehabil.*, vol. 96, no. 4, pp. S145–S155, 2015, doi: 10.1016/j.apmr.2014.07.418.
- [181] K. L. Bunday and M. A. Perez, "Motor recovery after spinal cord injury enhanced by strengthening corticospinal synaptic transmission," *Curr. Biol.*, vol. 22, no. 24, pp. 2355–2361, Dec. 2012, doi: 10.1016/j.cub.2012.10.046.
- [182] M. C. Ridding and J. C. Rothwell, "Is there a future for therapeutic use of transcranial magnetic stimulation?," *Nature Reviews Neuroscience*, vol. 8, no. 7. Nature Publishing Group, pp. 559–567, Jul-2007, doi: 10.1038/nrn2169.
- [183] Y.-H. Kim *et al.*, "Repetitive Transcranial Magnetic Stimulation–Induced Corticomotor Excitability and Associated Motor Skill Acquisition in Chronic Stroke," *Stroke*, vol. 37, no. 6, pp. 1471–1476, Jun. 2006, doi: 10.1161/01.STR.0000221233.55497.51.
- [184] J. Gomes-Osman and E. C. Field-Fote, "Improvements in hand function in adults with chronic tetraplegia following a multiday 10-Hz repetitive transcranial magnetic stimulation intervention combined with repetitive task practice," *J. Neurol. Phys. Ther.*, vol. 39, no. 1, pp. 23–30, Jan. 2015, doi: 10.1097/NPT.000000000000062.
- [185] S. W. Chung, A. T. Hill, N. C. Rogasch, K. E. Hoy, and P. B. Fitzgerald, "Use of theta-burst stimulation in changing excitability of motor cortex: A systematic review and meta-analysis," *Neurosci. Biobehav. Rev.*, vol. 63, pp. 43–64, Apr. 2016, doi: 10.1016/J.NEUBIOREV.2016.01.008.
- [186] M. Wischniewski and D. J. L. G. Schutter, "Efficacy and time course of theta burst stimulation in healthy humans," *Brain Stimulation*, vol. 8, no. 4. Elsevier Inc., pp. 685–692, 2015, doi: 10.1016/j.brs.2015.03.004.

- [187] Y. Z. Huang, R. S. Chen, J. C. Rothwell, and H. Y. Wen, "The after-effect of human theta burst stimulation is NMDA receptor dependent," *Clin. Neurophysiol.*, vol. 118, no. 5, pp. 1028–1032, May 2007, doi: 10.1016/j.clinph.2007.01.021.
- [188] J. T. H. Teo, O. B. Swayne, and J. C. Rothwell, "Further evidence for NMDA-dependence of the after-effects of human theta burst stimulation," *Clinical Neurophysiology*, vol. 118, no. 7. Clin Neurophysiol, pp. 1649–1651, Jul-2007, doi: 10.1016/j.clinph.2007.04.010.
- [189] Q. Yang *et al.*, "Independent replication of motor cortex and cervical spinal cord electrical stimulation to promote forelimb motor function after spinal cord injury in rats," *Exp. Neurol.*, vol. 320, p. 112962, Oct. 2019, doi: 10.1016/j.expneurol.2019.112962.
- [190] H. J. Fassett *et al.*, "Transcranial magnetic stimulation with intermittent theta burst stimulation alters corticospinal output in patients with chronic incomplete Spinal cord injury," *Front. Neurol.*, vol. 8, no. AUG, p. 380, Aug. 2017, doi: 10.3389/fneur.2017.00380.
- [191] J. F. Ditunno, M. E. Cohen, W. W. Hauck, A. B. Jackson, and M. L. Sipski, "Recovery of upper-extremity strength in complete and incomplete tetraplegia: A multicenter study," *Arch. Phys. Med. Rehabil.*, vol. 81, no. 4, pp. 389–393, 2000, doi: 10.1053/mr.2000.3779.
- [192] R. J. Morecraft, J. Ge, K. S. Stilwell-Morecraft, D. W. Mcneal, M. A. Pizzimenti, and W. G. Darling, "Terminal distribution of the corticospinal projection from the hand/arm region of the primary motor cortex to the cervical enlargement in rhesus monkey," *J. Comp. Neurol.*, vol. 521, no. 18, pp. 4205–4235, Dec. 2013, doi: 10.1002/cne.23410.
- [193] S. Sangari and M. A. Perez, "Distinct corticospinal and reticulospinal contributions to voluntary control of elbow flexor and extensor muscles in humans with tetraplegia," *J. Neurosci.*, vol. 40, no. 46, pp. 8831–8841, Nov. 2020, doi: 10.1523/JNEUROSCI.1107-20.2020.
- [194] S. H. Kozin, L. D'Addesi, R. S. Chafetz, S. Ashworth, and M. J. Mulcahey, "Biceps-to-Triceps Transfer for Elbow Extension in Persons With Tetraplegia," *J. Hand Surg. Am.*, vol. 35, no. 6, pp. 968–975, Jun. 2010, doi: 10.1016/j.jhsa.2010.03.011.
- [195] A. Curt, M. E. Keck, and V. Dietz, "Functional outcome following spinal cord injury: Significance of motor- evoked potentials and ASIA scores," *Arch. Phys. Med. Rehabil.*, vol. 79, no. 1, pp. 81–86, 1998, doi: 10.1016/S0003-9993(98)90213-1.
- [196] R. Nardone *et al.*, "Functional brain reorganization after spinal cord injury: Systematic review of animal and human studies," *Brain Research*, vol. 1504. Brain Res, pp. 58–73, 04-Apr-2013, doi: 10.1016/j.brainres.2012.12.034.
- [197] P. N. Gad, E. Kreydin, H. Zhong, K. Latack, and V. R. Edgerton, "Non-invasive Neuromodulation of Spinal Cord Restores Lower Urinary Tract Function After Paralysis," *Front. Neurosci.*, vol. 12, p. 432, Jun. 2018, doi: 10.3389/fnins.2018.00432.
- [198] H. J. Fassett, C. V Turco, J. El-sayes, and A. J. Nelson, "Alterations in Motor Cortical

- Representation of Muscles Following Incomplete Spinal Cord Injury in Humans,” *Brain Sci.*, vol. 8, no. 225, 2018, doi: 10.3390/brainsci8120225.
- [199] T. L. Bender Pape, A. A. Herrold, A. Guernon, A. Aaronson, and J. M. Rosenow, “Neuromodulatory interventions for traumatic brain injury,” *J. Head Trauma Rehabil.*, vol. 35, no. 6, pp. 365–370, Nov. 2020, doi: 10.1097/HTR.0000000000000643.
- [200] P. Spagnolo, J. Parker, S. Horovitz, and M. Hallett, “Cortic limbic Modulation via Intermittent Theta Burst Stimulation as a Novel Treatment for Functional Movement Disorder: A Proof-of-Concept Study,” *Brain Sci.*, vol. 11, no. 6, Jun. 2021, doi: 10.3390/BRAINSKI11060791.
- [201] A. Pink, C. Williams, N. Alderman, and M. Stoffels, “The use of repetitive transcranial magnetic stimulation (rTMS) following traumatic brain injury (TBI): A scoping review,” *Neuropsychol. Rehabil.*, vol. 31, no. 3, pp. 479–505, 2021, doi: 10.1080/09602011.2019.1706585.
- [202] J. Korzhova *et al.*, “High-frequency repetitive transcranial magnetic stimulation and intermittent theta-burst stimulation for spasticity management in secondary progressive multiple sclerosis,” *Eur. J. Neurol.*, vol. 26, no. 4, pp. 680–e44, Apr. 2019, doi: 10.1111/ENE.13877.
- [203] R. J. Butts, M. B. Kolar, and R. D. Newman-Norlund, “Enhanced motor skill acquisition in the non-dominant upper extremity using intermittent theta burst stimulation and transcranial direct current stimulation,” *Front. Hum. Neurosci.*, vol. 8, p. 451, Jun. 2014, doi: 10.3389/fnhum.2014.00451.
- [204] N. Mittal, B. C. Majdic, A. P. Sima, and C. L. Peterson, “The effect of intermittent theta burst stimulation on corticomotor excitability of the biceps brachii in nonimpaired individuals,” *Neurosci. Lett.*, vol. 764, p. 136220, Nov. 2021, doi: 10.1016/J.NEULET.2021.136220.
- [205] N. Sollmann *et al.*, “Clinical Factors Underlying the Inter-individual Variability of the Resting Motor Threshold in Navigated Transcranial Magnetic Stimulation Motor Mapping,” *Brain Topogr.* 2016 301, vol. 30, no. 1, pp. 98–121, Nov. 2016, doi: 10.1007/S10548-016-0536-9.
- [206] D. T. Corp *et al.*, “Large-scale analysis of interindividual variability in theta-burst stimulation data: Results from the ‘Big TMS Data Collaboration,’” *Brain Stimul.*, vol. 13, no. 5, pp. 1476–1488, 2020, doi: <https://doi.org/10.1016/j.brs.2020.07.018>.
- [207] F. Ferreri *et al.*, “Age-related changes of cortical excitability and connectivity in healthy humans: non-invasive evaluation of sensorimotor network by means of TMS-EEG,” *Neuroscience*, vol. 357, pp. 255–263, Aug. 2017, doi: 10.1016/j.neuroscience.2017.06.014.
- [208] V. Noreika, M. R. Kamke, A. Canales-Johnson, S. Chennu, T. A. Bekinschtein, and J. B. Mattingley, “Alertness fluctuations when performing a task modulate cortical evoked responses to transcranial magnetic stimulation,” *Neuroimage*, vol. 223, p. 117305, Dec. 2020, doi: 10.1016/j.neuroimage.2020.117305.
- [209] N. De Geeter, G. Crevecoeur, A. Leemans, and L. Dupré, “Effective electric fields along realistic

- DTI-based neural trajectories for modelling the stimulation mechanisms of TMS,” *Phys. Med. Biol.*, vol. 60, no. 2, pp. 453–471, Jan. 2015, doi: 10.1088/0031-9155/60/2/453.
- [210] C. B. Ah Sen, H. J. Fassett, J. El-Sayes, C. V. Turco, M. M. Hameer, and A. J. Nelson, “Active and resting motor threshold are efficiently obtained with adaptive threshold hunting,” *PLoS One*, vol. 12, no. 10, pp. 1–9, 2017, doi: 10.1371/journal.pone.0186007.
- [211] N. H. Jung, I. Delvendahl, N. G. Kuhnke, D. Hauschke, S. Stolle, and V. Mall, “Navigated transcranial magnetic stimulation does not decrease the variability of motor-evoked potentials,” *Brain Stimul.*, vol. 3, no. 2, pp. 87–94, Apr. 2010, doi: 10.1016/J.BRS.2009.10.003.
- [212] A. McGirr *et al.*, “Efficacy of Active vs Sham Intermittent Theta Burst Transcranial Magnetic Stimulation for Patients With Bipolar Depression: A Randomized Clinical Trial,” *JAMA Netw. Open*, vol. 4, no. 3, pp. e210963–e210963, Mar. 2021, doi: 10.1001/JAMANETWORKOPEN.2021.0963.
- [213] R. L. Harvey *et al.*, “Randomized Sham-Controlled Trial of Navigated Repetitive Transcranial Magnetic Stimulation for Motor Recovery in Stroke,” *Stroke*, vol. 49, no. 9, pp. 2138–2146, 2018, doi: 10.1161/STROKEAHA.117.020607.
- [214] M. Halaki and K. Gi, “Normalization of EMG Signals: To Normalize or Not to Normalize and What to Normalize to?,” in *Computational Intelligence in Electromyography Analysis - A Perspective on Current Applications and Future Challenges*, InTech, 2012.
- [215] K. M. Hasan and P. A. Narayana, “Computation of the fractional anisotropy and mean diffusivity maps without tensor decoding and diagonalization: Theoretical analysis and validation,” *Magn. Reson. Med.*, vol. 50, no. 3, pp. 589–598, Sep. 2003, doi: 10.1002/MRM.10552.
- [216] X. Li, P. S. Morgan, J. Ashburner, J. Smith, and C. Rorden, “The first step for neuroimaging data analysis: DICOM to NIfTI conversion,” *J. Neurosci. Methods*, vol. 264, pp. 47–56, May 2016, doi: 10.1016/J.JNEUMETH.2016.03.001.
- [217] M. Jenkinson, C. F. Beckmann, T. E. J. Behrens, M. W. Woolrich, and S. M. Smith, “FSL,” *Neuroimage*, vol. 62, no. 2, pp. 782–790, Aug. 2012, doi: 10.1016/J.NEUROIMAGE.2011.09.015.
- [218] J. Andersson and S. Sotiropoulos, “An integrated approach to correction for off-resonance effects and subject movement in diffusion MR imaging,” *Neuroimage*, vol. 125, pp. 1063–1078, Jan. 2016, doi: 10.1016/J.NEUROIMAGE.2015.10.019.
- [219] S. M. Smith, “Fast robust automated brain extraction,” *Hum. Brain Mapp.*, vol. 17, no. 3, pp. 143–155, Nov. 2002, doi: 10.1002/HBM.10062.
- [220] F. Syeda, A. Pandurangi, A. A. El-Gendy, and R. L. Hadimani, “Effect of Transcranial Magnetic Stimulation on Demyelinated Neuron Populations,” *IEEE Trans. Magn.*, vol. 53, no. 11, Nov. 2017, doi: 10.1109/TMAG.2017.2728006.

- [221] T. A. Yousry *et al.*, “Localization of the motor hand area to a knob on the precentral gyrus. A new landmark,” *Brain*, vol. 120, no. 1, pp. 141–157, 1997, doi: 10.1093/brain/120.1.141.
- [222] J. Anderson, N. J. Parr, and K. Vela, “Evidence Brief: Transcranial Magnetic Stimulation (TMS) for Chronic Pain, PTSD, TBI, Opioid Addiction, and Sexual Trauma,” *Evid. Br. Transcranial Magn. Stimul. Chronic Pain, PTSD, TBI, Opioid Addict. Sex. Trauma*, 2020.
- [223] A. Latorre, L. Rocchi, A. Berardelli, K. Bhatia, and J. Rothwell, “The interindividual variability of transcranial magnetic stimulation effects: Implications for diagnostic use in movement disorders,” *Mov. Disord.*, vol. 34, no. 7, pp. 936–949, Jul. 2019, doi: 10.1002/MDS.27736.
- [224] A. Herrold *et al.*, “Customizing TMS Applications in Traumatic Brain Injury Using Neuroimaging,” *J. Head Trauma Rehabil.*, vol. 35, no. 6, pp. 401–411, Nov. 2020, doi: 10.1097/HTR.0000000000000627.
- [225] R. F. H. Cash *et al.*, “Using Brain Imaging to Improve Spatial Targeting of Transcranial Magnetic Stimulation for Depression,” *Biol. Psychiatry*, Jun. 2020, doi: 10.1016/J.BIOPSYCH.2020.05.033.
- [226] G. Raffa *et al.*, “The Impact of Diffusion Tensor Imaging Fiber Tracking of the Corticospinal Tract Based on Navigated Transcranial Magnetic Stimulation on Surgery of Motor-Eloquent Brain Lesions,” *Neurosurgery*, vol. 83, no. 4, pp. 768–782, Oct. 2018, doi: 10.1093/NEUROS/NYX554.
- [227] N. Sollmann *et al.*, “Associations between clinical outcome and navigated transcranial magnetic stimulation characteristics in patients with motor-eloquent brain lesions: a combined navigated transcranial magnetic stimulation-diffusion tensor imaging fiber tracking approach,” *J. Neurosurg.*, vol. 128, no. 3, pp. 800–810, Mar. 2018, doi: 10.3171/2016.11.JNS162322.
- [228] H. Zhang, T. Schneider, C. Wheeler-Kingshott, and D. Alexander, “NODDI: practical in vivo neurite orientation dispersion and density imaging of the human brain,” *Neuroimage*, vol. 61, no. 4, pp. 1000–1016, Jul. 2012, doi: 10.1016/J.NEUROIMAGE.2012.03.072.
- [229] M. Bastiani *et al.*, “Improved tractography using asymmetric fibre orientation distributions,” *Neuroimage*, vol. 158, p. 205, Sep. 2017, doi: 10.1016/J.NEUROIMAGE.2017.06.050.
- [230] E. J. Wallace, J. L. Mathias, L. Ward, J. Fripp, S. Rose, and K. Pannek, “A voxel-based analysis of micro- and macro-structural changes to white matter following adult traumatic brain injury,” *Hum. Brain Mapp.*, vol. 41, no. 8, pp. 2187–2197, Jun. 2020, doi: 10.1002/HBM.24939.
- [231] M. Lu and S. Ueno, “Comparison of the induced fields using different coil configurations during deep transcranial magnetic stimulation,” *PLoS One*, vol. 12, no. 6, Jun. 2017, doi: 10.1371/journal.pone.0178422.
- [232] A. Zolj, S. N. Makarov, L. Navarro De Lara, and A. Nummenmaa, “Electrically Small Dipole Antenna Probe for Quasistatic Electric Field Measurements in Transcranial Magnetic Stimulation,” *IEEE Trans. Magn.*, vol. 55, no. 1, Jan. 2019, doi: 10.1109/TMAG.2018.2875882.

- [233] A. V. Peterchev *et al.*, “Fundamentals of transcranial electric and magnetic stimulation dose: Definition, selection, and reporting practices,” *Brain Stimulation*, vol. 5, no. 4. Elsevier, pp. 435–453, 01-Oct-2012, doi: 10.1016/j.brs.2011.10.001.
- [234] T. Wagner *et al.*, “Transcranial magnetic stimulation and stroke: A computer-based human model study,” *Neuroimage*, vol. 30, no. 3, pp. 857–870, Apr. 2006, doi: 10.1016/j.neuroimage.2005.04.046.
- [235] X. J. Wang, “Fast burst firing and short-term synaptic plasticity: A model of neocortical chattering neurons,” *Neuroscience*, vol. 89, no. 2, pp. 347–362, Mar. 1999, doi: 10.1016/S0306-4522(98)00315-7.
- [236] M. Memarian Sorkhabi, K. Wendt, M. T. Wilson, and T. Denison, “Estimation of the Motor Threshold for Near-Rectangular Stimuli Using the Hodgkin-Huxley Model,” *Comput. Intell. Neurosci.*, vol. 2021, 2021, doi: 10.1155/2021/4716161.
- [237] T. Xu *et al.*, “Rapid formation and selective stabilization of synapses for enduring motor memories,” *Nat. 2009 4627275*, vol. 462, no. 7275, pp. 915–919, Nov. 2009, doi: 10.1038/NATURE08389.
- [238] M. T. Wilson, B. D. Fulcher, P. K. Fung, P. A. Robinson, A. Fornito, and N. C. Rogasch, “Biophysical modeling of neural plasticity induced by transcranial magnetic stimulation,” *bioRxiv*, p. 175893, Aug. 2017, doi: 10.1101/175893.
- [239] F. Syeda, K. Holloway, A. A. El-Gendy, and R. L. Hadimani, “Computational analysis of transcranial magnetic stimulation in the presence of deep brain stimulation probes,” *AIP Adv.*, vol. 7, no. 5, p. 056709, May 2017, doi: 10.1063/1.4974062.
- [240] N. De Geeter, L. Dupré, and G. Crevecoeur, “Modeling transcranial magnetic stimulation from the induced electric fields to the membrane potentials along tractography-based white matter fiber tracts,” *J. Neural Eng.*, vol. 13, no. 2, p. 026028, Mar. 2016, doi: 10.1088/1741-2560/13/2/026028.
- [241] J. Albert, “A hybrid of the chemical master equation and the gillespie algorithm for efficient stochastic simulations of sub-networks,” *PLoS One*, vol. 11, no. 3, Mar. 2016, doi: 10.1371/journal.pone.0149909.
- [242] C. L. Vestergaard and M. Génois, “Temporal Gillespie Algorithm: Fast Simulation of Contagion Processes on Time-Varying Networks,” *PLoS Comput. Biol.*, vol. 11, no. 10, p. 1004579, 2015, doi: 10.1371/journal.pcbi.1004579.